DEVELOPMENT OF 3D PRINTING FRAMEWORK USING PC-BASED PLC

VINCENT HOONG YONG SHENG

A project report submitted in partial fulfilment of the requirements for the award of Bachelor of Engineering (Hons.) Mechatronics Engineering

Lee Kong Chian Faculty of Engineering and Science
Universiti Tunku Abdul Rahman

May 2018

DECLARATION

I hereby declare that this project report is based on my original work except for citations and quotations which have been duly acknowledged. I also declare that it has not been previously and concurrently submitted for any other degree or award at UTAR or other institutions.

Signature : _____

Name : Vincent Hoong Yong Sheng

ID No. : 13UEB03027

Date : 15/04/2018

APPROVAL FOR SUBMISSION

I certify that this project report entitled **"DEVELOPMENT OF 3D PRINTING FRAMEWORK USING PC-BASED PLC"** was prepared by **VINCENT HOONG YONG SHENG** has met the required standard for submission in partial fulfilment of the requirements for the award of Bachelor of Engineering (Hons.) Mechatronics Engineering at Universiti Tunku Abdul Rahman.

Approved by,

Signature : _____

Supervisor : Dr. Tey Jing Yuen

Date : _____

Signature : _____

Co-Supervisor : Mr. Chong Yu Zheng

Date : _____

ACKNOWLEDGEMENTS

I would like to thank everyone who had contributed to the successful completion of this project. I would like to express my gratitude to my research supervisor, Dr. Yogeswaran a/l Mohan, Dr. Tey Jing Yuen and Mr. Chong Yu Zheng for his invaluable advice, guidance and his enormous patience throughout the development of the research.

In addition, I would also like to express my gratitude to my loving parents and friends who had helped and given me encouragement and great support throughout my process of undertaking the project research. More of that, I would also like to express my appreciation towards Mr. Lim Kok Teong from JKS Engineering (M) Sdn. Bhd., Mr. Johnny Poh from Beckhoff Automation Sdn. Bhd. and Mr. Ren and Mr. Kevin from Iconix Technology Sdn. Bhd. for providing professional advises in terms of PLC programming knowledge throughout the project.

ABSTRACT

3D printing denotes to processes which material is fused and solidified under computer control to construct a three dimensional object. It can produce complex objects directly by using computer aided design. This technology has traditionally been applied by large companies to perform rapid prototyping before production. Moreover, there has also been a change to adopt the technology as customise printing solution in the recent years. The advent of 3D printers that are capable of multi-material printing such as ProJet MJP 5600 from 3D Systems has create a breakthrough that enables the users to create product with different mechanical properties over its structure. However, current multi-material printing solution only offers up to discrete selection of printed material matrix in a single printing process. Therefore, this project intends to develop a multi-material composite 3D printer that is capable in selecting wide variation of material matrix for printing through a single extruder. The framework for interpreting G-code generated and performing 3D printing process is designed and developed in this project. To ensure accurate and reliable system, configurations and experimentations are performed to measure the performance of the system. Accuracy and reliability of the system are determined and proven based on the experimental results obtained. Low accuracy and performance system will be calibrated based on the system behaviour. Furthermore, this project also covers the techniques to link user interface with system framework. System framework will have certain level of flexibility of controls by the non-technical users via user interface. Critical status of the system will also be linked from the system framework to user interface for users to understand the system condition.

TABLE OF CONTENTS

LIST OF TABLES

LIST OF FIGURES

LIST OF SYMBOLS / ABBREVIATIONS

3D	Three dimensional
e.m.f	Electromagnetic force
AM	Additive Manufacturing
FDM	Fused Depostion Modelling
SLA	Stereolithography Apparatus
SLS	Selective Laser Sintering
RAM	Random Access Memory
HMI	Human Machine Interface
SSR	Solid State Relay
EMR	Electromechanical Relay
AC	Alternating Current
DC	Direct Current
BJT	Bipolar Junction Transistor
IC	Integrated Circuit
CNC	Computer Numerical Control
CPU	Central Processing Unit
Gr	Pinion to gear ratio, 1
T_P	Number of teeth of pinion
T_G	Number of teeth of gear
d	Distance travelled by the pinion per rotation, mm/rad
dpp	Pitch-to-pitch distance of the screw/auger, mm/rad
SF	Scaling factor
d_{rev}	Distance travelled per revolution
RMSE	Root Mean Square Error
n	Number of readings
y_i	Measured reading
$\hat{y}_i$	Actual reading
$\omega_{maxpinion}$	Maximum angular velocity of pinion
$v_{maxgear}$	Maximum velocity of gear
f_{base}	Base frequency
f_{motor}	Motor frequency

$T_{measured}$	Measured temperature
$T_{thermocouple}$	Thermocouple temperature
$T_{calibrated}$	Calibrated temperature
e_{actual}	Actual percentage error
$e_{calibrated}$	Calibrated percentage error

LIST OF APPENDICES

CHAPTER 1

INTRODUCTION

1.1 General Introduction

There is an increasing demand for customising products to fragment the market in the middle of the 1950's (Kaplan & Haenlein, 2006). Consequently, in order to facilitate the demand of more tailored products, business decisions were directed towards a certain degree of customisation. The unprecedented 3D shaping abilities of additive manufacturing have lately influenced areas as diverse as medicine, anthropology and design (Kokkinis, Schaffner and Studart, 2015). To fulfil the need of customisation, inventors have sought new fabrication techniques to increase the flexibility in structure of an output product. One such emerging technique is 3D printing. 3D printing is a process used to create a customised three dimensional objects via extruding molten materials, cooling and solidifying it. It is often known as additive manufacturing (AM) process.

Depending on the physical and chemical properties of the final printed products, the materials used for 3D printing is selected. In some occasions, there are a need to create product with varying physical or chemical properties over the product. Current multi-material additive manufacturing systems have encountered severe shortcomings of technology in achieving this condition (Sitthi-Amorn et al., 2015). The current 3D printer technology can concurrently use, at most, only three different materials (Sitthi-Amorn et al., 2015). More of that, the ideas of using multiple extruders can only produce a discrete selection on the material properties. The hardware and software architectures of the current multi-material 3D printers are exclusive and inextensible. Therefore, this project intends to develop a 3D printers that is capable of printing product with varying local chemical composition over the product. The general methodology of the stated idea is by controlling the mixing ratio of two types of materials with different matrix properties. Accuracy and reliability of the framework are two important criteria to be considered before performing investigation and study on the chemical fusion of the materials.

1.2 Importance of the Study

The importance of the undertaking project is to propose and develop a new method of 3D printing where the mechanical, electrical, chemical and optical properties of the output product can be controlled. This is achieved by modifying the mother matrix of a material with different proportion of additive added. Depending on the mixing ratio, a product with different properties can be produced. With a success in the respective proposed method, a complex structure like badminton racquet which require a softer texture on the gripper but rigid structure on the other parts can be easily produced. Furthermore, this idea can also create a gradient transition over the mechanical structure to reduce the maximum concentrated stress applied on the structure. Due to time limitation, the project only be focusing on the framework development. In summary, the importance of this project is to act as a stepping stone in the future progress of constructing a 3D printer which allows variable material properties printing with a single extruder.

1.3 Problem Statement

In the current 3D printing technology, the outcome of the printed products is almost impossible to be possessed with different material properties over the products. This often creates an issue especially on complicated products which requires to have mild flexibility and soft texture over its product. A solution to this problem can be applied by using a multi-material feeding 3D printer that is capable of multi-material mixing. With the ability to print products that contained the composition of multiple materials, the printer can provide an additional control over the local chemical composition of the printed material.

However, a question remains on whether the multi-material feeding 3D printer is capable of printing desired output products with different composition of material over the product. To resolve this problem, the framework of the printer with close consideration on the performance of the machine is developed. Electrical control system of the printer is designed and constructed to ensure proper and stable

connections for system to perform command and control operation. In addition, the accuracy and reliability of the system are also investigated to ensure proper printing operation. The parameters are fine-tuned to produce a machine with better accuracy. Human Machine Interface is developed to interface the users with machine's command and response.

1.4 Aims and Objectives

The main aim of pursuing this development project is to construct a 3D printer framework to innovate new techniques in producing a product with variable material properties over its body. With a success in the respective research, a 3D printer framework that is capable of perform correct motion positioning and temperature measurement is created. In order to achieve this, three objectives had been clearly stated out to achieve and extend the capabilities of the stated goal.

- Develop 3D printing framework and electrical system controls of the machine.
- Improve the reliability and accuracy of the printer prototype by performing calibration on the machine.
- Integrate 3D printing framework with Human Machine Interface.

1.5 Scope and Limitation of the Study

The physical and chemical behaviour of the plastic pellets are the aspect of the 3D printing which is essential in ensuring expected quality products. It is to be highlighted that to understand chemical behaviour especially the chemical fusion of the two plastic materials required high level of chemical fusion knowledge and many chemical experiments to be done. All properties including the fluidity and the fusion rate must be considered properly in order to ensure that the particular mixing ratio can be printed out at the right moment.

Therefore, the inadequate knowledge of material fusion behaviour became one of the limitation for the study. The study of thermoplastic material is not involved in the scope of this project. Other than that, with an open-loop control system of stepper motor used, there will also be a slight inaccuracy being generated. In other words, there can be tolerance on the distance travelled by the stepper motor as compare with the expected distance.

1.6 Contribution of the Study

With the completion of this project, one essential contribution is the limitation of the variety in printing material of a 3D printer. From the view of engineering, it helps by providing information on the integrating process of the structure and the factor on the printer that needs to be to be closely considered. From the view of end-users, this technology paves a new and better ways of printing product. End-users without professional technical knowledge will be able to print a high quality product with ease.

Furthermore, 3D printing technology can also be expanded to more fields with the breakthrough on the limitation. For instance, the base of the shoes can be printed with a harder bottom base and softer upper base to deal with floor impact while at the same time provide comfort for users.

1.7 Outline of the Report

The main chapters that will be covered in this report will be the literature review and methodology. Literature review summarises the relevant researches that had been done on the 3D printing concepts, technology and their limitations. Fundamental 3D printing concepts such as the control system, components required and the processing techniques will be discussed in literature review.

The methodology will be discussed on the techniques used in constructing the 3D printer using the information that had been gathered through reviewing the literature. Detailed plan of the designing and constructing of the physical structure and

framework will be included. Electronics components selection and its arrangement will also be considered in methodology chapter.

CHAPTER 2

LITERATURE REVIEW

2.1 Introduction

Additive manufacturing (AM), colloquially recognised as 3D printing, is currently being introduced as the spark of an innovative industrial revolution. The technology permits one to make customised products without acquiring any cost penalties in manufacturing as neither molds nor tools required (Weller, Kleer and Piller, 2015). Many techniques has been proposed based on the AM technologies to extend the capabilities to customised products. Fused Deposition Modelling (FDM), Stereolithography (SLA) and Selective Laser Sintering (SLS) are methods that are commonly used in current society to perform AM.

Each of the AM techniques have their unique specifications and pros and cons in terms of cost, printing speed and structure of printed products. However, among all the AM techniques mentioned, FDM is one of the most recommended method used for rapid prototyping. One of the main factor leading to this conclusion is due to the cost-effective printing operations and high speed printing. FDM perform its 3D printing operation by heating up production-grade thermoplastics to glass transition phase and extrude it on a platform known as heat bed according to the commands given to the machine.

The temperature is set by using an electrically, usually pulse width modulated, controlled heater to heat up the extruder for plastic to melt. Sensors are used to control the temperature of the system by controlling the modulation sent to the heater based on the temperature configured. It uses motors to move the extruder around a 3D platform to print an object. To be more precise, depending on the situation, stepper motors are usually used in FDM 3D printing due to its accurate motion. To further enhance the motion accuracy of the printer, a higher step angle stepper motor or a stepper motor with encoder closed-loop feedback controller is equipped.

As mentioned in importance of this study, this project aims to develop a 3D printer which is capable of printing product with varying chemical composition along the product. The direction to achieve this is by feeding two different materials into an extruder barrel to melt and fuse it based on the mixing ratio. In other words, the extruder barrel acts as a path for fusing a new blend of material with different composition to printed out. Temperature is increased along the extruder barrel towards the nozzle to safeguard printed output quality.

Finally, controls and commands display are another important aspects to study before proceeding into practical hands-on. Important information should be summarise and displayed to speed up printing configuration and process. Data presentation is a key focus when designing the user interface. Furthermore, techniques to interface between back-end configuration and front-end user display is to be study. In conclude, the data presentation and interfacing methods are to be reviewed.

2.2 Additive Manufacturing

AM is a manufacturing method which involves the fusing of materials, usually layer-upon-layer, to construct objects from 3D model data (Mellor, Hao and Zhang, 2014). The advantages of this methodology include removal of tooling requirements, new design freedom and economically low volumes (Weller, Kleer and Piller, 2015). AM was mostly used for fabrication of conceptual and functional prototypes which is also known as rapid prototyping during its early years of invention. It suggested that AM production can reduce waste, offers design customisation, has shorter lead times and allows economical custom products (Holmström et al., 2010). There are several technologies which employ this method of manufacturing such as fused deposition modelling, stereolithography and selective laser sintering. However, AM technologies are commonly limited to rapid prototyping as they do not allow matrix of the engineering materials to be processed (Holmström et al., 2010).

One of the most commonly used methods of AM in nowadays 3D printing technology is the FDM. This method builds parts with production-grade

thermoplastics which are equipped with excellent mechanical, thermal and chemical qualities as shown in Figure 2.1 (Sidambe, 2014). FDM technology produces 3D object by heating and extruding thermoplastic filament over a platform from bottom up, layer by layer ("Types of 3D printers or 3D printing technologies overview | 3D Printing from scratch", 2018). Thermoplastic is heated to its glass transition temperature by the printer and extruded out from the extruder nozzle onto a platform along the calculated path. After the printed layer binds to the layer beneath it, the plastic cools down and hardens. Once a layer is finished, either the platform is lowered or the extruder is raised to proceed print on the next layer.

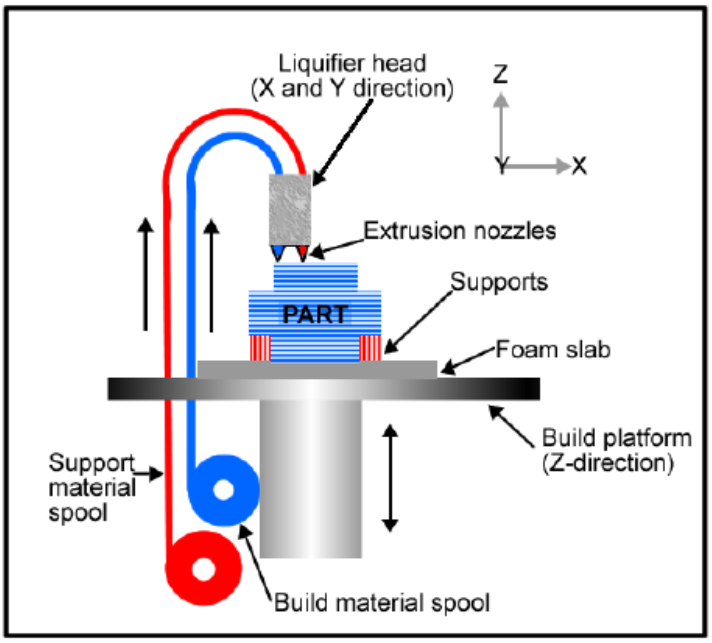

Figure 2.1 Fused Deposition Modelling
(Sidambe, 2014)

FDM utilises multiple extruders for printing different colours of materials simultaneously. Furthermore, it also has good geometric accuracy and compact machine structure (Negi, Dhiman and Kumar Sharma, 2014). However, FDM has its limitations on the resolution of the printed products (Jose, 2014). The methods used by FDM can often cause ribbing around the printed products. FDM also required supporting frames to be printed under overhanging structures. Without a supporting frames, the 3D printed product will deformed due to the lack of existence of printing

platform. In short, FDM has good accuracy, compact machine structure, required supporting frames for overhanging structures and limited printing resolution.

Similar to FDM, SLA is another techniques of AM. SLA creates 3D models in a layer by layer manner using a method by which light causes the chains of molecules to link and formed polymers, known as photopolymerization. A general idea of SLA can be seen in Figure 2.2. SLA can produced high part building accuracy and smooth surface finish (Negi, Dhiman and Kumar Sharma, 2014). Although SLA can be used to create virtually synthetic design, the photopolymers resins which is used as a printing material is often expensive (Ngo, 2015). Apart from that, the post-processing time is usually longer than the common AM techniques for SLA (Negi, Dhiman and Kumar Sharma, 2014).

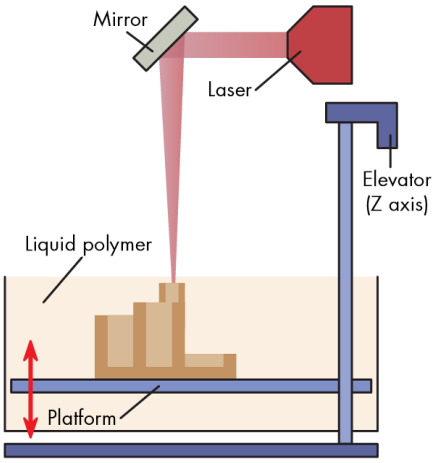

Figure 2.2 Stereolithography

(Kerns J.,2015)

Lastly, SLS utilises the AM technology by using a laser to selectively scan and sinter thin layer of powder particles. To summarize the working principle of SLS, the powder in a container is swept upon the construction stage by a recoater. Then, a laser selectively scans through the thin layer of powder, sintering the powder particles together. The build platform is then lowered by one layer depth and a new coat of powder is applied by a recoater as shown in Figure 2.3. The advantages of SLA includes the capability to use wide variation of thermoplastics, no necessities for support structure and it is easy for post-processing (Negi, Dhiman and Kumar Sharma,

2014). This allows intricate and complicated geometries to be constructed easily. However, similar to SLA, the cost of a machine is pretty steep.

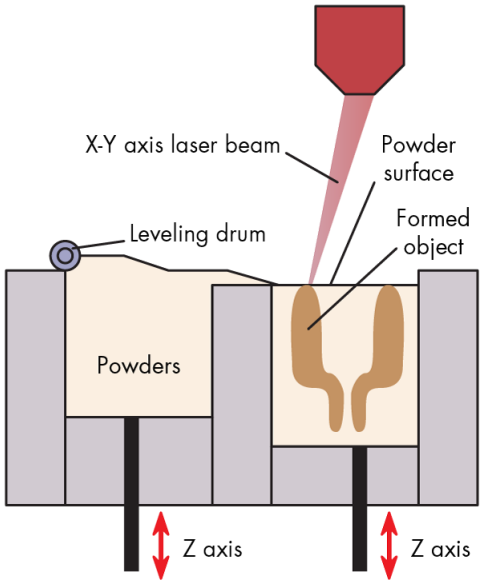

Figure 2.3 Selective Laser Sintering

(Kerns J., 2015)

2.3 Working Principle of 3D Printer

Stepper Control System for 3D Printer

The main control system that required close consideration is the motor selected for the axes and extruder. There are essential in ensuring accuracy. The most frequently used system in 3D printer world is the simple stepper control where the system is an open loop unit driving the stepper motor. Figure 2.4 shows a clearer picture on the operation of simple stepper control (Reprap.org, 2017).

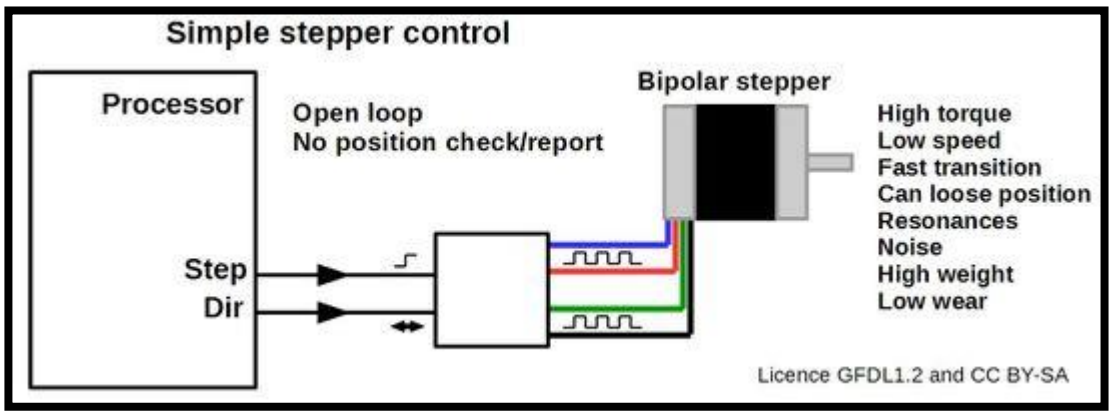

Figure 2.4 Simple Stepper Control

(Source: Reprap.org, 2012)

Another type of stepper motor which is known as 'hybrid' stepper control is less commonly used in 3D printing. This 'hybrid' stepper control operate with a similar function as compare to the simple stepper control but with an additional sensor which constantly provides information about the effective movement. The 'hybrid' stepper control can be understood much further by referring to Figure 2.5.

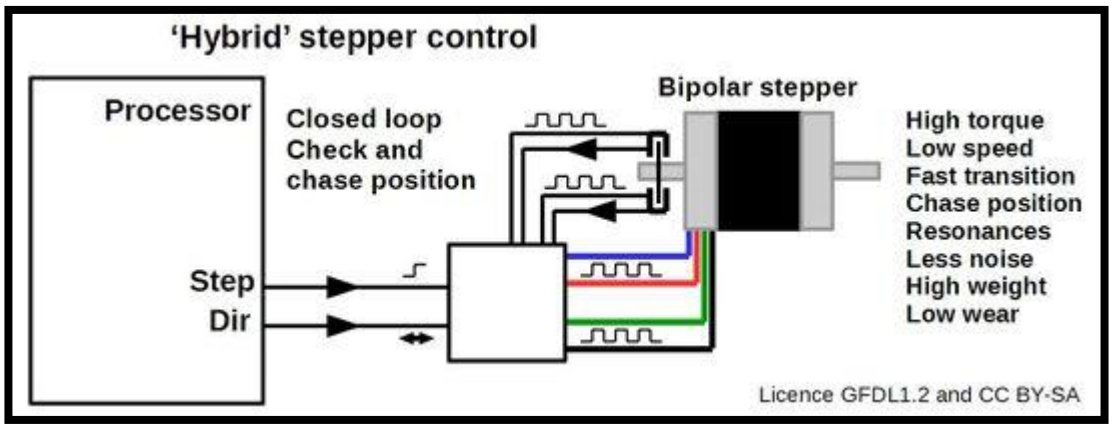

Figure 2.5 'Hybrid' Stepper Control

(Source: Reprap.org, 2012)

Stepper motors are used to drive the dynamic motion of the machine. In many automation problems and machine control, there could be two or more axes of motion that must be coordinated (Automation.com, n.d.). The terms "multi-axis synchronisation" refers to the techniques used to achieve control of motion and the motion requires for coordination (Kim et al., 1996). When there are two or more axes

of motion are executed in a single operation, the machine is commissioning multi-axis motion. The axes may be working individually or moving together.

Multi-axis synchronisation is necessary whenever the axes are required to move together. The relationship between their respective motions can be important. The most familiar example of the multi-axis synchronisation application is the X-Y Plotter. The motion at the X and Y direction may move individually from each other but their motion must be coordinated. Figure 2.6 shows the problems encountered to a 45 degree straight line if the X axis starts and ends its motion later than the Y axis. The synchronisation based on position and velocity relationship between the axes are important for proper operation of the machine (Automation.com, n.d.).

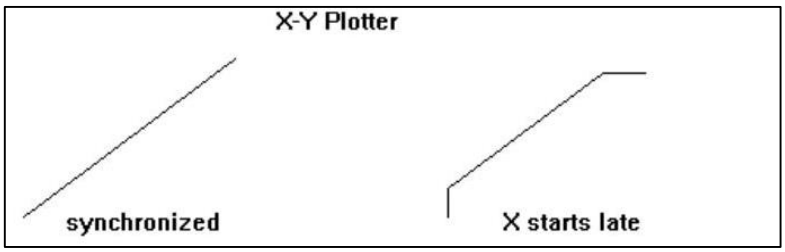

Figure 2.6 Difference between Multi-axis Synchronisation and Non-Synchronisation Motion

(Source: Automation.com, n.d.)

G-code Interpreter

3D printing is performed via a combination set of skills in mechanical, electronics and programming. To command a stepper motor we need a way to easily turn our human desires into machine instruction into stepper motor steps (Dan, 2013). In effect we need our robot brain to be interpreter. For the 3D printer, it uses a machine instruction known as G-code to allow the machine to understand and perform the command operation. G-code is one of the many interpreters that has been used for human-machine communication (Shin, Suh and Stroud, 2007). It consists of an uppercase letter which is the action command followed by a number which is the value used for either action command or position declaration (Shin, Suh and Stroud, 2007).

Each line of G-code tells the machine to execute one discrete action, including position, rotation and velocity (Rapid S., 2016). Shapes are formed by stringing together point-by-point sets of instructions (Shin, Suh and Stroud, 2007). All the commands are usually read as a string without information understood by the machines. Parsing and extraction of information are required in order to allow the machine to understand the steps or procedures and the actions to be made in every step. The interpreter should be flexible in interpreting all variety length of commands and able to extract the relevant details.

One example of G-code that is commonly used for motion control is the G01 which is linear interpolation. G01 executes a movement following a straight line at a set feed rate as shown in Figure 2.7. The feed rate that is programmed into the G01 command is the actual feed rate along the proposed tool path rather than the feed rate of each axis (CNC Machining Handbook, 2010). On motion that involved two or more axes movement, all the slides have to execute exactly the same length of time in order to generate a single vector move. The machine controller will calculate the separate feed rate of each axes, allowing the vector feed rate to be equal to that stated in G01 command.

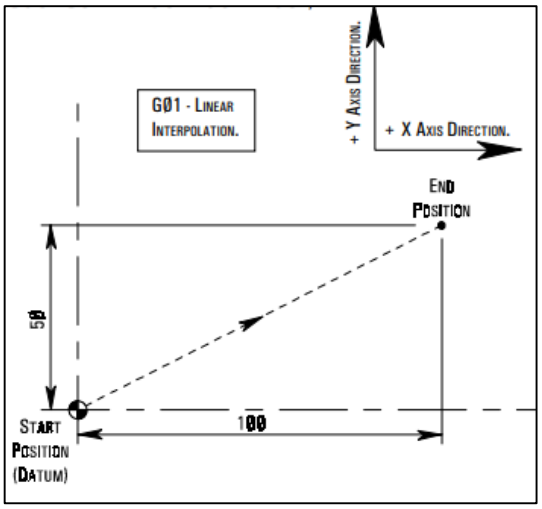

Figure 2.7 Linear Interpolation

(Source: Denford G and M Programming for CNC Milling Machines, n.d.)

Circular interpolation is also one of the common G-code command that is used for CNC control. G02 and G03 are clockwise and counter-clockwise circular interpolation commands (CNC Machining Handbook, 2010). The letters I and J are

addressed to program an arc motion. I relates to the address of X and its incremental value and direction from the initial point of the arc on the X axis to the arc centre as shown in Figure 2.8 (Denford G and M Programming for CNC Milling Machines, n.d.).. J relates to the address of Y and is the incremental value and direction from the initial point of the arc on the Y axis to the arc center (Denford G and M Programming for CNC Milling Machines, n.d.).

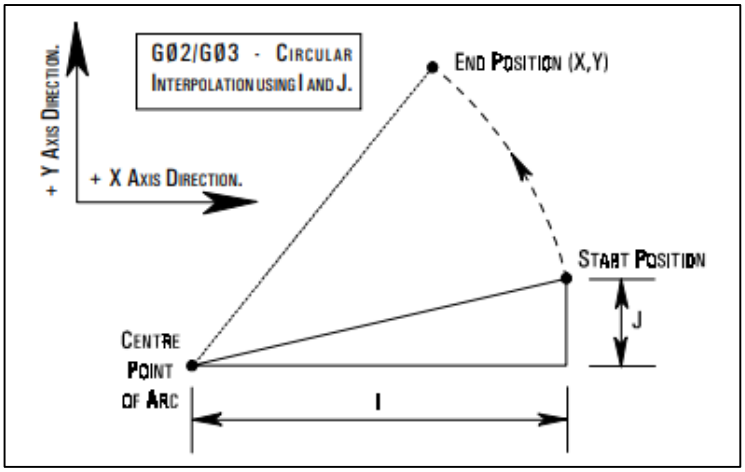

Figure 2.8 Circular Interpolation

(Source: Denford G and M Programming for CNC Milling Machines, n.d.)

2.4 Temperature Sensor

Temperature sensor is mainly used in temperature control application within a system. There are various types of temperature sensor being introduced and the selection of type of temperature sensor also depending on the application requirements. Negative temperature coefficient (NTC) thermistor, resistance thermometer detectors (RTD), thermocouple and integrated silicon sensors are a few of the typical temperature sensors that are used in circuits. Trade-offs amongst these devices include cost to operate, stability, operating temperature range and noise immunity (Ametherm, 2017). Stable devices will yield lesser output signal drift over time as compare to the unstable devices which reduces the need for repeat calibrations.

Thermocouples are inexpensive, operate over a wide range, stable, rugged, and are relatively linear over a wide range but deviate significantly at extremely cold or

hot temperatures. A thermocouple adhere the Seeback effect to generate voltage that correlates to the temperature. To improve the accuracy of a thermocouple, a controller equipped with a Seeback coefficients and look-up table of thermoelectric voltages is required to generate linear signal. Thermocouples also have a faster response time as compare to NTC thermistors followed by RTDs (Brei T. M., 2013).

RTD elements have a varying resistance value depending on temperature change. RTDs are offered in several different kinds of metals which includes nickel, platinum, nickel-iron and copper. The platinum RTD is the most accurate temperature sensor of all types of other sensors. RTDs have a better accuracy and repeatability as compare to thermocouples and it is easier to be calibrated (Brei T. M., 2013). Platinum RTD is stable, can covers a wide range of temperature, demonstrates good noise immunity and has excellent repeatability and linearity (Heath, 2016). However, it is very costly to purchase and apply platinum RTD unless the measurand condition is critical. More of that, RTDs required stable current for accurate measurement of the resistance value.

Thermistors are temperature sensitive resistors which are known for a rapid response. Resemble to RTDs, thermistors also have a varying resistance value depending on the temperature change and require excitation. Thermistors generally have higher resistance value as compare to RTDs. Therefore, it is operated under lower reference currents and thus required lesser energy consumption. NTC thermistor usually has a temperature drift of lower than 0.2 ℃ per year while thermocouple has a lower stability which gives a 1 ℃ to 2 ℃ temperature drift per year (Ametherm, 2017). However, thermistors do not have good linearity between temperature and its resistance value. In result, a look-up table or equation is needed to interpret the temperature values in relation to the output. Figure 2.9 shows a comparison graph of resistance against temperature between various thermistors and platinum RTD.

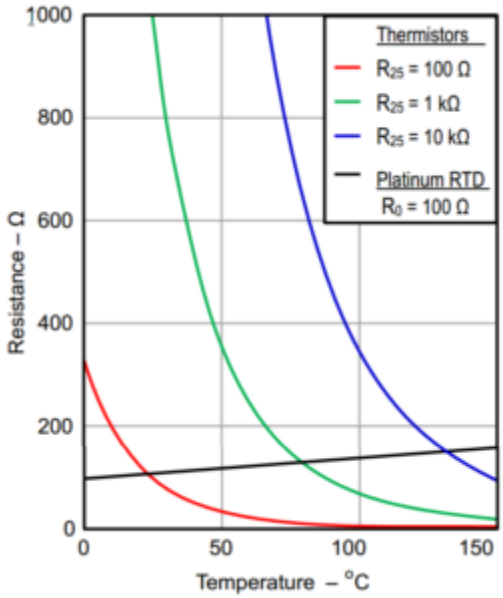

Figure 2.9 Graph of resistance against temperature for RTD and various thermistors (Source: Texas Instruments)

Lastly, integrated silicon sensors are semiconductor temperature sensors that measure and identify its temperature based on temperature-dependent relationship between the collector current of a BJT and the base-emitter voltage. It is easily integrated within semiconductor ICs therefore it is small in size. However, it has slow respond on fast temperature changes. An overview of the comparison between thermocouples, RTDs, NTC thermistors and integrated silicon sensor are as shown in Table 2.1.

Table 2.1 Comparison between NTC thermistors, thermocouples and RTDs (Heath, 2016)

Factor	**Thermocouples**	**RTDs**	**NTC thermistors**	**Integrated Silicon Sensor**
Temperature range	-270 to 1800 ˚C	-250 to 900 ˚C	-100 to 450 ˚C	-55 to 150 ˚C
Sensitivity	±0.5 ˚C	±0.01 ˚C	±0.1 ˚C	±0.15 ˚C
Linearity	Requires at least a 4th order polynomial or	Requires at least a 2nd order	Requires at least a 3rd order	At best within ±1 ˚C.

	equivalent lookup table	polynomial or equivalent lookup table	polynomial or equivalent lookup table	No linearization required
Excitation	None required	Current source	Voltage source	Typically: supply voltage
Output Type	Voltage	Resistance	Resistance	Typically: supply voltage
Typical Size	Bead diameter = 5 x wire diameter	0.25 x 0.25 in	0.1 x 0.1 in	0.88mm x 0.88mm

2.5 Extrusion Process

It is declared that the concept of producing 3D printer plastic at home can be developed using single screw extruder as shown in Figure 2.10 (“3D Printing for Beginners”, 2016). The working principles of a single screw extruder starts from a hopper. All materials are fed in from the hopper into the barrel containing a screw, which is the main part of the extruder (Wagner, Mount and Giles, 2014). On one end, the screw, or sometimes referred to as auger is connected to an electric motor which helps to transport the fed pellets towards the tip of the extruder or also known as the extruder nozzles. A heater is placed as the extruder nozzles to soften and melt the material in order to allow it to be extruded and form continuous filament strand.

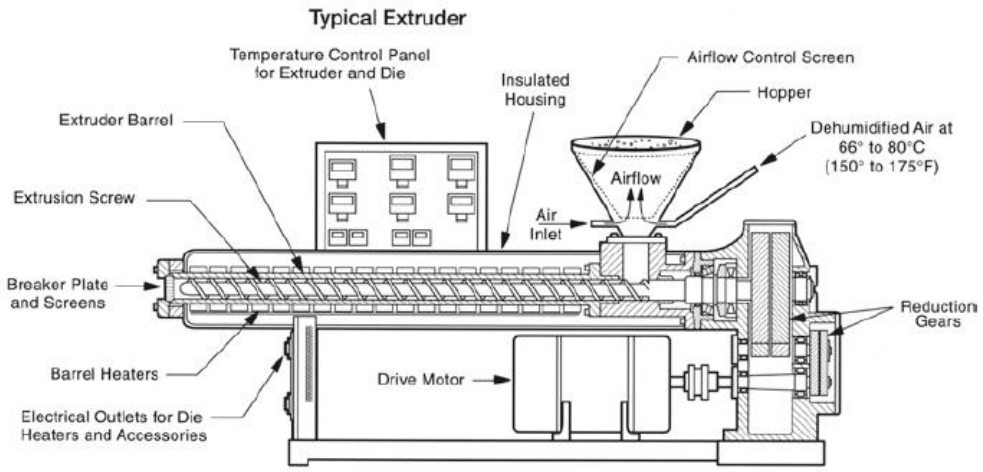

Figure 2.10 Cross-section of a Single Screw Extruder
(Rao & Schott, 2012)

The materials that is fed into the hopper are usually tiny solid pellets to speed up heating and reduce friction on the screw. A progressive increased in temperature profile with the setpoints temperature increasing continually from the hopper to the extrusion nozzle is necessary to prevents premature melting and reduces melt plug formation around the screw of bridging the throat in the hopper wall (Wagner, Mount and Giles, 2014). This can avoid polymers or additives to becoming sticky and adhering to the hopper wall.

To clearly define the temperature profile along the extruder barrel, the temperature zone is separated into four zones; the feed zone, transition zone and metering zone wall as shown in Figure 2.11 (Wagner, Mount and Giles, 2014). Resins are input through the feed zone and the root diameter along this zone is constant. The transition zone has a progressively increasing root diameter as compression is applied (Whelan and Dunning, 1988). This zone is where the solid pellets is melted into molten material. Finally, the metering zone has a uniform flight depth that transfers the melt and controls the volumetric flow rate through the extruder into the die (Whelan and Dunning, 1988).

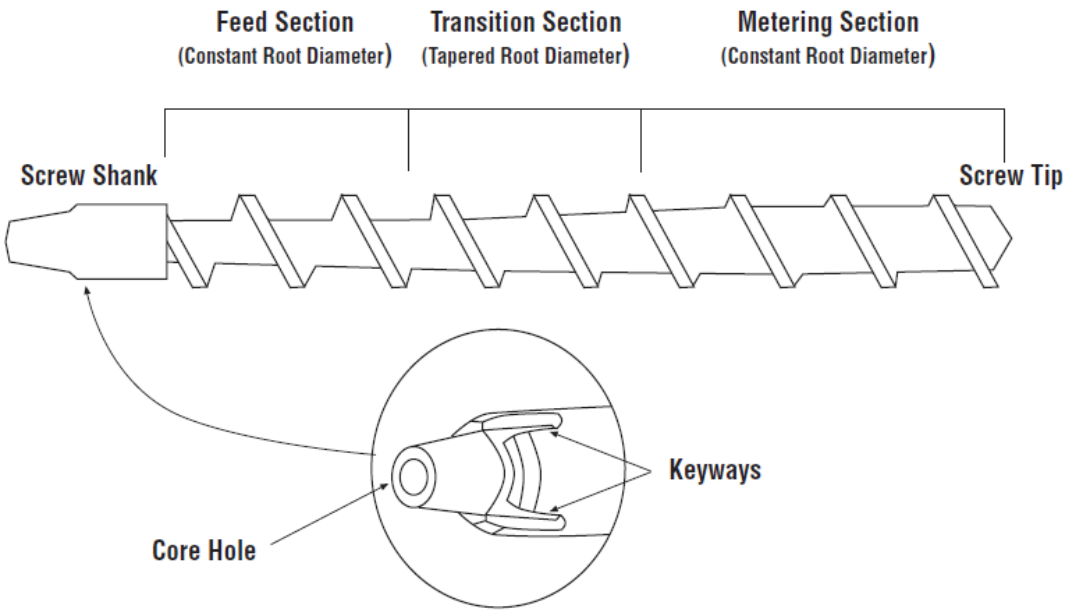

Figure 2.11 Extrusion Screw
(Whelan and Dunning, 1988)

2.6 System Controller

2.6.1 Programmable Logic Controller (PLC)

Programmable logic controller, in short, known as PLC is an industrial solid-state computer control system that has been introduced in the late 1960s by an inventor named Richard Morley (Mary R., 2011). Its ability to perform modular programming allow PLC system to mix and match and monitor the types of inputs and outputs devices and automate the process based on logical decisions. It was first designed and developed to replace relay logic systems due to the unreliability and time delay created by the relay system.

These controllers excluded the needs for rewiring and adding extra hardware devices for each new configuration of logic. With that, it drastically reduced the cabinet space that housed the logic while increasing the functionality of the controls. PLC contained of CPU, inputs and outputs logical port as shown in Figure 2.12. The CPU directs the PLC to perform control instructions, perform logic and arithmetic operations, connect with other devices and execute internal diagnostics. Apart from

that, CPU also performs memory routines, constantly inspecting the PLC to avoid programming errors and to protect the memory from being damaged.

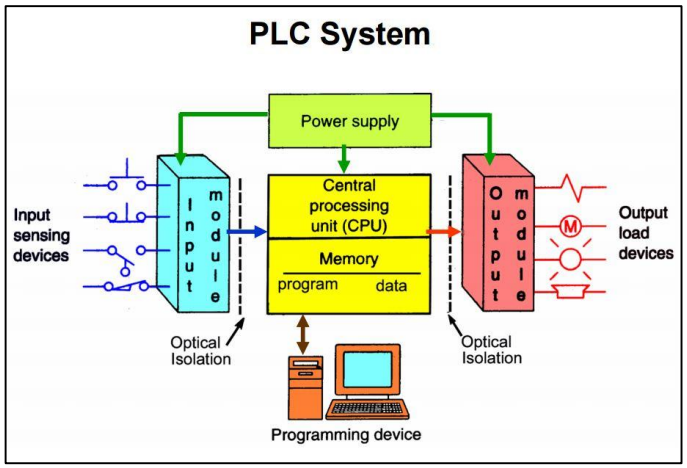

Figure 2.12 Internal Architecture of PLC

(Gonzalez, 2015)

There are four fundamental procedures in the process of all PLCs; input scan, internal program execution, output update and internal checks as shown in Figure 2.13 (Agarwal T., 2015). Input scanning operation detects the condition of all input devices that are linked to PLCs while the output update process energize or de-energize the output devices based on the CPU internal response. Most PLCs provide libraries of function blocks for complicated controls such as temperature control and motion control. Components can simply be control by setting the basic parameters needed into the function block and the output is linked to the devices required to take response. Internal program execution run the program logic created by the user. Lastly, internal checks performs housekeeping operation which helps communicate PLCs with programming terminals and execute internal diagnostics.

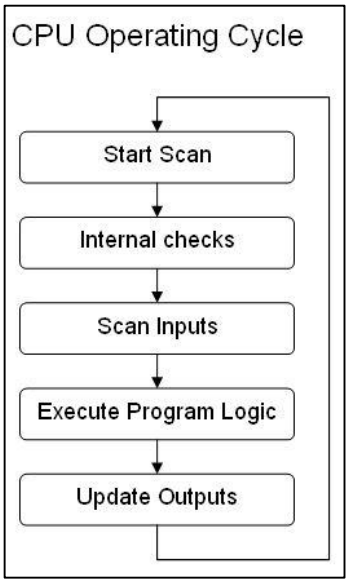

Figure 2.13 Internal Program Flow of PLCs

(Gonzalez, 2015)

PLCs uses five type of high level programming languages that are defined by the international standard IEC-61131 (Gonzalez, 2015). Its solid standardization and simple programming techniques speed up the production process of a machine maker. Ladder logic is one of the most frequently used PLC languages where it utilises the use of symbols and rungs for input and output logical control. Function block diagram is another programming languages used in PLC where it describes the functions between input and output variables. Structured text is a high-level language that resembles modern C programming language. It uses sentenced commands to create programs. Instruction list, on the other hand, is a low level language that contains functions and variables defined by a simple list (Gonzalez, 2015). Sequential function chart language is a technique of programming complex control system where it divides large and complicated programming operations into simpler and more manageable tasks.

2.6.2 Microcontroller

Microcontrollers are special purpose logic controllers that execute one operation repeatedly. They are dedicated for single task execution. Similar to a PLC, they also have CPU to execute the programs, RAM for data storage and input and output ports that are capable for microcontrollers to process user command and perform a specific

response on the output. Microcontrollers contained their programs in a flash program memory while the variables data are stored in Data RAM. The logical processing within a microcontrollers are performed by the ALU as shown in Figure 2.14. General Purpose Register stored the configuration of microcontroller input and output ports. All these units are linked together via a network bus system. From the aspects of system architecture, unlike PLC, microcontrollers are incapable of running an operating system and do not have the same amount of computing power or resources as compare to PLC. Therefore, they are not an infinitely expandable input and output logic controller.

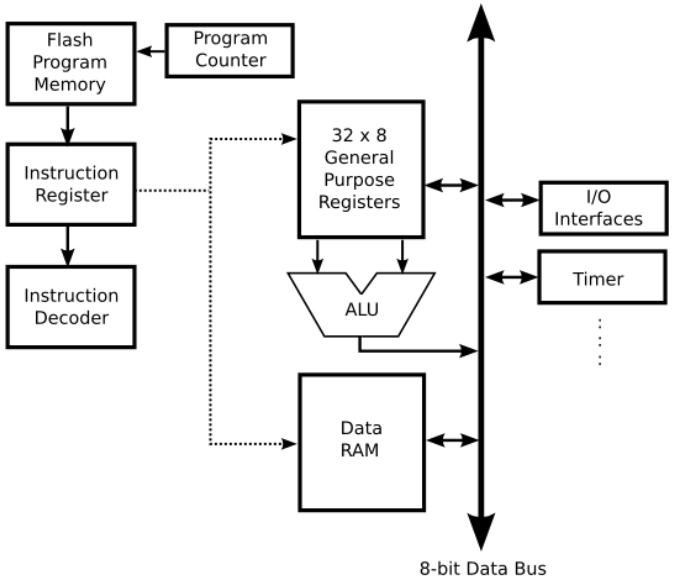

Figure 2.14 Microcontroller Architecture

(Source: ATmega32 datasheet p. 6)

The development time taken for microcontrollers is longer than PLC due to their usage of tedious machine language. More of that, microcontrollers do not offers a standard user interface platform. The interfacing features might need to be programmed manually onto an LCD or LED display.

However, microcontrollers are necessary and useful as a platform to perform simpler computing tasks such as flipping a switch or controlling small components. They are commonly used due to their low-powered consumption and low-memory which make them to be low cost.

2.7 Modular Programming

Structured programming, or sometimes known as modular programming, is a subcategory of procedural programming that implements a logical structure on the program that is being written to improve the efficiency and ease understanding and modification (Rouse M., 2005). Several programmers can easily work on individual programs at the same time and join programs in the end. This programming technique helps to easily control the scoping variables and less code has to be written as individual programs are simpler to code than combining all individual programs in a single program. Modular programming is a type of top-down design programming approach that breaks down program functions into modules (SearchSoftwareQuality, n.d.)

In this approach, most of the variables are passed from one module to another whenever the other module is called. In short, modular programming has similar behaviour with plugin where the function are added whenever it is needed. Versioning is considered to be one of the most popular approach to ensure those independent functions to work together (Chapter 2: The Benefits of Modular Programming, 2007). Basically, it means that every module will have a consistent passing variables. The modification of each module will be done only in the process being programmed in the module.

2.8 Human Machine Interface

Human Machine Interface, or also known as Graphical User Interface (GUI), is a simplified use of computers by presenting relevant information in a manner that enables rapid assimilation and manipulation (Toby, 2001). The use of graphic constructs that mimic physical objects such as “buttons” and “switches” can speed learning, by applying an intuitive technique to provide input to the computer. An implementation of user interface is not always an improvement to a system. As

demonstrated by some commonly used commercial programs, a poor user interface implementation can obscure its functionality. Significant amount of learning time is required for the program to be used efficiently if the user interface is organized in a counter-intuitive manner or if the commonly performed operations required several unexpected indirect steps to be performed (Toby, 2001). A good user interface does not require user to memorise procedures required for task execution. Multiple step operations can be simplified by executing all operations in a single step shortcuts.

In order to compile multiple steps into a single shortcuts, operations need to be compiled as a single function via back-end programming. Modularity of components has enormous benefits on assisting steps compilation when building interactive applications. Functional units can be isolated to its most simplified form to ease application designer in understanding, modifying and compiling each particular unit (Krasner and Pope, 1988). More of that, it is demonstrated that one particular form of modularity is the three separation of application components which are the model, the view and the controller as shown in Figure 2.15 (Krasner and Pope, 1988). The model represents the functional units that contained multiple steps operations while the view represents the display of the application's state. As for the controller, it signifies the user communication with the model and the view.

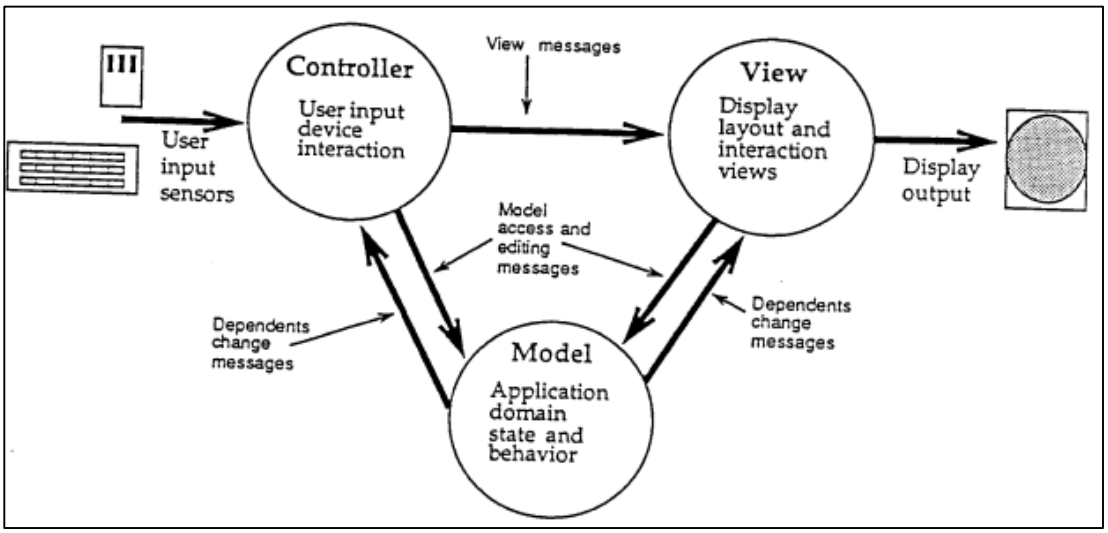

Figure 2.15 Model-View-Controller Setting and Message Sending

(Krasner and Pope, 1988)

CHAPTER 3

METHODOLOGY AND WORK PLAN

3.1 Introduction

Multi-material 3D printing holds great promises towards allowing the automated construction of 3D models with complex structures, appearances and properties to physical equivalents. It has accelerated the potential of innovation to create objects that has been previously impossible or difficult to be fabricated. There have been significant efforts from the industry as well as the academic community in building multi-material fabrication platforms.

Motion control plays an important role in producing quality 3D printed products. Accuracy of the motion control need to be calibrated to avoid producing defected objects. Other than that, 3D printer system should be made reliable for low maintenance cost during long run. Intelligent system is one of the example of reliable system where it can perform self-diagnosis and self-calibration. In order to achieve good accuracy and reliability, statistical methods are utilised for measuring the performance of the system. More of that, proper electrical connection can also yield a more reliable system. Suitable grounding techniques are relevant to reduce the noise being induced in the signal circuits. Appropriate components are selected to optimise between cost and system performance. In short, the objective for electrical wiring planning and design is to improve system stability while considering the safety measures.

From the aspects of software configuration, the first step for a 3D printing process is reading and interpreting the language used for human-machine communication. This required machine to have its knowledge to identify and understand the command. The system should made capable in performing actions based on the command interpreted. Further than that, simplified information and settings should be presented and accessible by end users. This involves interfacing the

system program with end users via user interface. Linkage is made for end users to have appropriate level of control on the system actions.

3.2 Applied Theories

3.2.1 Program Flow

There are two main operations that are executed by the system during the operation; motion control and temperature control. Temperature control input setpoint temperature value from the HMI while performing controlling feedback operation on the temperature at different zone. Motion control reads file from HMI to perform interpretations and printing actions based on the file command. The general flow of the concept for the framework will be described in Figure 3.1.

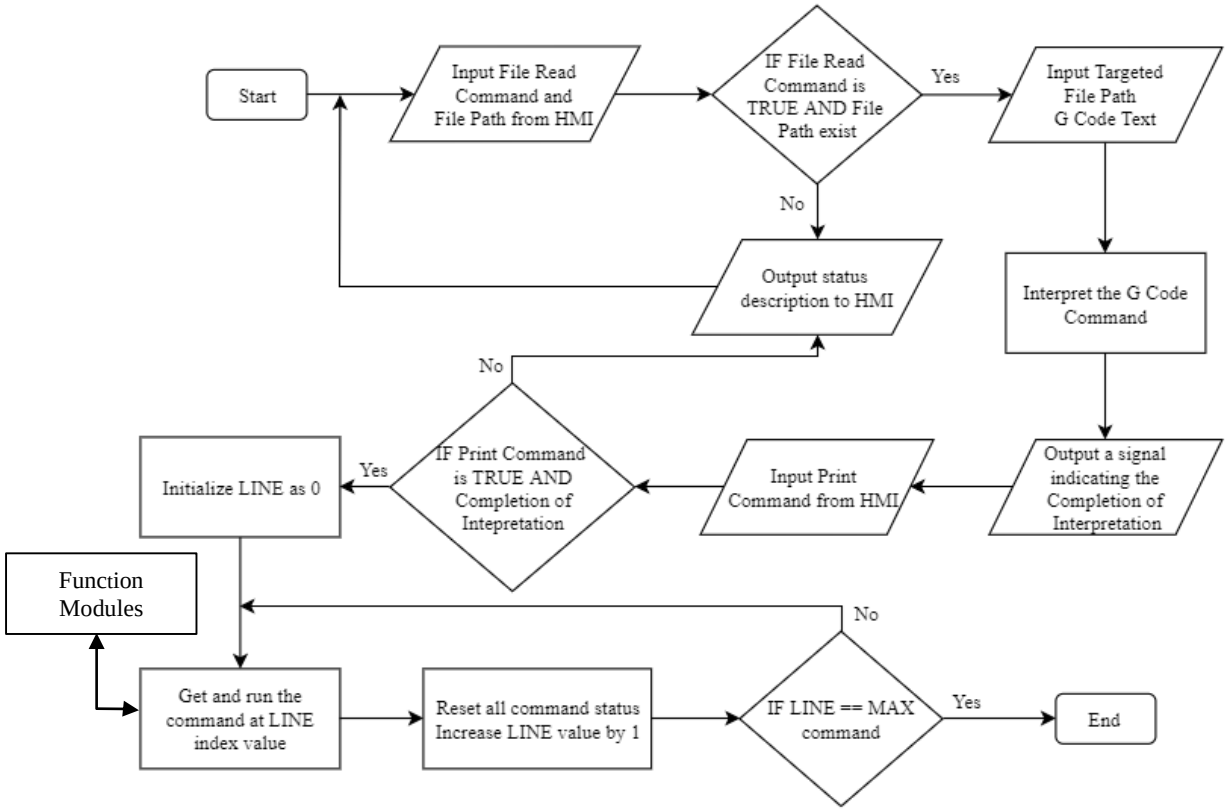

Figure 3.1 General Program Flowchart

As a further explanation of the flowchart, prior to the feeding of material, there are parameters that require close consideration. These parameters may consist of the auger or extruder feed rate, the feed rate for the material source located before the mixer and the average total flow rate of the material pellets feed into the mixer.

3.2.2 Pre-processing Technique

Based on the literature that have been reviewed previously, some of the basics languages are required in order to allow human to interact with a machine which includes the usage of G-code. Moreover, machine required to be equipped with the knowledge to understand the language ‘spoken’ by a human to them. The knowledge is induced into the machines by equipping G-code Interpreter in the machines. The objective for such implementation to allow the machine to extract the relevant information out from the commands and perform operation.

The length of commands can be varied in length. For instance, a single ‘G01’ command can have all X, Y and Z position and might also only contain the X position. Furthermore, in order to ensure robust G-code Interpreter, the position of each information in a string of command should also be considered. One method proposed is by first finding all the alphabets of relevant data that might exist in the string of command. Rearranging and identify which data is before or after another.

Lastly, extract the value of the particular alphabet by taking the middle information between the alphabet and the one after it. Each line of commands is extracted and stored in an array of structure, where the structure is the final information of all positions and extrusion rate. In order to ensure reliable and stable G-code Interpreter, several samples of G-code is used to test the interpreter as shown in Appendix A and Appendix B. An overview flowchart of the G-code Interpreter is as shown in Figure 3.2.

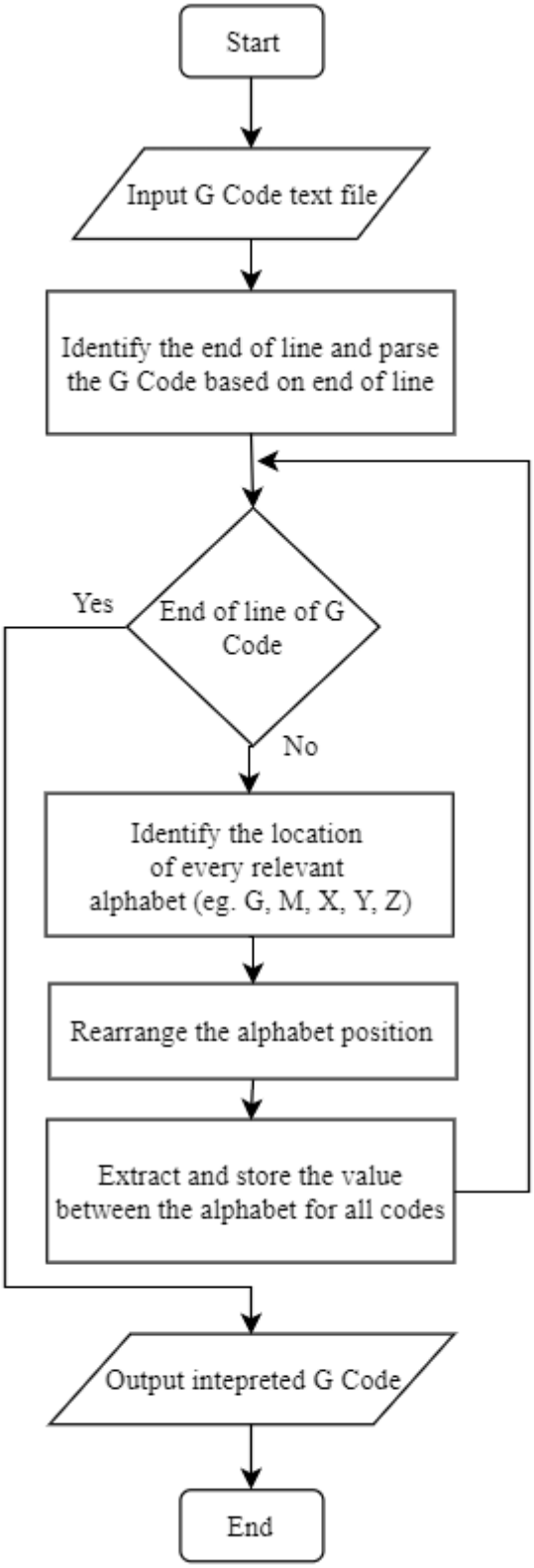

Figure 3.2 Program Flow of G-code Interpreter

3.2.3 Process Framework

The information extracted from G-code Interpreter during the pre-processing is then used for the main 3D printing process. This is also considered as the main framework for the 3D printing. The framework will starts by initializing and resetting all position value and velocity relevant for the normal function of the 3D printer.

After that, it will read the first structure of instruction from the array of G-code information. All commands are grouped into a separate function block. G command being extracted will go through each and every command and check for a match. The particular function block will be run when it found a match. All function blocks are programmed according to the modular programming approach to ease future improvements. The G-code and M-code being included in the program are shown in Table 3.1 and Table 3.2.

Table 3.1 G-code Description

G-code	Description
G0	Rapid Coordinated Movement X Y Z E
G1	Coordinated Movement X Y Z E
G10	Retract filament according to settings of M207
G11	Retract recover filament according to settings of M208
G28	Home one or more axes
G90	Use Absolute Coordinates
G91	Use Relative Coordinates
G92	Reset Current Coordinate as 0 Position

Table 3.2 M-code Description

M-code	Description
M0	Unconditional stop - Wait FOR user button press on UI
M17	Enable/Power all stepper motors
M23	Access File Information
M80	Turn on Power Supply. (Requires POWER_SUPPLY)

M81	Turn off Power Supply. (Requires POWER_SUPPLY)
M82	Set E codes absolute (default)
M83	Set E codes relative while in Absolute (G90) mode
M104	Extruder Temperature input and control not set. Set extruder target temp
M106	Fan on
M107	Fan off
M110	Set Current Line Number
M112	Emergency stop
M114	Report current position
M120	Enable endstops detection
M121	Disable endstops detection
M140	Bed Temperature input and control not set. Set bed target temp
M201	Set max acceleration in units/s^2 for print moves
M202	Set max acceleration in units/s^2 for travel moves
M203	Set maximum feedrate
M205	Set advanced settings
M206	Set additional homing offset
M207	Set Retract Length
M220	Set Feedrate Percentage

Each of the code has its individual breakdown program flow. For instance, the G-code G28 which is homing function initialize by commanding rapid motion for all 3 axes towards the direction of hardware configured home position. Each of the axis stop when it reaches the minimum limit of the system and touches the end stop limit switch. The stop command is completed by utilising the M112 emergency stop command of the M Code. The absolute position is reset when all 3 axes reaches its minimum limit. The program flow is as shown in Figure 3.3.

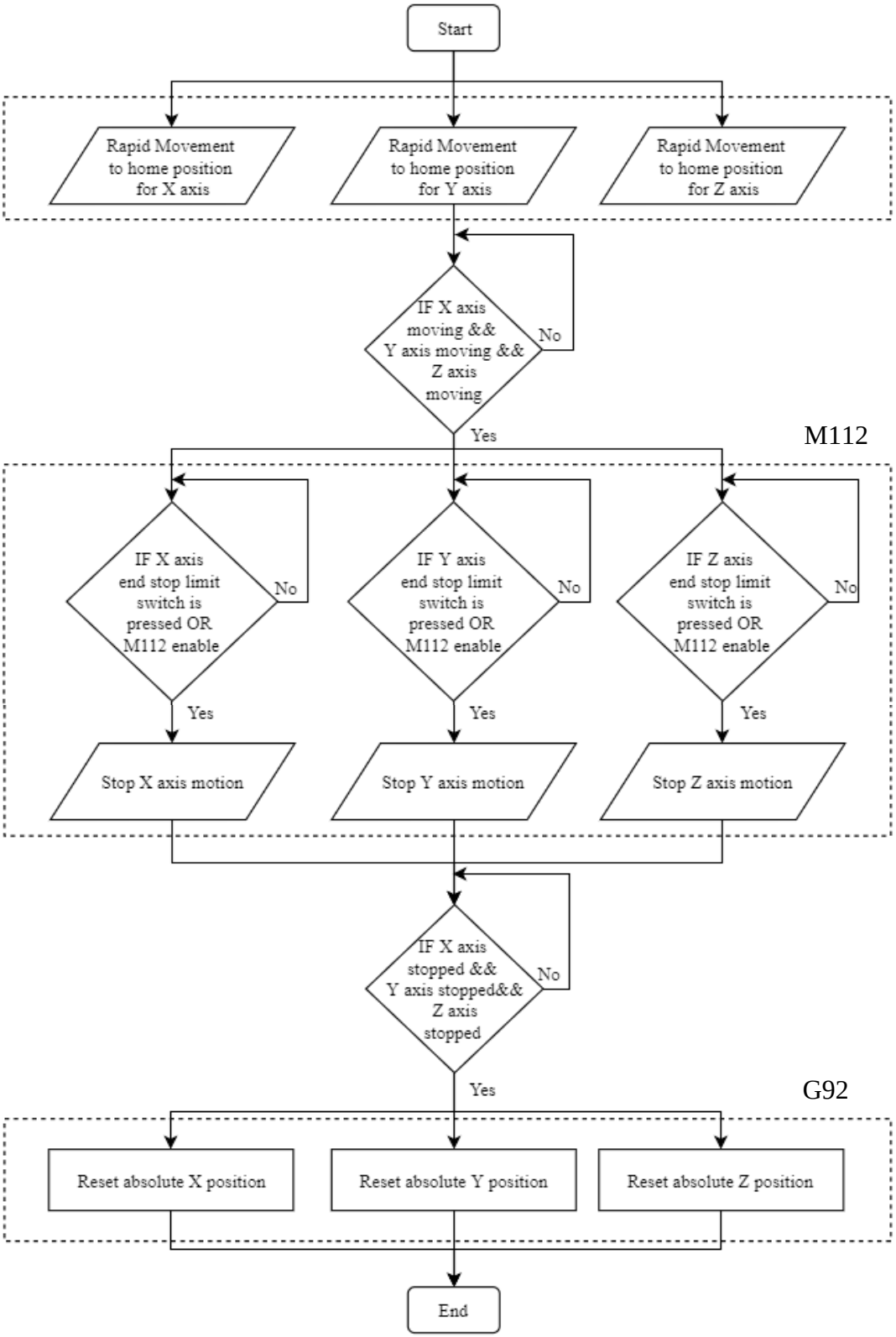

Figure 3.3 G28 Program Flow

After completing the executed function block, the next structure of instruction will be read and the loop of flow continues. All other motion correction, temperature

control and emergency stop tasks are added in the loop of the framework as separate task. Each task execution is weight by using the priority set.

Concurrently, the value such as the position of 3D printer, temperature of heat bed and extruder, percentage of printing completion and relevant information for displaying to user will be displayed on the HMI.

3.3 Hardware Configuration

3.3.1 Circuit Wiring

Planning and designing are the initial procedures to construct an electrical system. Cooling fan is mounted on the control panel to assist air ventilation within the control panel. The arrangement of the devices in the control panel is arranged based on the heat dissipation capability of the device. The larger the heat dissipated by the device, the nearer it should be placed in the control panel to improve ventilation on the device.

TB6600 motor drivers are selected for mixer stepper motor control due to the limited cost available for purchasing EL7031 Beckhoff stepper motor card. This motor driver, with its controller board mounted on a heat sink, has larger heat dissipation capability. Therefore, it is placed beside the cooling fan as shown in Figure 3.4. Power supplies are isolated from the controller to reduce the risk of short circuit. Power and ground terminals are introduced to redirect and complete all connections.

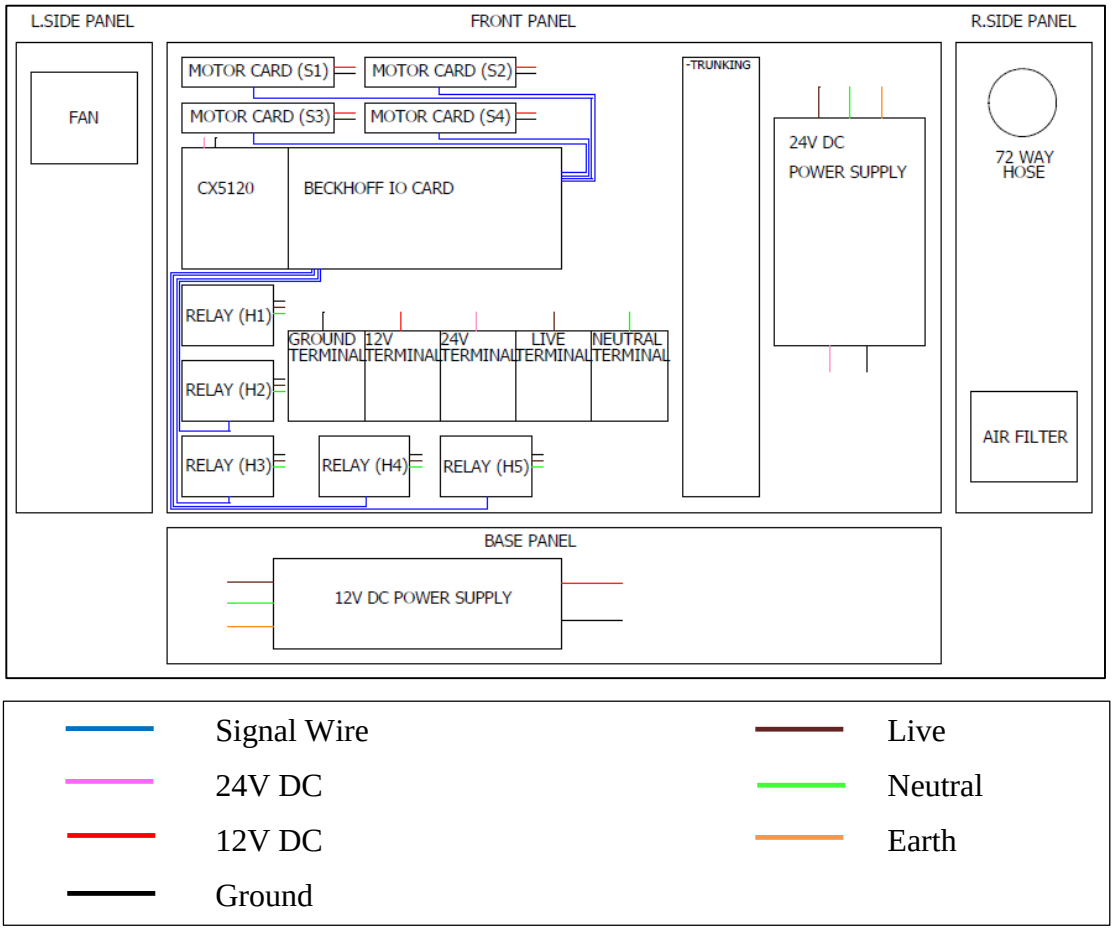

Figure 3.4 Control Panel Layout

Labelling has been tagged on each cables to ease future development. Larger cables are used for heavy duty applications such as triggering the heating of the heat cartridge through a SSR. Shielded wires are used as signalling wire to reduce the risk of e.m.f disturbance. Trunking is built to ensure proper arrangement of wires in the control panel. Capacitive and inductive coupling can happen when all wires are arranged and direct through the trunking. However, with shielded wires, the disturbance can be reduce and it can reduce the effect of noise.

Grounding is categorized into 3 categories which is the power earth, safety earth and signal earth. All 24V, 12V and 5V direct current supply are grounded to the power earth. Alternating current is grounded to safety earth. Lastly, instead of separating logic earth and analogue earth, all signals including digital and analogue signals' wires are grounded to signal earth. The electrical schematic is drawn as shown in Appendix H before connection process begin.

3.3.2 Selection of Relay

There are two relays that are recommended to be applied in controlling the response of the heat cartridge which is the SSR and EMR due to its suitability in input response. However, SSR is selected to be used instead of EMR. This is because SSR generate relatively smaller electrical disturbance as compare to EMR. More of that, SSR also required lower input power for switching loads as compare to EMR.

Switching debouncing is another factor to consider when it comes to switching devices. SSRs do not generate electric arcs or sparks and do not bounce mechanically or electrically (Wendt, 2017). As comparing to SSR, EMR has longer switch debouncing time and response time. However, SSR generates more heat as compare to EMR. This issue can be solved by mounting a cooling fan in the control panel to ventilate the heat being produced.

3.3.3 Selection of Temperature Sensor

Based on the literature reviewed, it is concluded to use thermocouples as the temperature measuring devices for all the critical points along the extruder and heat bed. This is mainly due to its good linearity capability within small range of temperature and fast response time. A minor accuracy is sacrificed when thermocouples are used but it will not affect the system as a minor tolerance on the temperature will not affect much on the quality of the plastic materials.

Furthermore, according to the literature reviewed, thermocouples can detect extremely high temperature which is up to 1800℃. The working principle of 3D printer is to melt materials for easy printing and solidify it after cooling. Therefore, for the considerations of further future applications where higher melting point materials can be used as printing materials, thermocouple is selected. Other than that, it is also easier

and more compatible by pairing thermocouple with EL3314 Beckhoff Thermocouple Card.

The 3D printer aims to print plastic materials which are usually melted below 540 ℃ and the heat bed temperature should be above room temperature to avoid deflected printed product. Therefore, type K thermocouple is used as it has better linearity among all the other type of thermocouple, good resistance against oxidation below 1000 ℃ and it is the most stable among thermocouple of inexpensive material.

3.3.4 Thermocouple Cable Extension

Thermocouple extension cables is used to extend the thermocouple from the machine to the control panel which directly linked into the EL3314 Beckhoff 4-channel thermocouple input terminal. However, in order to standardize all cables extension through a 72 ways socket crimp connectors, thermocouple wires are extended through a normal crimp connectors instead of a standard thermocouple extension connectors. Therefore, the measured value of thermocouple might experience a slight differ in temperature from the actual due to the potential drop between different materials of connectors and thermocouple.

Experiments are performed to determine the accuracy of the thermocouple. The experiments will be conducted within a range of temperature and the thermocouple measured temperature is plotted based on the temperature measured using infrared thermometer. The behaviour and performance of the thermocouple within the range can be determined via the graph. An offset calibration is recommended if the behaviour of the thermocouple shows a linear error when compare with the temperature measured by infrared thermometer. If the thermocouple shows a non-linear error behaviour, either a system response should be equate or a lookup table is to be generated and configure into the software for calibration purposes.

3.4 Control Configuration

3.4.1 Motion and Scale Factor Configuration

The stepper motor used in all axes has a specification of 1.8˚ angular displacement per pulse and it is not equipped with any encoder feedback control. It is controlled by system framework via EL7031 Beckhoff stepper card as shown in Figure 3.5.

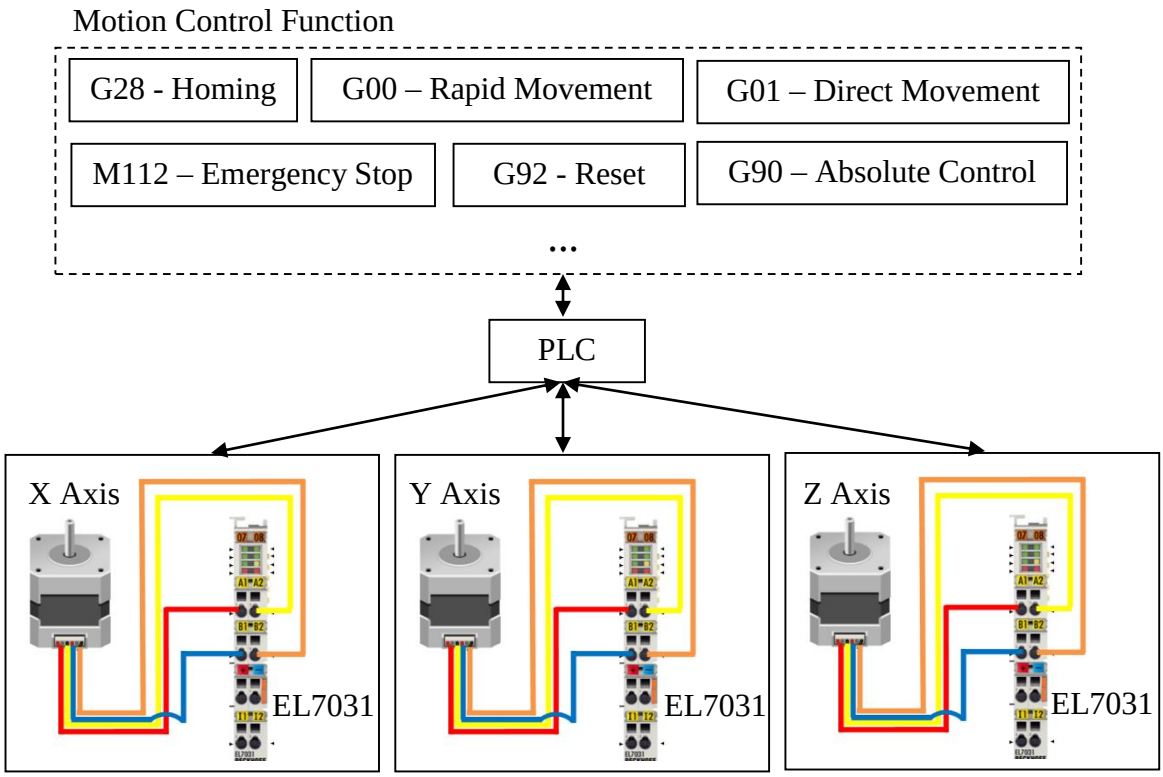

Figure 3.5 Stepper Motor Electrical Schematic

Moreover, the X, Y and Z axis stepper motor is equipped with a gear transition and a lead screw which converts rotational motion to translational motion. The gear ratio and the pitch-to-pitch distance of the lead screw is determined for accurate positioning. The distance travelled per revolution of the axis motor is determined by utilising the equation 3.1. The EL7031 Beckhoff stepper card required a software configuration of scaling factor based on the motion transition for synchronisation purpose with the stepper motor. Equation 3.2 is an equation provided by Beckhoff to determine the software scaling factor required to configure for stepper motors without

encoder feedback control. By combining equation 3.1 and 3.2, the total equivalent equation for determining the scaling factor is as shown in equation 3.3.

$$d = Gr\ x\ dpp \tag{3.1}$$

$$SF = \frac{d_{rev}}{full\ steps\ x\ microsteps} \tag{3.2}$$

$$SF = \frac{Gr\ x\ dpp}{full\ steps\ x\ microsteps} \tag{3.3}$$

The number of teeth for pinion and gear is identified to be 12 and 30 respectively while the pitch-to-pitch distance is measured to be 5mm using vernier calliper as shown in Figure 3.6. Microsteps is fixed by Beckhoff with a value of 64 microsteps. Lastly, the stepper motor of X axis has a 1.8 ° step angle per pulse. Therefore, the stepper motor required 200 pulses in order for it to rotate a complete revolution. Utilising the information collected, the software scaling factor of X axis is determined to be 1.5625 x 10^{-4} as shown below using equation 3.3. Other than that, the scaling factor is also the maximum precision that can be achieved by the stepper system.

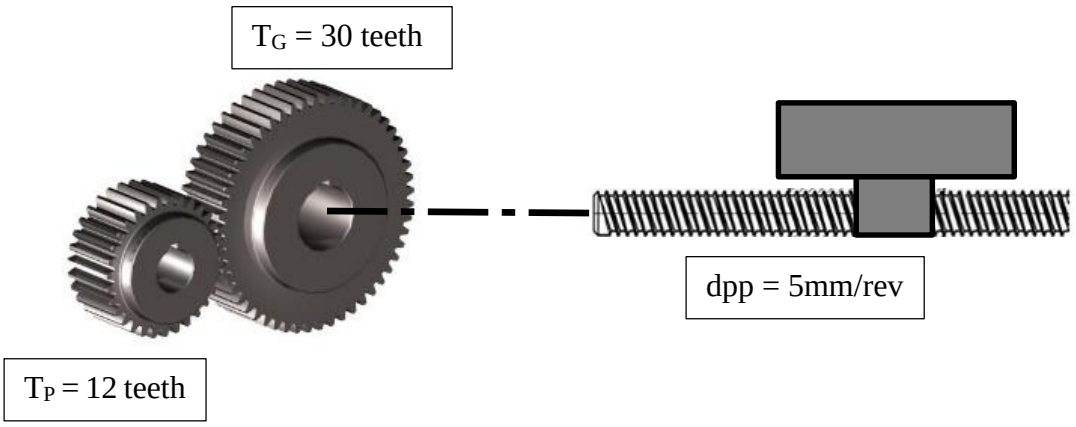

Figure 3.6 Power Transmission Schematic of Axis Motion

$$SF = \frac{Gr * dpp}{full\ steps\ x\ microsteps}$$

Tp	= 12 teeth	*full steps*	= 200 steps/rev
T_G	= 30 teeth	*microsteps*	= 64 microsteps
dpp	= 5mm/rev		

$$SF = \frac{\frac{T_P}{T_G} * dpp}{full\ steps\ x\ microsteps}$$

$$SF = \frac{\frac{12\ teeth}{30\ teeth} * 5mm}{200\frac{steps}{rev}\ x\ 64\ microsteps}$$

$$SF = 1.5625\ x\ 10^{-4}\ mm/steps$$

The maximum angular velocity that can be achieved by the stepper motors is determined by using the equation 3.4 according to the documentation stated in the commissioning techniques of Beckhoff EL7031 stepper motor card. The base frequency is configured to 8000 fullsteps/s while the motor frequency, depending on the stepper motor used, is 200 fullsteps/rev. By using the parameters identified, the maximum velocity is calculated as shown below.

$$\omega_{maxpinion} = \frac{f_{base}}{f_{motor}} \tag{3.4}$$

$$v_{maxgear} = \frac{\omega_{maxpinion}}{Gr\ x\ dpp} \tag{3.5}$$

However, the maximum configurable angular velocity calculated is the maximum angular velocity of the stepper motor. Gear ratio is also required to be taken into account for this situation. Therefore, the actual allowable maximum velocity is calculated using equation 3.5 as below.

$$v_{maxgear} = \frac{\frac{8000}{200}}{\frac{12}{30}x5}$$

$$v_{maxgear} = 20\ mm/s$$

The distance travelled per revolution for the stepper motors at feeder and mixer are also calculated using equation 3.1. The accuracy and reliability of the stepper

motors using the calculated scaling factor is determined by using mean root square error and correlation method respectively. The accuracy can be determined from the equation 3.4. The lower the root mean square error, the better the accuracy. As for the reliability measurement, it is determined via correlation formula as shown in equation 3.5. Similar to correlation, the higher the correlation value, the higher the reliability of the system.

$$RMSE = \sqrt{\frac{1}{n}\sum_{i=1}^{n}(y_i - \hat{y}_i)^2} \tag{3.6}$$

$$r = \frac{n\sum_{i=1}^{n} xy - \sum_{i=1}^{n} x \sum_{i=1}^{n} y}{\sqrt{[n\sum_{i=1}^{n} x^2 - (\sum_{i=1}^{n} x)^2][n\sum_{i=1}^{n} y^2 - (\sum_{i=1}^{n} y)^2]}} \tag{3.7}$$

3.4.2 Thermocouple Configuration

The main materials that will be used in this project will be thermoplastics. In order for it to be melted, fused and extruded successfully, the temperature along the extruder should be controlled. There are total three thermocouples and two heaters along the barrel for extrusion and one thermocouple and heater is placed at the tip of the extruder which is the nozzle to keep the temperature in control. The temperature will be increasing along the barrel up until the extruder nozzle. The extruder nozzle temperature will be at or slightly above the maximum glass transition temperature of both fused thermoplastic.

Furthermore, temperature being measured by the thermocouple will also be experimented to ensure accurate reading. The performance of the thermocouple will also be determined by comparing the data with the measured data using thermistor from the existing 3D printer. The thermocouple is mounted into the heater plate of the extruder nozzle. Accuracy and reliability is identified through the similar equation used for motion control which is equation 3.4 and 3.5.

Graph of the temperature behaviour will be plotted to determine the relationship between the actual and measured value. Offset calibration will be performed based on the behaviour of the plotted graph to ensure the temperature can be measured accurately within the temperature range. The feedback control system of the heat cartridge is controlled by thermocouples feeding data into a software PID temperature controller function block preconfigured in the TwinCAT3 libraries.

3.5 Human Machine Interface (HMI)

The final part for the 3D printer is on the HMI. This will be a user friendly interface that is built to ease non-technical personnel to key in relevant information for the printer to print an object. The interface will have a direct link to the variables of the program during the execution phase. Commands that are needed to be added into the interface will be such as the text reading, commence printing, emergency stop and some basic resets, homing control and temperature control. An overview of the HMI is shown in Figure 3.7.

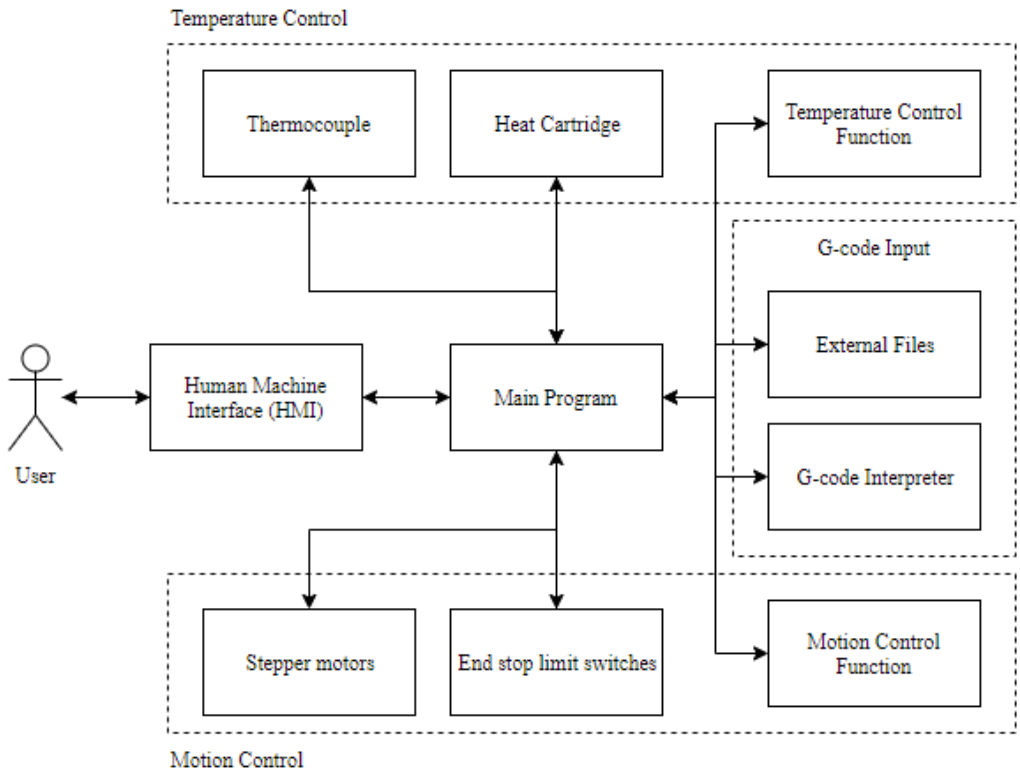

Figure 3.7 Overview Architecture of HMI

File reading operation is interfaced with HMI to obtained direct command from the user. It awaits for a trigger from the File Read button and input the file path from the HMI. The operation check for file existence before commencing reading operation. Error description will be displayed on the HMI if the file cannot be found and it will wait for another triggering of file read operation. The program flow of the file reading task interfacing via HMI is shown in Figure 3.8.

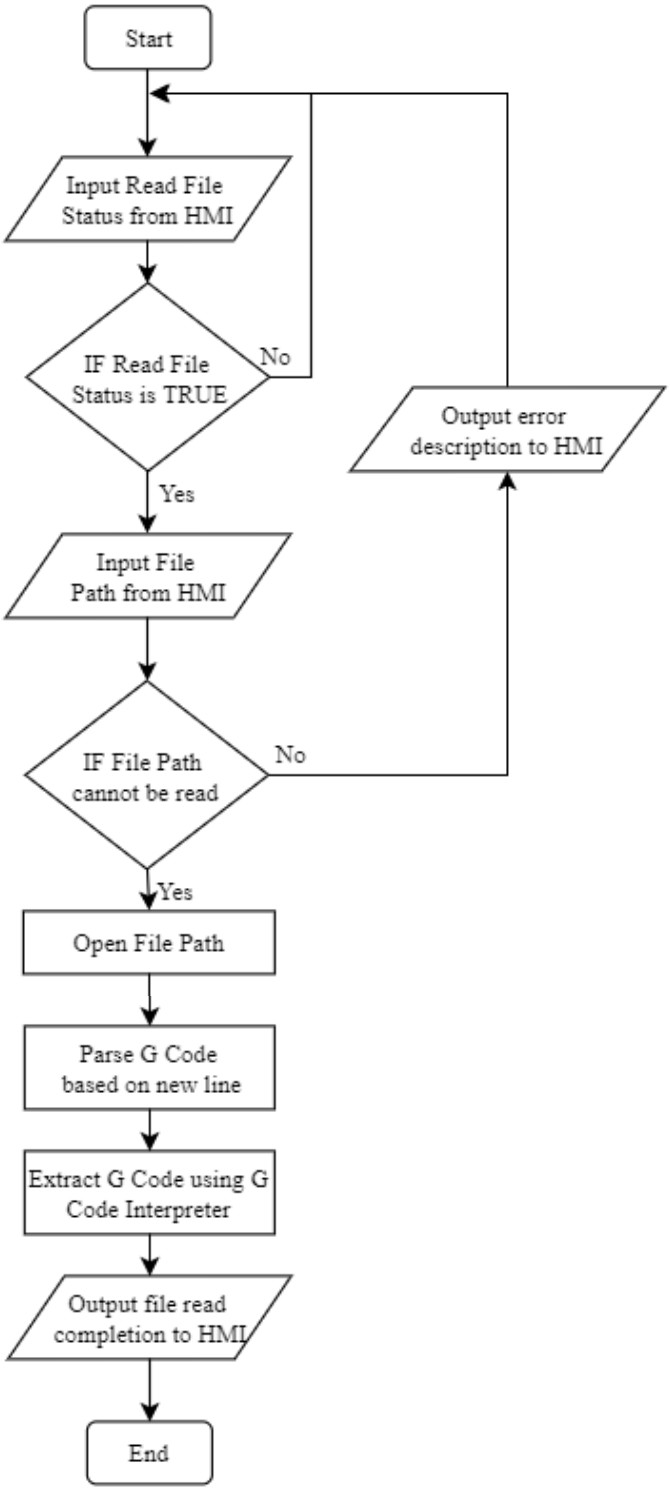

Figure 3.8 Program Flow of File Reading Operation Interfaced with HMI

The HMI should display the actual temperature measured by the thermocouple and the setpoint temperature configured by the user. Temperature is controlled by background temperature controller function interfacing with HMI. The temperature controller compare setpoint temperature obtained from HMI with the actual

temperature measured by thermocouple and uses PID to control the heat cartridge response accordingly. For instance, if setpoint temperature is higher than actual temperature, the temperature controller will trigger the heat cartridge to heat up to the respective temperature. A logical flow of temperature controlling via HMI is shown in Figure 3.9.

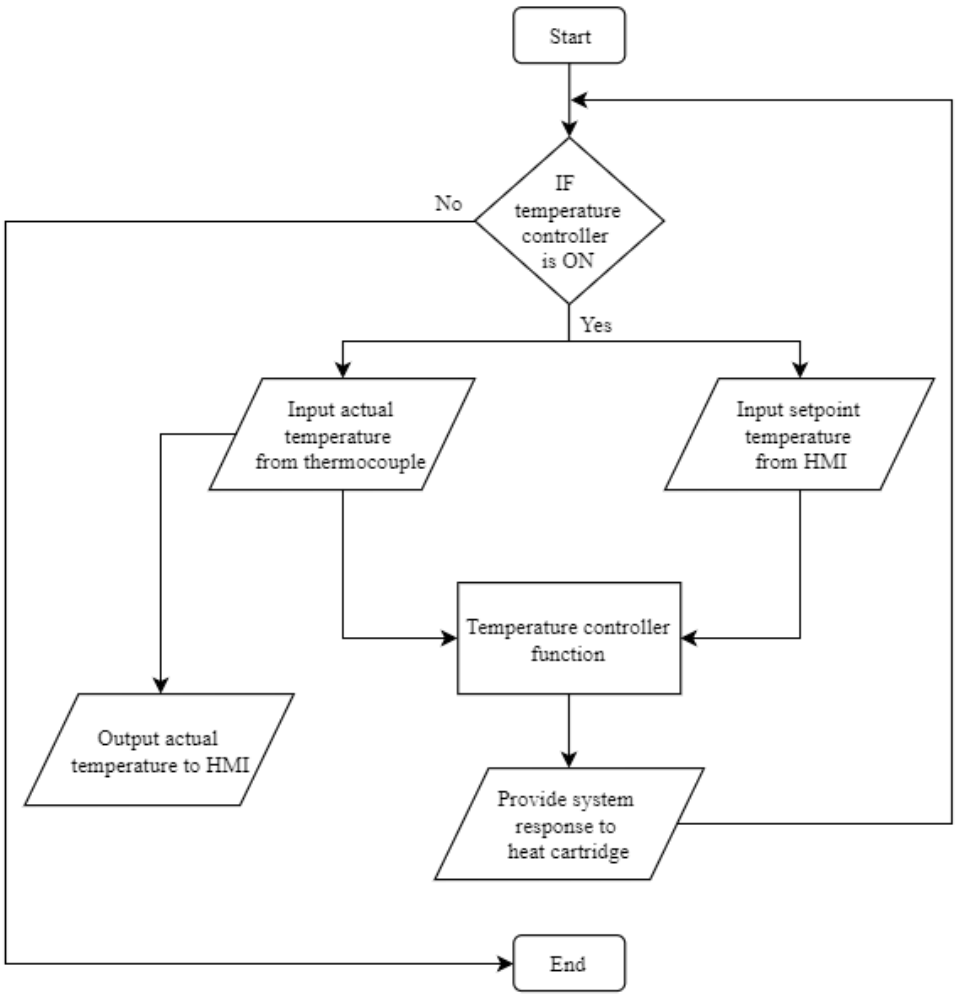

Figure 3.9 Program Flow of Temperature Control Interfaced with HMI

CHAPTER 4

RESULTS AND DISCUSSIONS

4.1 Introduction

The first step for a 3D printing process is receiving and interpreting the language used for human-machine communication. This required machine to have its knowledge to identify and understand the command. After interpreting the command, 3D printer should have its ability to perform operation automatically and pause or stop the process when the process might harm the surrounding. The reliability of the interpreter is determined by measuring the flexibility and repeatability of the interpreter in reading and extracting the correct information from random orientated G-code.

Experiments are conducted on determining the accuracy and reliability of the motion and temperature response. The accuracy and reliability of the system is derived by applying root mean square error and correlation formulas on the experimental results. Graphs are plotted to determine the behaviour of the response. The optimization of the system is achieved by using the nominal value for the best accuracy.

HMI is inspired by the conventional 3D printer display. Clean and simple layout design is considered for good user experience. Fundamentals information especially on the filament extruder including temperature for all heater zone and heat bed and cooling fans are added into the HMI. Certain level of flexibility is allowed for users to configure product for printing, temperature of the materials and calibration.

4.2 G-code Interpreter

This subsection will provide a little recap on the experiment carried out during the first part of this project and also some of the improvements made. The early experiment instilled thoughts and critical thinking in enhancing the interpreter framework to

ensure stability and reliability. The following content will summarise the details of the experiment, results and the improvements made to obtain a better interpreter.

G-code Interpreter commenced by reading all the G-code from a declared text file and storing it in a buffer. The raw data from the text file is not relevant in the future process of 3D printing. Therefore, a temporary buffer with limited size is used to read the text file. When the buffer is filled, G-code Interpreter will parse the raw data and stored in into lines of code by identifying the next line command being read. After that, it will check for end of file state from the text file being read and repeat if it is not the end of file. The code will proceed to the extraction of information from every line of G-code for the next step.

In extraction of information, the first attempt of coding the G-code Interpreter was to hardcode the order of all alphabetical code in the order of G, X, Y and Z from left to right in a line of code. The value of each code is obtain by finding the value between its code and the next alphabetical code. For instance, the value of G is obtained by finding the value between G position and X position. However, in some situations there are more alphabetical code such as I, J, F, M, and R. And it is often difficult to identify which alphabetical code comes after another in a line of code. Using the mentioned technique can cause incorrect or invalid extraction of information.

The interpreter is improvised to be fully soft-coded in order to solve the issue. This proposed initialize by finding all location of possible alphabetical code. Using program to interpret which alphabetical code comes after another, the value of each code can be extracted by finding the value between the respective alphabetical code and its next nearest alphabetical code. All the relevant information being extracted is then stored into a structure of code that is later used for printing process. In short, this proposed techniques read, extract and store all G-code information before commencing the printing process. Different from 3D printing Marlin firmware, which it performs printing and reading process concurrently. After completion, a Boolean logic of 1 will be output from the G-code Interpreter to indicate interpretation complete.

The results of the G-code Interpreter using the sample G-code shown in Appendix A is shown in Table 4.1. More of that, the result of the testing for G-code Interpreter on the G-code shown in Appendix B is shown in Table 4.2. All commented lines of G-code is filtered at the first stage of G-code Interpreter which is the reading from text file stage.

Table 4.1 "testpieces1.txt" extracted G-code at 11th & 12th command

Expression		Value
GCodeData[11]	X	G1
	Y	0
	Z	0
	I	0.5
	J	0
	E	0
	F	0
	Ss	0
	T	0
	N	0
GCodeData[12]	X	G1
	Y	100
	Z	0
	I	0
	J	0
	E	8
	F	1000
	Ss	0
	T	0
	N	0

Table 4.2 “testpieces2.txt” extracted G-code at 11th & 12th command

Array of Structure Variable Name	Variables in Structure	Interpreted Value
GCodeData[11]	X	G1
	Y	0
	Z	0
	I	0
	J	0
	E	-1
	F	300
	Ss	0
	T	0
	N	0
GCodeData[12]	X	G0
	Y	-20
	Z	-20
	I	0.5
	J	0
	E	-1
	F	9000
	Ss	0
	T	0
	N	0

From the results of the 2nd attempted G-code Interpreter, it is shown that all the G-code from the sampled code is extracted correctly in stored in correct location. All extracted data of the G-code is stored within an array of structure known as the “GCodeStructure”. The size of the array is set up to 20,000 during the testing to ensure all lines of G-code in the sample can be stored.

4.3 G-code Functions

The 3D printing operation is a customised printing operation where it contains different mixing ratio over the time for printing. The G-code generated should also include a parameter for configuring the mixing ratio. To perform that, the standard CNC control available in TwinCAT3 cannot be used as it cannot process mixing ratio parameter. Therefore, NC operation which required manual programming of G-codes and M-codes is used.

For simplification purposes, G-code and M-code included are only the fundamentals codes required to complete basic printing process. All codes are programmed based on modular programming approach. The code function takes in enable bit from the main program to trigger the code execution and sends a completion bit back to the main program when the process is completed. The progress of the code completion is shown in Table 4.1. The completed code functions are used for testing the performance of motion control. Code functions that are still under progress are related to temperature controlling. Experiments are yet to be completed for temperature control, therefore, it is not stable for actual use.

Table 4.3 Progress of Code Completion

G0		**M0**		**M85**		**M114**		**M206**	
G1		**M1**		**M92**		**M115**		**M207**	
G10		**M17**		**M104**		**M117**		**M208**	
G11		**M18**		**M105**		**M119**		**M209**	
G28		**M48**		**M106**		**M120**		**M218**	
G29		**M80**		**M107**		**M121**		**M220**	
G30		**M81**		**M109**		**M140**		**M221**	
G90		**M82**		**M110**		**M145**		**M226**	
G91		**M83**		**M111**		**M190**		**M540**	
G92		**M84**		**M112**		**M205**		**M600**	

	In progress
	Completed
	Tested
	Probe Function
	Report Function

4.4 Hardware Configuration

The testing of the operation for motion and temperature control required implementation on hardware structure. The connections and position of all hardware are configured before testing is performed on the machine as shown in Figure 4.1.

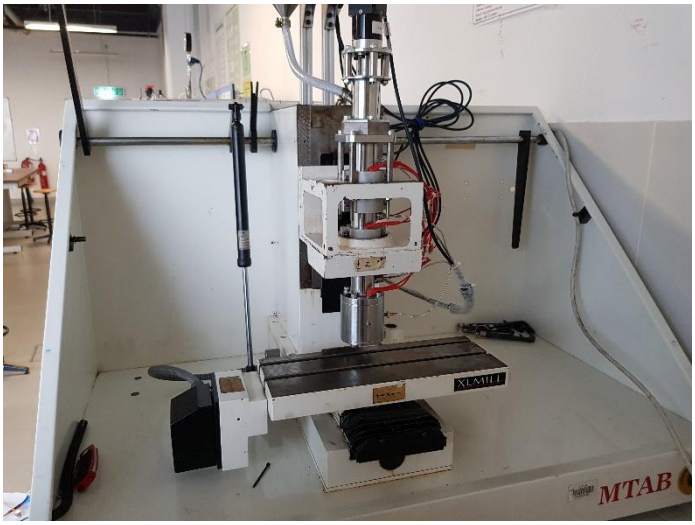

Figure 4.1 Hardware Structure of 3D Printer

The mechanical end-stop switch is mounted on the end of each axis to perform homing operation and to avoid machine from exceeding minimum or maximum allowable travel limit for machine safety purposes. End-stop switch is mounted only at one end of each axis for homing configuration and minimum allowable travel limit. The maximum allowable travel limit is set via software configuration of limit switch. An overall schematic of the end-stop is shown in Figure 4.2.

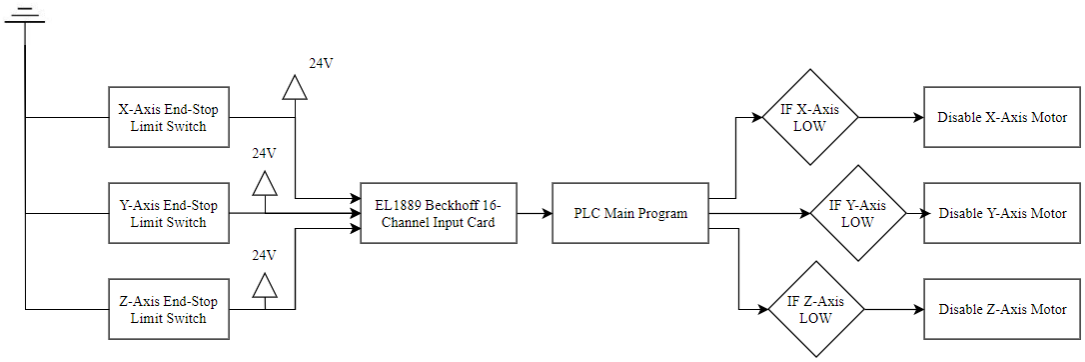

Figure 4.2 Schematic Flow of End-Stop Limit Switch

The temperature control also required heating the heat cartridges and obtaining feedback temperature value from thermocouples. Heat cartridges is triggered by SSR and controlled by temperature control function of Beckhoff libraries using setpoint temperature obtained from HMI and actual temperature fed from thermocouples. The schematic flow of the temperature control is shown in Figure 4.3.

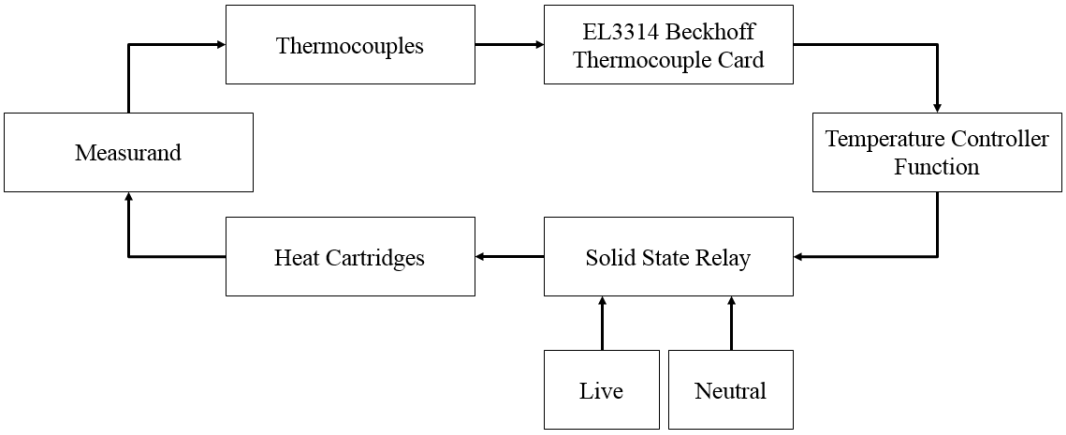

Figure 4.3 Schematic Flow of Temperature Control

4.5 Electrical Wiring

The electronic components wiring from the machine are connected to the 72 ways socket female connector on the back of the machine accordingly. Similarly, another set of wires are connected from the 72 ways socket male connector into the control panel to complete the wiring connections. Cooling fans within the control panel which is driven by AC supply is directly connected to the main AC power supply to constantly ventilate the control panel. Testing is done and is concluded that the electrical wiring for the device is completed.

There are total three stepper motors that are mainly driven by stepper motor driver. And the control of stepper motor required a 5V pulse. Therefore, voltage regulators are applied to step down digital voltage output from Beckhoff digital output card. 5V pulse is successfully sent into the motor driver. An overview of the circuit connection in the control panel is as shown in Figure 4.4.

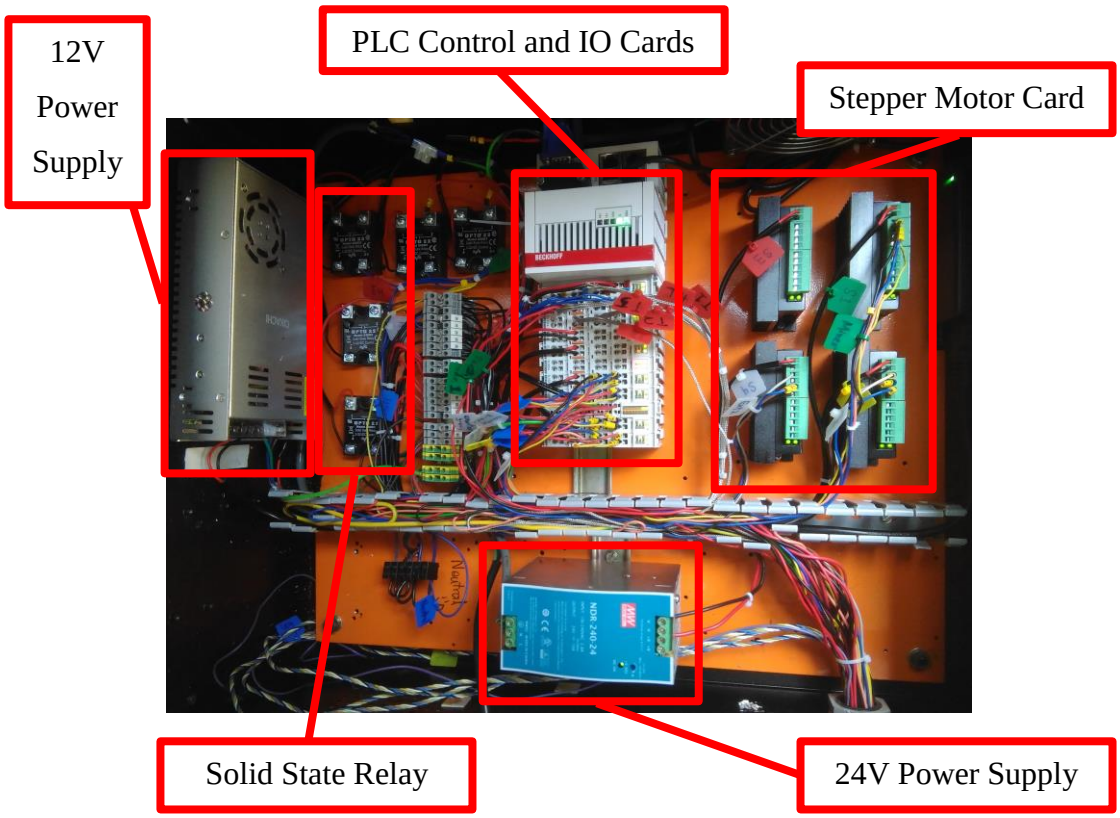

Figure 4.4 Circuit Connection of Control Panel

4.6 Human Machine Interface (HMI)

The HMI of the 3D Printer is shown in Figure 4.5. It is separated into 3 sets which is the overall system status, control and configuration and selection box. Overall system status is shown in the left side of the HMI. It gives an overview of temperature in all points of the extruder and heat bed. The control and configuration box is positioned in the middle, allowing user to have manual control and simple configuration of the system. User can commands any of the axes to jog or perform auto homing via user interface. Furthermore, temperature for all points in the system is also configured via the control and configuration box. Lastly, the selection box consists of categories of control and configuration. User can configured system temperature by selecting the “Settings” in the selection box. Other than that, manual interrupt such as pause and emergency stop which is used for safety and flexibility purpose can also be controlled via selection box.

Figure 4.5 Human Machine Interface with ABS Temperature Configuration

4.7 Motion Control

Experiments are conducted to identify the accuracy and reliability of the scale factor configured and the stepper motor performance as shown in Appendix F. The root mean square error and correlation of the translated motion is calculated using excel sheet based on the experimental data. The root mean square and correlation is 0 and 1 respectively. There are no tolerance between the actual and programmed. By referring to Graph 1, it is shown that the programmed travelled distance has a perfect linear relationship with actual travelled distance. Similar position is experimented repeatedly to ensure reliable performance. In conclude, the motion of the system is measured to be accurate and reliable.

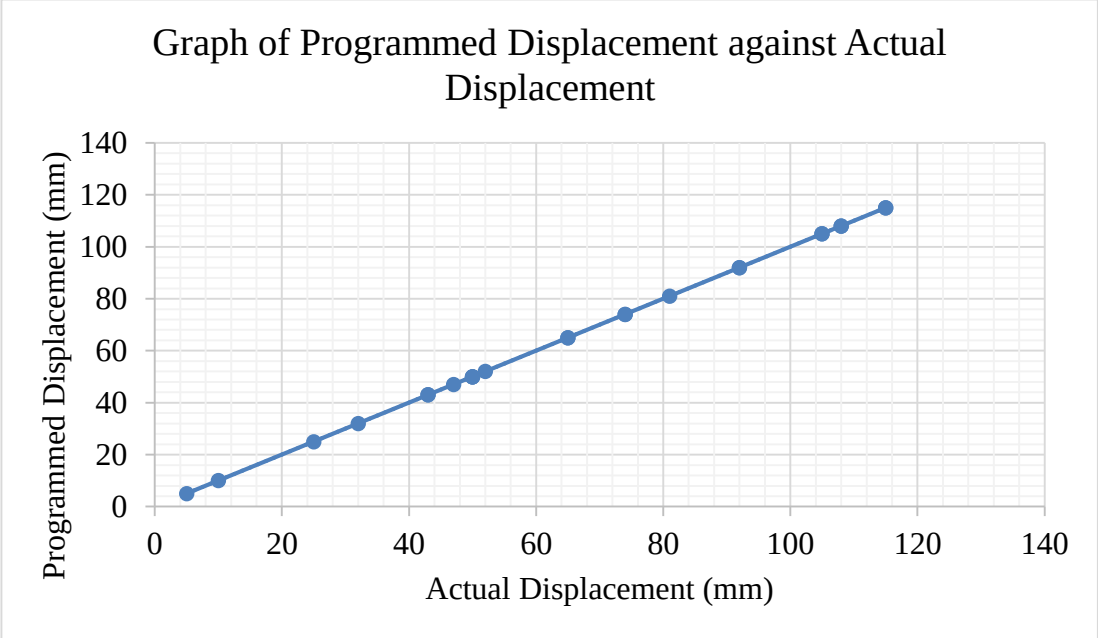

Graph 1 Graph of Programmed Displacement against Actual Displacement

Furthermore, calibration has been made and the printing volume is identified to be 210 x 158 x 76mm. However, the printing volume is scale down to 200mm x 150mm x 76mm to avoid the hardware structure from over run that can cause damage.

4.8 Temperature Control

Temperature is directly measured using thermocouple connected into Beckhoff EL3314 thermocouple card. The experimental data collected is as shown in Appendix G.

It is identified from Appendix G that a tolerance of maximum ±0.3 ℃ exist between the thermocouple measured temperature and the thermistor measured temperature at standard room temperature which is 26.6 ℃. This might be due to the different material used between the connector for the extension of thermocouple or the inaccurate temperature measured by thermistor thermometer. The root mean square error and the correlation is calculated to be 1.2229 and 0.9874 using excel sheet.

According to the Graph 2 and the correlational value, it is shown that the temperature measured by thermocouple shows a near to linear relationship with respect

to temperature measured by thermistor. However, the accuracy of the temperature measured is low when the temperature increases. In other words, the higher the temperature the lower the accuracy. By referring to the graph, it can be clearly identified that the relationship between the parameters are not perfectly directly proportional. Therefore, a second order polynomial equation is generated via excel to input into the system for calibration as shown in Graph 2.

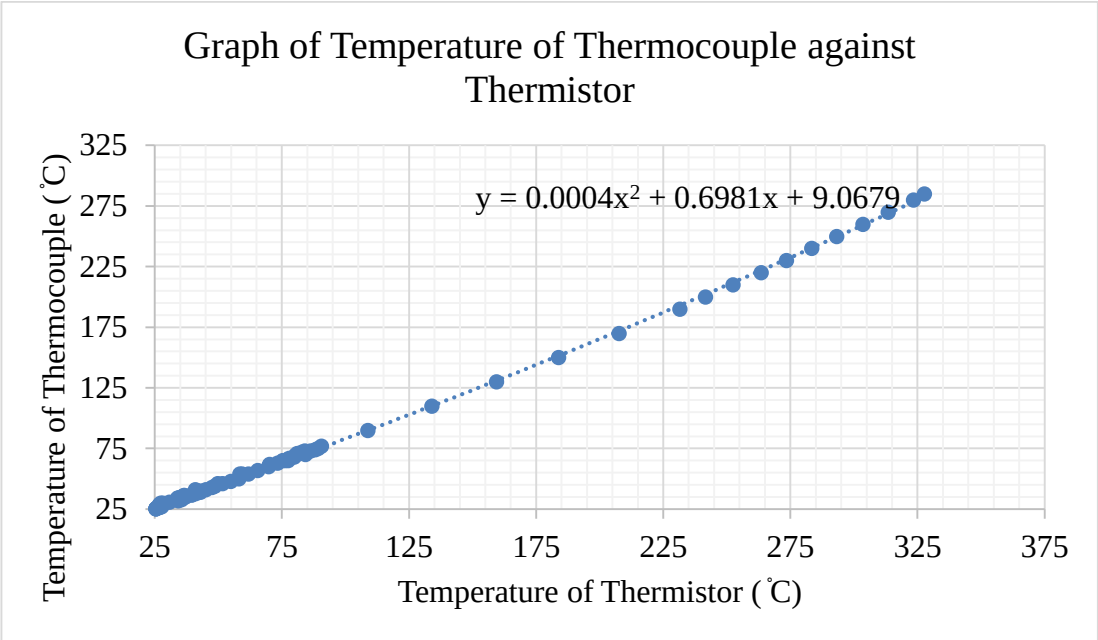

Graph 2 Graph of Temperature of Thermocouple against Infrared Thermometer

The percentage error for temperature at 200 ℃ with a thermocouple measured temperature of 241.6 ℃ is shown as below.

$T_{thermocouple}$ = 241.6 ℃

$T_{measured}$ = 200.0 ℃

$$Percentage\ error, e_{actual} = \frac{T_{thermocouple} - T_{measured}}{T_{measured}}\ x\ 100\%$$

$$Percentage\ error, e_{actual} = \frac{241.6 - 200}{241.6}\ x\ 100\%$$

$$Percentage\ error, e_{actual} = 20.8\%$$

By using the calibrated equation generated, the percentage error using the stated equation can be identified. The percentage error is reduced by 20.3% from the actual thermocouple measurement. In conclusion, the accuracy can be improved by using the polynomial equation generated. However, further calibration need to be performed to refined the accuracy of the thermocouple system response.

$$T_{calibrated} = 0.0004(T_{thermocouple})^2 + 0.6981\left(T_{thermocouple}\right) + 9.0679$$

$$T_{calibrated} = 0.0004(241.6)^2 + 0.6981(241.6) + 9.0679$$

$$T_{calibrated} = 201.0℃$$

$$Percentage\ error, e_{calibrated} = \frac{T_{calibrated} - T_{measured}}{T_{measured}}\ x\ 100\%$$

$$Percentage\ error, e_{calibrated} = \frac{201.0 - 200.0}{200.0}\ x\ 100\%$$

$$Percentage\ error, e_{calibrated} = 0.5\%$$

CHAPTER 5

CONCLUSIONS AND RECOMMENDATIONS

5.1 Conclusions

Based on the results obtained with the assessment of the performance of the framework and reliability of the system, the main aim of developing a PC based 3D printer is fulfilled. The minimum objective which is to develop a framework for the 3D printing process is accomplished through the development of G-code Interpreter techniques which provides flexibility in reading codes with inconsistent arrangement of position and the motion control of the printer.

The reliability and accuracy of the motion positioning system of the printer is guaranteed via configuration of scale factor. Experiments were conducted to prove the accuracy and reliability of the motion positioning system. The accuracy is very high as the root mean square error calculated using the data obtained is 0. The reliability of the system is very high as the programmed distance travelled has perfect linear relationship with the measured distance travelled.

The behaviour of the thermocouple is experimented on a heating block and compared with the value measured from a thermistor. The temperature measured by thermistor is taken as actual value in this experiments. It is shown that the error of the thermocouple is close to a linear error as the error increased as the temperature increased. Therefore, a polynomial equation is generated to compensate and calibrate the temperature measured by the thermocouple. The percentage error of the calibrated value as compared to the actual temperature is low after calibration. In short, the accuracy is enhanced after calibration. Reliability is high as it shows a correlational value of 0.9874.

The other objectives are also initiated and in progress throughout the period of development. Tasks are taken to paves way for future development. The practice of printer development in different areas which includes the arrangement of wires,

labelling of wires, modular programming, variables declaration, version control and mechanical assembly techniques are standardized.

The hardware configuration of the system is completed with the end-stop switch mounted at each axis and gear ratio is considered during gear ratio calculation. However, further modifications are required to be done for heat bed with critical considerations on the allowable travel space for Z axis. Bulky design of heat bed can scale down the allowable printing volume of the machine. Mounting of fans for feedback and cooling control of the extruder should also be reconsidered to ensure that the heat will not be transmitted up to the stepper motor as it can easily damage the stepper motor. Electrical wiring is completed and tested with direct AC power supply connected the system. All wires are safely grounded and connected with minimal exposure of conductive area.

In addition, from the aspects of programming, G-code is successfully read from external files with the file type of txt. G-codes are interpreted and stored into the system command correctly for printing process. There are two main categories of processing to be focused after G-code interpretation; the motion operations of the G-code. Motion control is programmed and completed by including all fundamentals and relevant G and M Codes required for 3D printing process. However, temperature control is yet to be completed as the parameters for PID temperature controlling required to be tested and fine-tuned.

The fundamental structure of HMI is accomplished with close consideration on user experience, ease of configuration and simple presentation. HMI is designed to have minimal complexity by categorizing all selection and using diagrams representation. Due to the issue in temperature control, HMI can also yet to be fully completed as the temperature is not completely configured.

5.2 Recommendations for future work

Future development can be done by ***fine tuning the PID temperature control function*** of the system. The temperature system response is required to be configured to optimise the temperature control system. Overshoot can be implemented to speed up the heating process. However, the overshoot percentage should not be too high to avoid time taken required for the temperature to reach stable condition.

More of that, more improvements can also be done on the HMI by ***adding more features to the HMI***. Due to time limitations and many literatures are required to review and development work are required, HMI is only completed up to the minimal requirements of controlling the motion. In the current state, the buttons for most of the features are created for future progress but not all features are fully programmed and equipped.

Finally, ***increasing printing volume*** is also another issue to be considered for further improvements. The current design of the extruder barrel is large and bulky limiting the motion range of the Z axis. The maximum printable height of the current design is only limited to 150mm. By shrinking down the size of the extrusion barrel, a larger printing limit can be achieved. However, close considerations need to be done on the temperature control as the plastic pellets materials required gradual temperature increase to avoid the material quality from degrading. Small extrusion barrel are not capable to achieve a change of 80 ℃ while ensuring a gradual increase in temperature with such a short distance.

REFERENCES

SearchSoftwareQuality. (n.d.). *What is structured programming (modular programming)? - Definition from WhatIs.com*. [online] Available at: http://searchsoftwarequality.techtarget.com/definition/structured-programming-modular-programming [Accessed 1 Apr. 2018].
Chapter 2: The Benefits of Modular Programming. (2007). Sun Microsystems, pp.1-4.

Rao, N. and Schott, N. (2012). *Understanding Plastic Engineering Calculations: Hands-on Examples and Case Studies*. Cincinnati: Hanser Publishers, pp.2-4.

Dan (2016). *How to build an 2-axis Arduino CNC Gcode Interpreter*. [online] Available at: https://www.marginallyclever.com/2013/08/how-to-build-an-2-axis-arduino-cnc-gcode-interpreter/ [Accessed 1 Apr. 2018].

Reprap.org. (2017). *Motor control loop - RepRapWiki*. [online] Available at: http://reprap.org/wiki/Motor_control_loop [Accessed 1 Apr. 2018].

Brei, T. (2008). *RTD vs Thermocouple - What's the difference?*. [online] Sure Controls. Available at: http://www.surecontrols.com/rtd-vs-thermocouple/ [Accessed 1 Apr. 2018].

Heath, J. (2016). *Temperature Sensors: thermocouple vs. RTD vs. thermistor vs. semiconductor IC*. [online] Analog IC Tips. Available at: http://www.analogictips.com/temperature-sensors-thermocouple-vs-rtd-vs-thermistor-vs-semiconductor-ic/ [Accessed 1 Apr. 2018].

Reprap.org. (2012). *Prusa i3 - RepRapWiki*. [online] Available at: http://reprap.org/wiki/Prusa_i3 [Accessed 13 Apr. 2018].

Ametherm. (2017). *Temperature Sensors. Thermistors vs Thermocouples*. [online] Available at: https://www.ametherm.com/blog/thermistors/temperature-sensors-thermistors-vs-thermocouples [Accessed 1 Apr. 2018].

Chen, K. (2015). *Choice of Wiring System & Types of Cables Used In Internal Wiring*. [online] Linkedin. Available at: https://www.linkedin.com/pulse/choice-wiring-system-types-cables-used-internal-kevin-chen [Accessed 1 Apr. 2018].

Kain, A., Mueller, C. and Reinecke, H. (2009). High aspect ratio- and 3D- printing of freestanding sophisticated structures. *Procedia Chemistry*, 1(1), pp.750-753.

Argawal, T. (2015). *Different Types of Relays used in Protection System and their Workings*. [online] ElProCus - Electronic Projects for Engineering Students. Available at: https://www.elprocus.com/different-types-of-relays-used-in-protection-system-and-their-workings/ [Accessed 1 Apr. 2018].

Wendt, Z. (2017). *Solid State vs. Electromechanical Relays*. [online] Available at: https://www.arrow.com/en/research-and-events/articles/crydom-solid-state-relays-vs-electromechanical-relays [Accessed 1 Apr. 2018].

Sidambe, A. (2014). Biocompatibility of Advanced Manufactured Titanium Implants—A Review. *Materials*, 7(12), pp.8168-8188.

Jefferies, K. (2014). *Info Zone*. [online] Au.rs-online.com. Available at: https://au.rs-online.com/web/generalDisplay.html?id=infozone&file=automation/good-practice-in-extending-thermocouple-cable [Accessed 1 Apr. 2018].

Texas Instruments (2007). *Removing Ground Noise in Data Transmission Systems*. SLLA268. [online] Texas Instruments, pp.1-7. Available at: http://www.ti.com/lit/an/slla268/slla268.pdf [Accessed 1 Apr. 2018].

Gregorec, J. (2018). *Preventing Electrical Shocks With Proper Grounding Techniques | IAEI Magazine*. [online] Available at: https://iaeimagazine.org/magazine/2005/05/16/preventing-electrical-shocks-with-proper-grounding-techniques/ [Accessed 1 Apr. 2018].

Jose, J. (2014). Design, Development and Analysis of FDM based Portable Rapid Prototyping Machine. *International Journal of Latest Trends in Engineering and Technology (IJLTET)*, [online] 4(4), pp.1-5. Available at: https://www.ijltet.org/wp-content/uploads/2014/11/1.pdf [Accessed 1 Apr. 2018].

Thiele, T. (2018). *Why Is Electrical Grounding So Important?*. [online] The Spruce. Available at: https://www.thespruce.com/what-is-grounding-1152859 [Accessed 1 Apr. 2018].

Krasner G. E. and Pope S. T. (1988). A Description of the Model-View-Controller User Interface Paradigm in the Smalltalk-80 System. *Byte, The Small Systems Journal, Special Smalltalk-80 Issue*, [online] pp.2-3. Available at: https://www.researchgate.net/profile/Stephen_Pope/publication/248825145_A_cookbook_for_using_the_model_-_view_controller_user_interface_paradigm_in_Smalltalk_-_80/links/5436c5f30cf2643ab9888926/A-cookbook-for-using-the-model-view-controller-user-interface-paradigm-in-Smalltalk-80.pdf [Accessed 1 Apr. 2018].

Argawal, T. (2015). *Understanding a Programmable Logic Controller (PLC)*. [online] Available at: https://www.elprocus.com/understanding-a-programming-logic-controller/ [Accessed 1 Apr. 2018].

Toby, B. (2001). EXPGUI, a graphical user interface forGSAS. *Journal of Applied Crystallography*, [online] 34(2), pp.210-213. Available at: https://ncnr.nist.gov/xtal/software/EXPGUI_reprint.pdf [Accessed 1 Apr. 2018].

Mary, R. (2011). *What is PLC? - PLC (Programmable Logic Controller) Tutorial*. [online] Available at: https://www.engineersgarage.com/articles/plc-programmable-logic-controller [Accessed 1 Apr. 2018].

Weller, C., Kleer, R. and Piller, F. (2015). Economic implications of 3D printing: Market structure models in light of additive manufacturing revisited. *International*

Journal of Production Economics, [online] 164, pp.43-56. Available at: https://www.researchgate.net/profile/Frank_Piller/publication/276898572_Economic_Implications_of_3D_Printing_Market_Structure_Models_Revisited/links/562a41f608aef25a243ff3f6/Economic-Implications-of-3D-Printing-Market-Structure-Models-Revisited.pdf [Accessed 1 Apr. 2018].

Gonzalez, C. (2015). *Engineering Essentials: What Is a Programmable Logic Controller?*. [online] Machine Design. Available at: http://www.machinedesign.com/engineering-essentials/engineering-essentials-what-programmable-logic-controller [Accessed 1 Apr. 2018].

Whelan, A. and Dunning, D. (1988). *The Dynisco extrusion processors handbook*. [London]: [Dynisco].

Negi, S., Dhiman, S. and Kumar Sharma, R. (2014). Basics and applications of rapid prototyping medical models. *Rapid Prototyping Journal*, [online] 20(3), pp.256-267. Available at: https://www.researchgate.net/profile/Sushant_Negi2/publication/262574639_Basics_and_applications_of_rapid_prototyping_medical_models/links/568cac2408ae153299b66f3d.pdf [Accessed 1 Apr. 2018].

Kaplan, A., & Haenlein, M. (2006). Toward a Parsimonious Definition of Traditional and Electronic Mass Customization. *Journal Of Product Innovation Management*, 23(2), 168-182. http://dx.doi.org/10.1111/j.1540-5885.2006.00190.x

Types of 3D printers or 3D printing technologies overview | 3D Printing from scratch. (2018). 3D Printing from scratch. Retrieved 1 April 2018, from http://3dprintingfromscratch.com/common/types-of-3d-printers-or-3d-printing-technologies-overview

Sitthi-Amorn, P., Ramos, J., Wangy, Y., Kwan, J., Lan, J., Wang, W. and Matusik, W. (2015). MultiFab. *ACM Transactions on Graphics*, 34(4), pp.129:1-129:11.

Holmström, J., Partanen, J., Tuomi, J. and Walter, M. (2010). Rapid manufacturing in the spare parts supply chain. *Journal of Manufacturing Technology Management*, 21(6), pp.687-697.

Ngo, D. (2015). *Formlabs Form 2 3D Printer review: An excellent 3D printer for a hefty price*. [online] CNET. Available at: https://www.cnet.com/products/formlabs-form-2-3d-printer/review/#! [Accessed 11 Apr. 2018].

Wagner, J., Mount, E. and Giles, H. (2014). *Extrusion*. Oxford [u.a.]: Andrew, Elsevier.

Kokkinis, D., Schaffner, M. and Studart, A. (2015). Multimaterial magnetically assisted 3D printing of composite materials. *Nature Communications*, [online] 6(1). Available at: https://www.nature.com/articles/ncomms9643.pdf [Accessed 1 Apr. 2018].

Automation.com. (n.d.). *Multi-Axis Synchronization in Motion Control*. [online] Available at: https://www.automation.com/library/articles-white-papers/motion-control/multi-axis-synchronization [Accessed 1 Apr. 2018].

Kim, N., Ryu, M., Hoo, S., Saksena, M., Choi, C. and Shin, H. (1996). Visual Assessment of a Real-Time System Design: A Case Study on a CNC Controller. *IEEE Real-Time Systems Symposium*. [online] Available at: https://www.researchgate.net/profile/Manas_Saksena/publication/3677999_Visual_Assessment_of_a_Real-Time_System_Design_A_Case_Study_on_a_CNC_Controller/links/00b49519f97e50a4d7000000/Visual-Assessment-of-a-Real-Time-System-Design-A-Case-Study-on-a-CNC-Controller.pdf [Accessed 1 Apr. 2018].

Shin, S., Suh, S. and Stroud, I. (2007). Reincarnation of G-code based part programs into STEP-NC for turning applications. *Computer-Aided Design*, [online] 39(1), pp.1-16. Available at: http://www.alvarestech.com/temp/ana/Reincarnation%20of%20G-code%20based%20part%20programs%20into%20STEP-NC%20for.pdf [Accessed 1 Apr. 2018].

CNC Machining Handbook. (2010). McGraw-Hill, pp.1-10.

Denford G and M Programming for CNC Milling Machines. (n.d.). West Yorkshire: Denford Limited, pp.30-33.

APPENDICES

APPENDIX A : “testpieces1.txt” G-code sample

```
;   thinWallAllowedOverlapPercentage,30
;   singleExtrusionMinLength,1
;   singleExtrusionMinPrintingWidthPercentage,50
;   singleExtrusionMaxPrintingWidthPercentage,200
;   singleExtrusionEndpointExtension,0.2
;   horizontalSizeCompensation,0 G90
M83
G28 ;z
G1 X50 Y0 Z10 F3000 ; move to wait position off table
M106 S0 ;fan speed
M190 R60 T0;stabalize heat bed temperature
M109 R235 T0;stabalize extruder temperature
M300 S1000 P400 ; Beep
M300 S1500 P400 ; Beep
G92 E0                ;zero the extruded length again
G1 Z0.5 ; position nozzle
G1 X100 Y0 E8 F1000; slow wipe
G92 E0
;Put printing message on LCD screen
M117 Printing...
G1 Z0.270 F1800
; process Process1
; layer 1, Z = 0.270
T0
; tool H0.300 W0.528
; skirt
G1 X76.713 Y120.897 F4000
G1 X77.683 Y120.495 E0.0212 F1440
G1 X97.694 Y120.495 E0.4036
G1 X98.126 Y120.567 E0.0088
G1 X98.572 Y120.721 E0.0095
G1 X98.957 Y120.930 E0.0088
G1 X100.218 Y121.913 E0.0323
```

APPENDIX B : “testpieces2.txt” G-code sample

```
G28 ; home all axes
G29
M109 S[first_layer_temperature]
G92 E0
G1 F200 E4
G92 E0
G1 X100 Y100 F-4000;and End Gcode:
M104 S0 ;extruder heater off
M140 S0 ;heated bed heater off (if you have it)
G91 ;relative positioning
G1 E-1 F300 ;retract the filament a bit before lifting the nozzle, to release some of the pressure
G0 Z+0.5 E-1 X-20 Y-20 F9000 ;move Z up a bit and retract filament even more
G28 X0
G90 ;move X/Y to min endstops, so the head is out of the way
G0 Y180
M84 ;steppers off
G90 ;absolute positioning
```

APPENDIX C: Part 1 Gantt Chart

No.	Project Activities	W1	W2	W3	W4	W5	W6	W7	W8	W9	W10	W11	W12	W13	W14
M1	Research on methods proposed by other parties in 3D Printing and controller used.														
M2	Research on techniques to interpret and perform G-code function for Beckhoff PLC.														
M3	Assemble mechanical structure for mixer and extruder.														
M4	Perform wiring connection for stepper motor, thermocouple and switches with Beckhoff IO Card.														
M5	Study on the programming techniques of required sensors and actuators and Beckhoff PLC programming.														

APPENDIX D : Part 2 Gantt Chart

No.	Project Activities	W1	W2	W3	W4	W5	W6	W7	W8	W9	W10	W11	W12	W13	W14
M1	Fine tuning the extruder structural support and position														
M2	Planning, designing and drawing electrical schematic														
M3	Rewiring all circuit connections into 72 ways socket connector														
M4	Rearranging and labelling all electrical wiring in the control panel and machine														
M5	Testing and fine tuning G-code Interpreter														
M6	Brainstorming 3D Printer firmware architecture														
M7	Planning and designing User Interface														
M8	Testing all G-code and M Code functions														

APPENDIX E : Z Axis Spacer Design

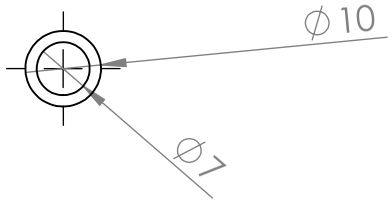

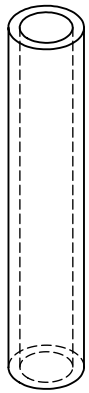

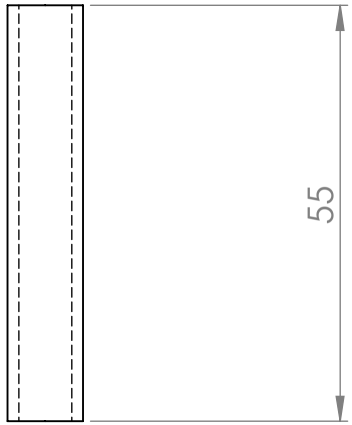

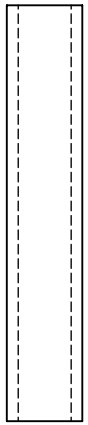

UNLESS OTHERWISE SPECIFIED: DIMENSIONS ARE IN MILLIMETERS SURFACE FINISH: TOLERANCES: LINEAR: ANGULAR:		FINISH:			DEBURR AND BREAK SHARP EDGES	DO NOT SCALE DRAWING	REVISION
	NAME	SIGNATURE	DATE			TITLE:	
DRAWN	Vincent Hoong		06/09/17				
CHK'D							
APPV'D							
MFG							
Q.A				MATERIAL: Mild Steel		DWG NO. Z Axis Spacer1	A4
				WEIGHT:		SCALE:1:1	SHEET 1 OF 1

APPENDIX F : Experimental data of the translated motion with 1.5625×10^{-4} scale factor

Programmed travelled distance (mm)	Actual travelled distance (mm)	Difference between programmed and actual distance (mm)
5.00	5.00	0
10.00	10.00	0
25.00	25.00	0
32.00	32.00	0
43.00	43.00	0
43.00	43.00	0
47.00	47.00	0
50.00	50.00	0
50.00	50.00	0
50.00	50.00	0
52.00	52.00	0
65.00	65.00	0
65.00	65.00	0
74.00	74.00	0
74.00	74.00	0
81.00	81.00	0
92.00	92.00	0
92.00	92.00	0
105.00	105.00	0
105.00	105.00	0
108.00	108.00	0
108.00	108.00	0
115.00	115.00	0
115.00	115.00	0
120.00	120.00	0

APPENDIX G : Experimental and Actual Data of the Temperature Measured

Temperature measured with thermocouple (°C)	Temperature measured with infrared thermometer (°C)	Difference between temperature measured by thermocouple and infrared thermometer (°C)
26.5	26.8	0.3
26.5	26.8	0.3
26.5	26.8	0.3
27.0	26.8	0.2
26.5	26.3	0.2
26.5	26.3	0.2
25.6	25.5	0.1
25.5	25.5	0.0
25.3	25.5	0.2
25.4	25.5	0.1
35.0	35.3	0.3
34.3	34.5	0.2
36.4	36.5	0.1
36.4	36.5	0.1
34.2	34.0	0.2
34.0	34.0	0.0
33.8	34.0	0.2
30.8	30.8	0
27.8	27	0.8
42.8	40	2.8
40.9	41	0.1
58.1	50	8.1
84.3	70	14.3
108.8	90	18.8
134	110	24
159.4	130	29.4

183.8	150	33.8
207.6	170	37.6
231.5	190	41.5
241.6	200	41.6
252.4	210	42.4
263.5	220	43.5
273.5	230	43.5
283.4	240	43.4
293.2	250	43.2
303.6	260	43.6
313.5	270	43.5
323.5	280	43.5
327.7	285	42.7
90.6	77	13.6
89.3	75	14.3
88.1	74	14.1
86.3	73	13.3
84	73	11
82.8	72	10.8
81	71	10
80.1	69	11.1
79.9	68	11.9
77.9	67	10.9
77.1	66	11.1
75.3	65	10.3
73.3	63	10.3
70.2	62	8.2
69.8	60	9.8
65.5	57	8.5
61.9	54	7.9
54.9	48	6.9
51.6	46	5.6

47.5	43	4.5
45.1	41	4.1
43	39	4
39.8	37	2.8
37.1	35	2.1
35.6	33	2.6
34.3	32	2.3
34.2	32	2.2
28.1	30	1.9
27.4	30	2.6
26.9	29	2.1
26.6	28	1.4
77.4	65	12.4
76.3	65	11.3
59.3	54	5.3
58.4	54	4.4
49.8	46	3.8
48.6	44	4.6
41.2	38	3.2
39.4	36.5	2.9

APPENDIX H : Electrical Schematic Diagram

1-PC-BASED 3D PRINTER

Drawing	Function	Location	Revision	Date	Created by	Description	Folder designation
01	F1	L1	0	27/1/2018	Vincent	COVER PAGE	
02	F1	L1	0	27/1/2018	Vincent	Drawing list	
03	F1	L1	0	27/1/2018	Vincent	COLORS OF CABLES	
04	F1	L1	0	27/1/2018	Vincent	CONTROL PANEL LAYOUT	
05	F1	L1	0	27/1/2018	Vincent	POWER SCHEMATIC CIRCUIT	
06	F1	L1	0	28/1/2018	Vincent	POWER SCHEMATIC CIRCUIT 2	
08	F1	L1	0	27/1/2018	Vincent	SOLID STATE RELAY	
09	F1	L1	0	28/1/2018	Vincent	STEPPER MOTOR CARD	
10	F1	L1	0	28/1/2018	Vincent	EL7031(X AXIS)	
11	F1	L1	0	28/1/2018	Vincent	EL7031(Y AXIS)	
12	F1	L1	0	28/1/2018	Vincent	EL7031(Z AXIS)	
13	F1	L1	0	28/1/2018	Vincent	EL7031(E AXIS)	
14	F1	L1	0	27/1/2018	Vincent	EL2008 OUTPUT (1)	
15	F1	L1	0	28/1/2018	Vincent	EL2008 OUTPUT (2)	
16	F1	L1	0	28/1/2018	Vincent	EL1889 INPUT	
17	F1	L1	0	28/1/2018	Vincent	72 WAY SOCKET DETAILS	
18	F1	L1	0	28/1/2018	Vincent	END-STOP AND EMERGENCY SWITCH	
19	F1	L1	0	28/1/2018	Vincent	STEPPER MOTOR	
20	F1	L1	0	28/1/2018	Vincent	THERMOCOUPLE	
21	F1	L1	0	28/1/2018	Vincent	HEAT CATRIDGE	

1	2	3	4	5	6	7	8	9	10

ELECTRICAL UTILITIES : SINGLE PHASE AC240V 50HZ + NEUTRAL + EARTH

COLORS OF CABLES

MAIN DIAGRAM	SINGLE PHASE AC240V	L : RED/BROWN
		N : BLUE/BLACK
		PE : GREEN/YELLOW
CONTROL DIAGRAM	24VDC	P24 : RED
		G : BLACK
	12VDC	P12 : RED
		G : BLACK

COLORS SHORT LIST

1) BLUE : BL
2) YELLOW : YE
3) RED : RD
4) BLACK : BK
5) BROWN : BN
6) WHITE : WH
7) GREEN : GN
8) ORANGE : OG

SOLIDWORKS Electrical

PROJECT: PC-BASED 3D PRINTER	TITLE: COLORS OF CABLES					PREVIOUS 02	REVISION 0
		0	27/1/2018	Vincent		NEXT 04	SCHEME 03
		REV.	DATE	NAME	CHANGES		
CONTRACT:	UTAR	DRAWN BY: Vincent Hoong			APPROVED BY:		

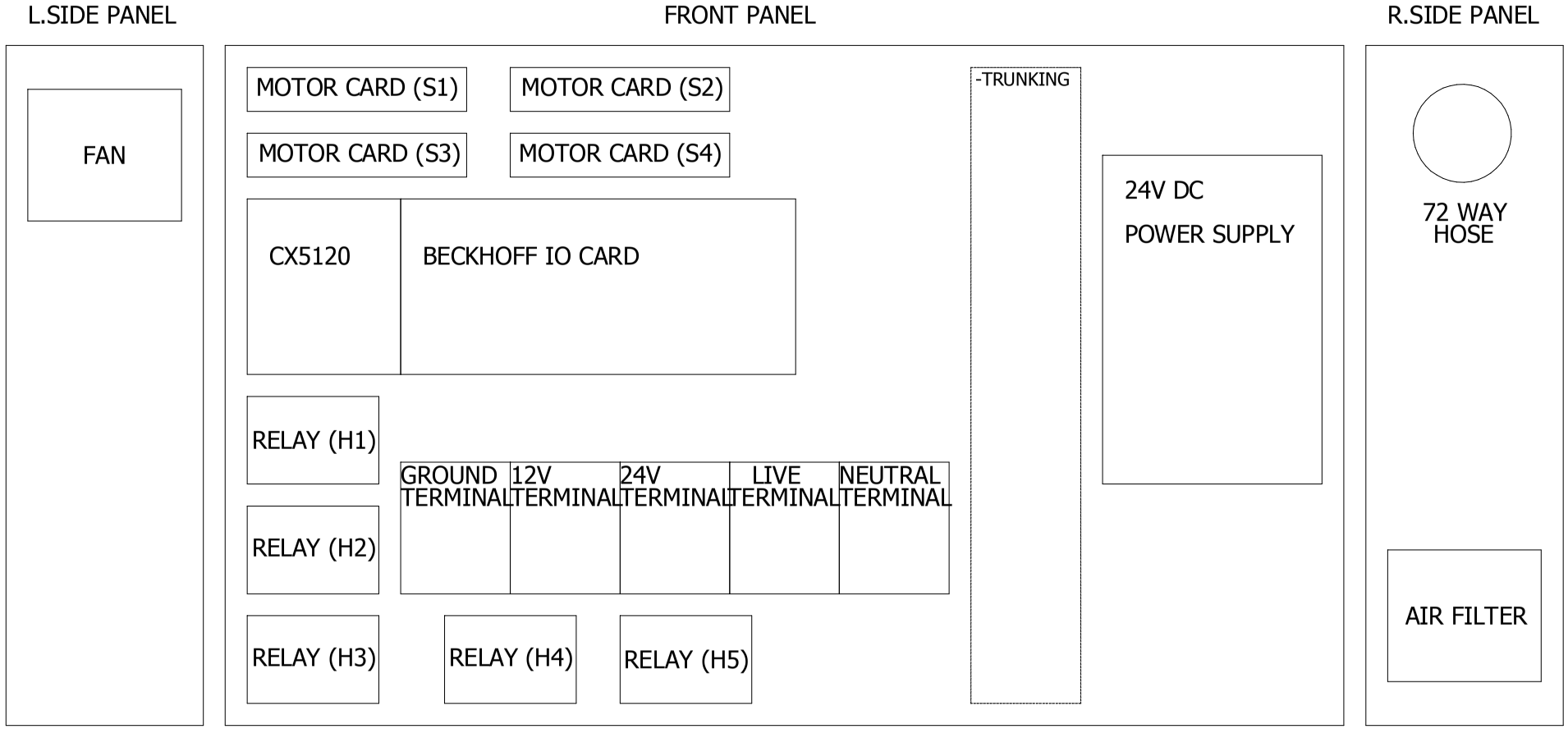

PROJECT: PC-BASED 3D PRINTER	TITLE: CONTROL PANEL LAYOUT	PREVIOUS 03	REVISION 0
CONTRACT:	UTAR	NEXT 05	SCHEME 04

REV.	DATE	NAME	CHANGES
0	27/1/2018	Vincent	

DRAWN BY: Vincent Hoong

APPROVED BY:

SOLIDWORKS Electrical

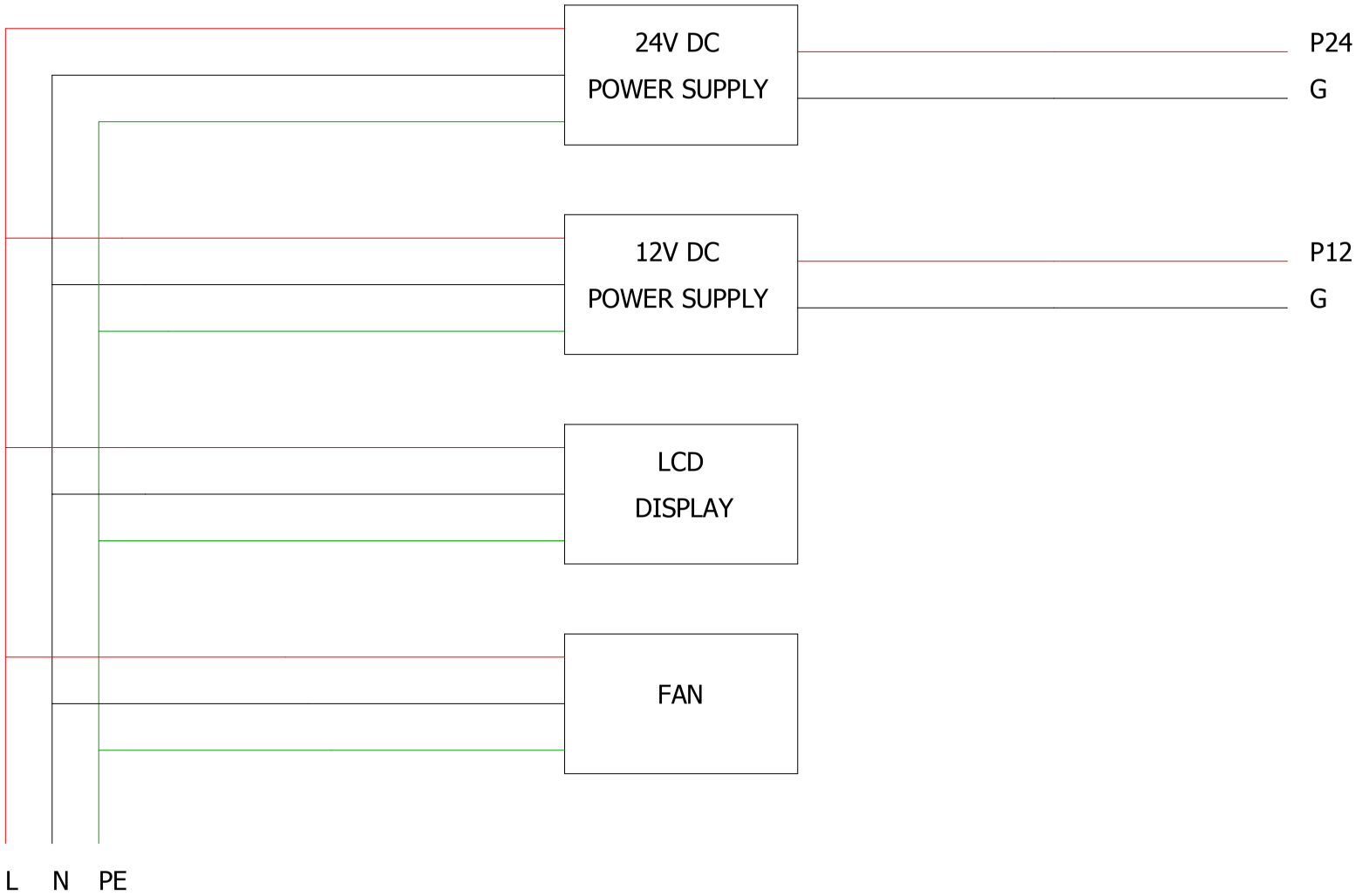

PROJECT: PC-BASED 3D PRINTER	TITLE: POWER SCHEMATIC CIRCUIT						PREVIOUS 04	REVISION 0
							NEXT 06	SCHEME 05
CONTRACT:	UTAR	0	27/1/2018	Vincent				
		REV.	DATE	NAME	CHANGES			
		DRAWN BY: Vincent Hoong			APPROVED BY:			

SOLIDWORKS Electrical

Document realized with version :2015.0.3.24

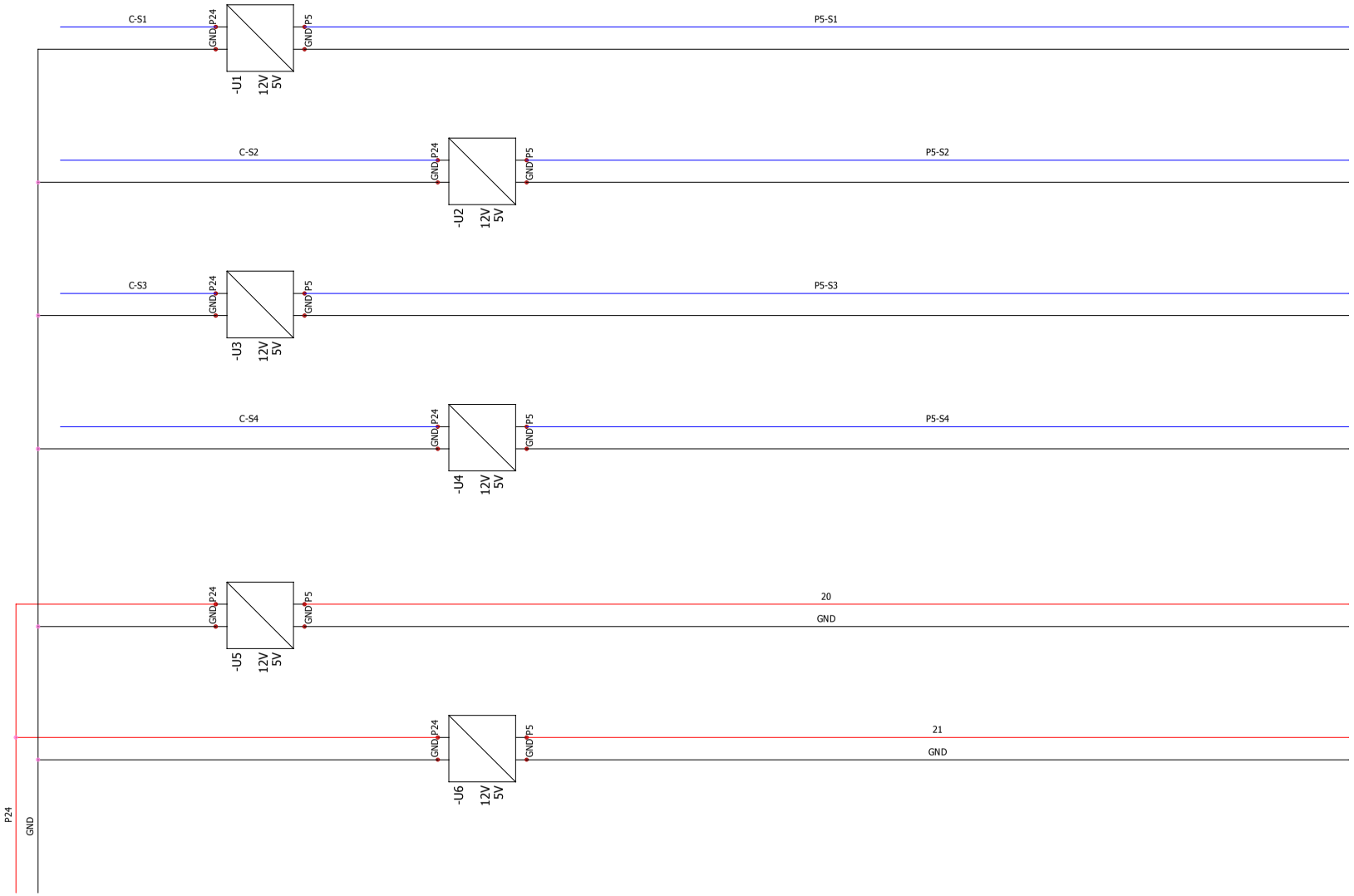

1	2	3	4	5	6	7	8	9	10

SOLIDWORKS Electrical

PROJECT: PC-BASED 3D PRINTER	TITLE: POWER SCHEMATIC CIRCUIT 2				PREVIOUS 05	REVISION 0
		0	28/1/2018	Vincent	NEXT 08	SCHEME 06
CONTRACT:	UTAR	REV.	DATE	NAME	CHANGES	
		DRAWN BY: Vincent Hoong		APPROVED BY:		

Document realized with version :2015.0.3.24

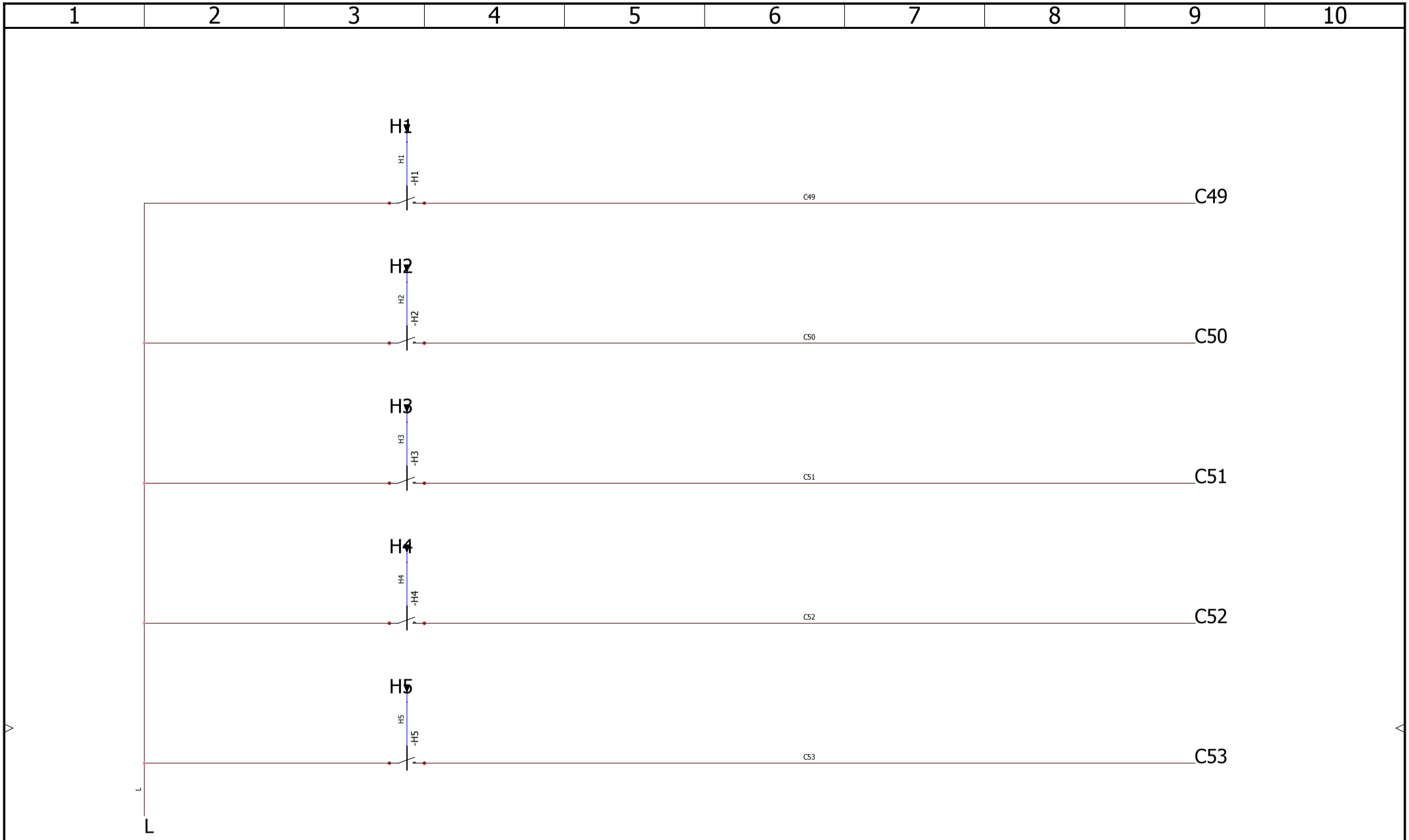

PROJECT: PC-BASED 3D PRINTER	TITLE: SOLID STATE RELAY					PREVIOUS 06	REVISION 0
		0	27/1/2018	Vincent		NEXT 09	SCHEME 08
CONTRACT:	UTAR	REV.	DATE	NAME	CHANGES		
		DRAWN BY: Vincent Hoong			APPROVED BY:		

SOLIDWORKS Electrical

Document realized with version :2015.0.3.24

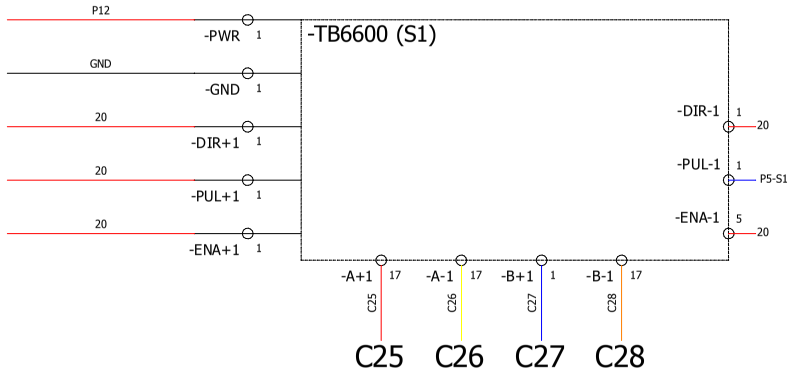

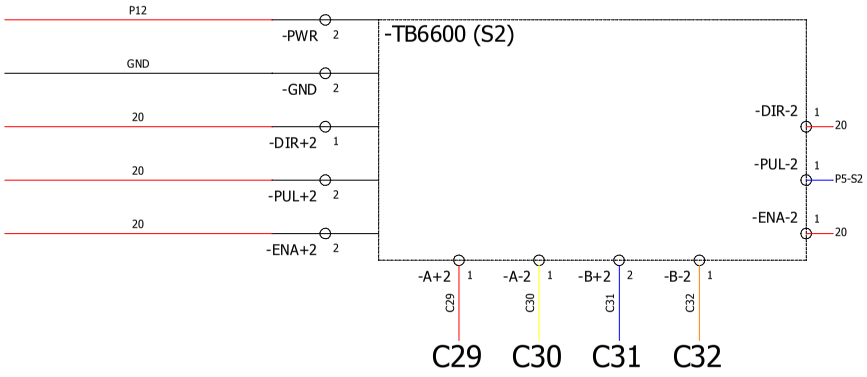

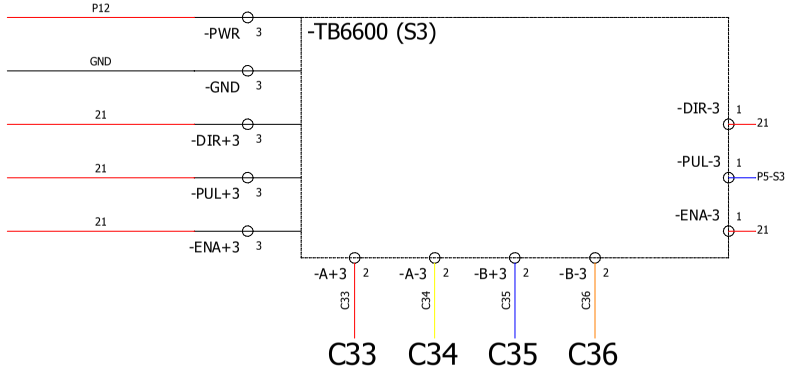

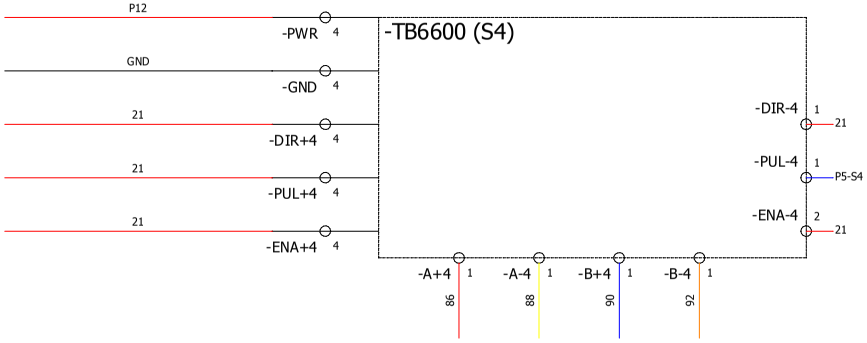

PROJECT: PC-BASED 3D PRINTER	TITLE: STEPPER MOTOR CARD			PREVIOUS 08	REVISION 0
		0	28/1/2018 Vincent	NEXT 10	SCHEME 09
CONTRACT:	UTAR	REV. DATE NAME CHANGES		DRAWN BY: Vincent Hoong	APPROVED BY:

SOLIDWORKS Electrical

Document realized with version :2015.0.3.24

1	2	3	4	5	6	7	8	9	10

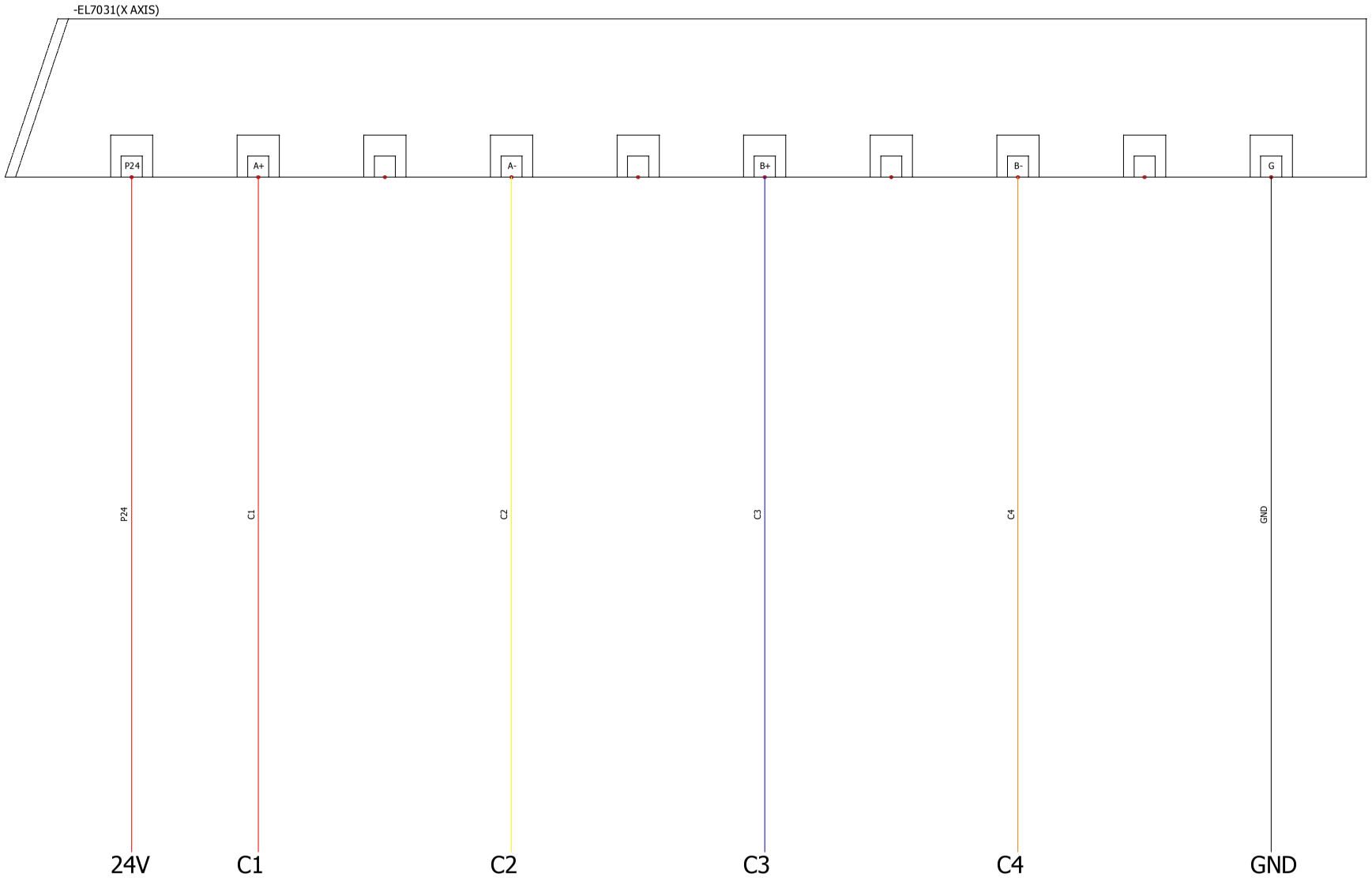

PROJECT: PC-BASED 3D PRINTER	TITLE: EL7031(X AXIS)			PREVIOUS 09	REVISION 0
		0	28/1/2018	Vincent	NEXT 11 / SCHEME 10
CONTRACT:	UTAR	REV.	DATE	NAME / CHANGES	
		DRAWN BY: Vincent Hoong		APPROVED BY:	

SOLIDWORKS Electrical

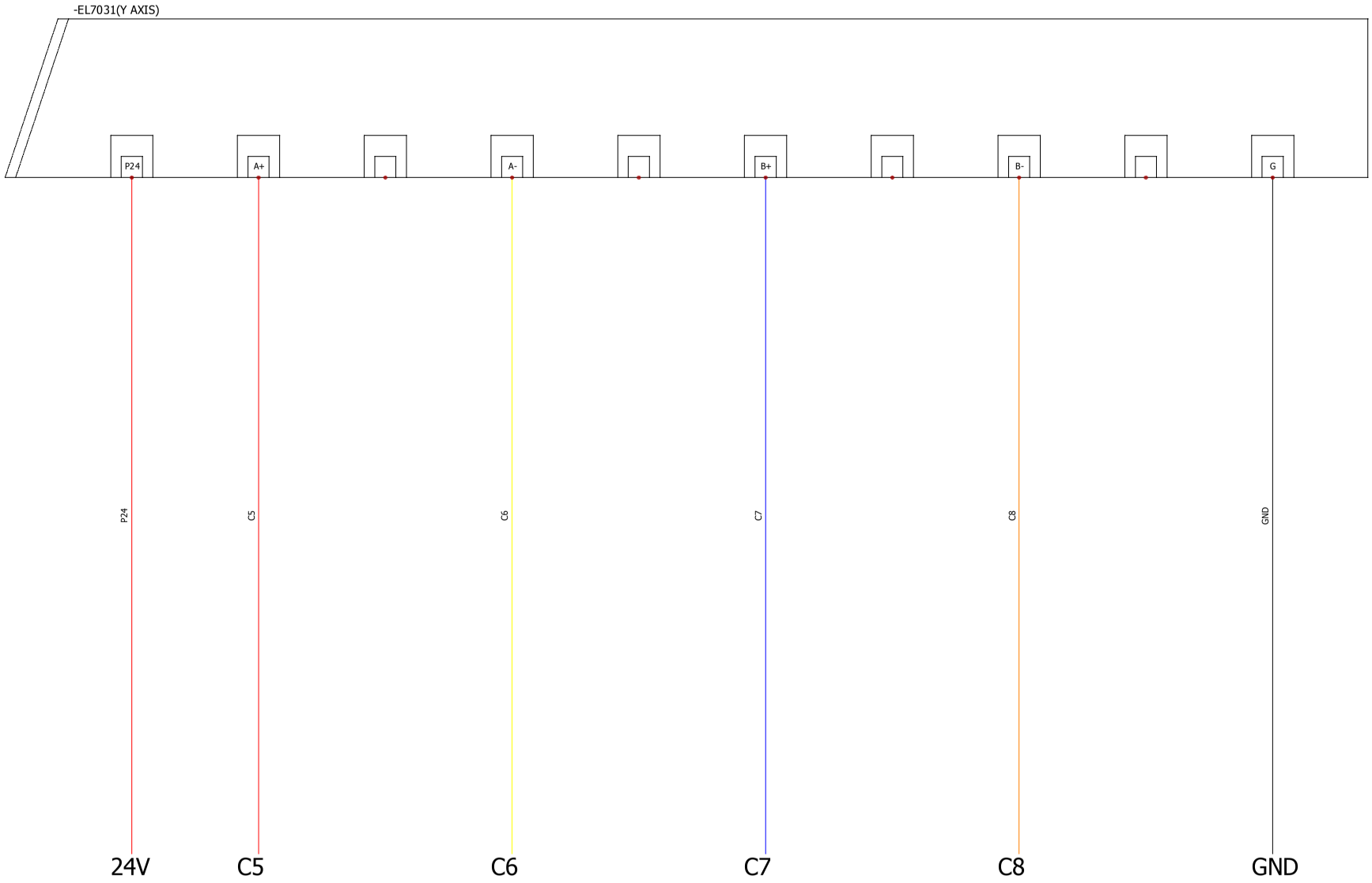

1	2	3	4	5	6	7	8	9	10

PROJECT: PC-BASED 3D PRINTER	TITLE: EL7031(Y AXIS)			PREVIOUS 10	REVISION 0
		0	28/1/2018	Vincent	NEXT 12 / SCHEME 11
		REV.	DATE	NAME	CHANGES
CONTRACT:	UTAR	DRAWN BY: Vincent Hoong		APPROVED BY:	

SOLIDWORKS Electrical

1	2	3	4	5	6	7	8	9	10

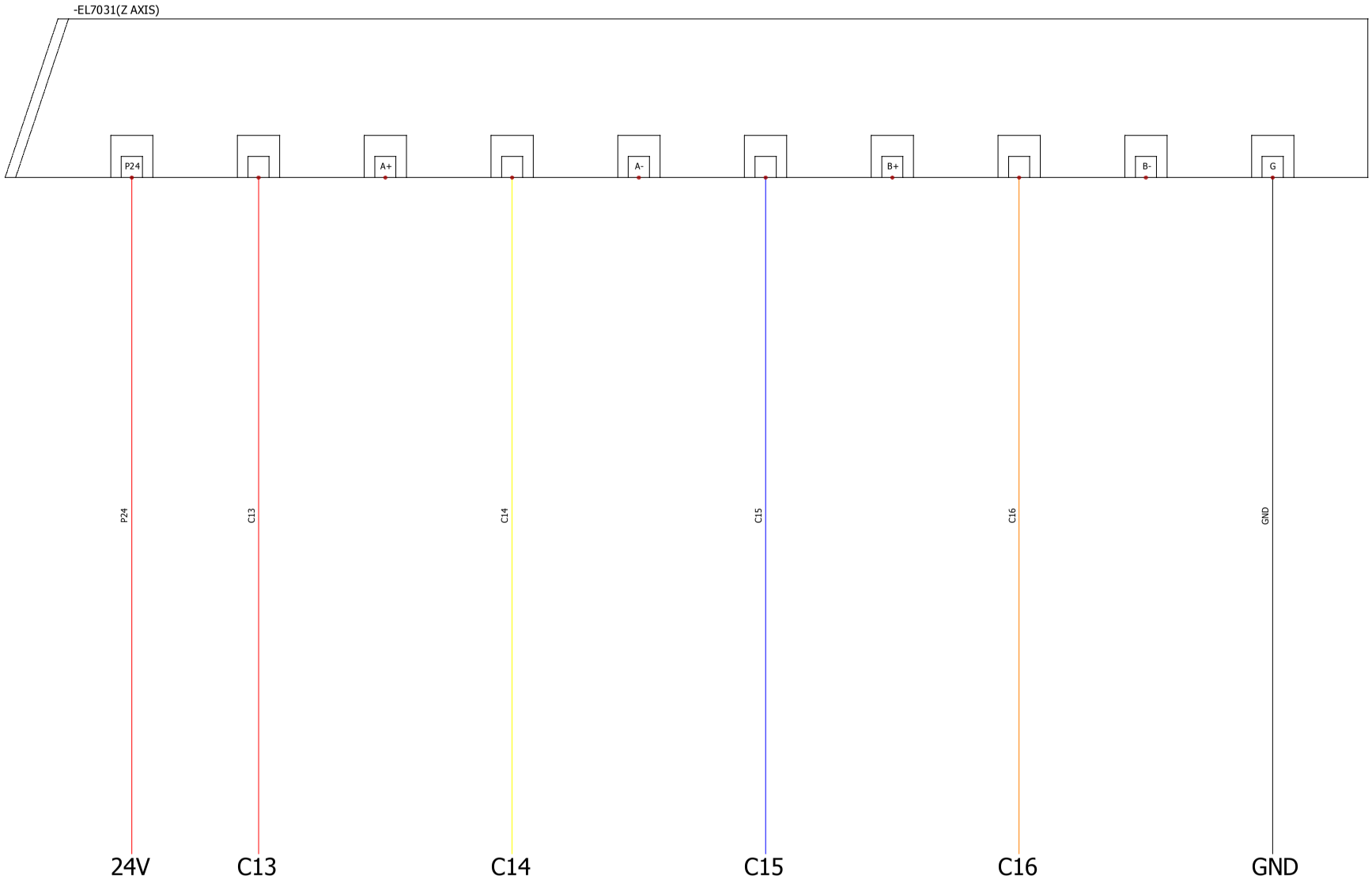

PROJECT: PC-BASED 3D PRINTER	TITLE: EL7031(Z AXIS)	PREVIOUS 11	REVISION 0
CONTRACT:	UTAR	NEXT 13	SCHEME 12

REV.	DATE	NAME	CHANGES
0	28/1/2018	Vincent	

DRAWN BY: Vincent Hoong

APPROVED BY:

SOLIDWORKS Electrical

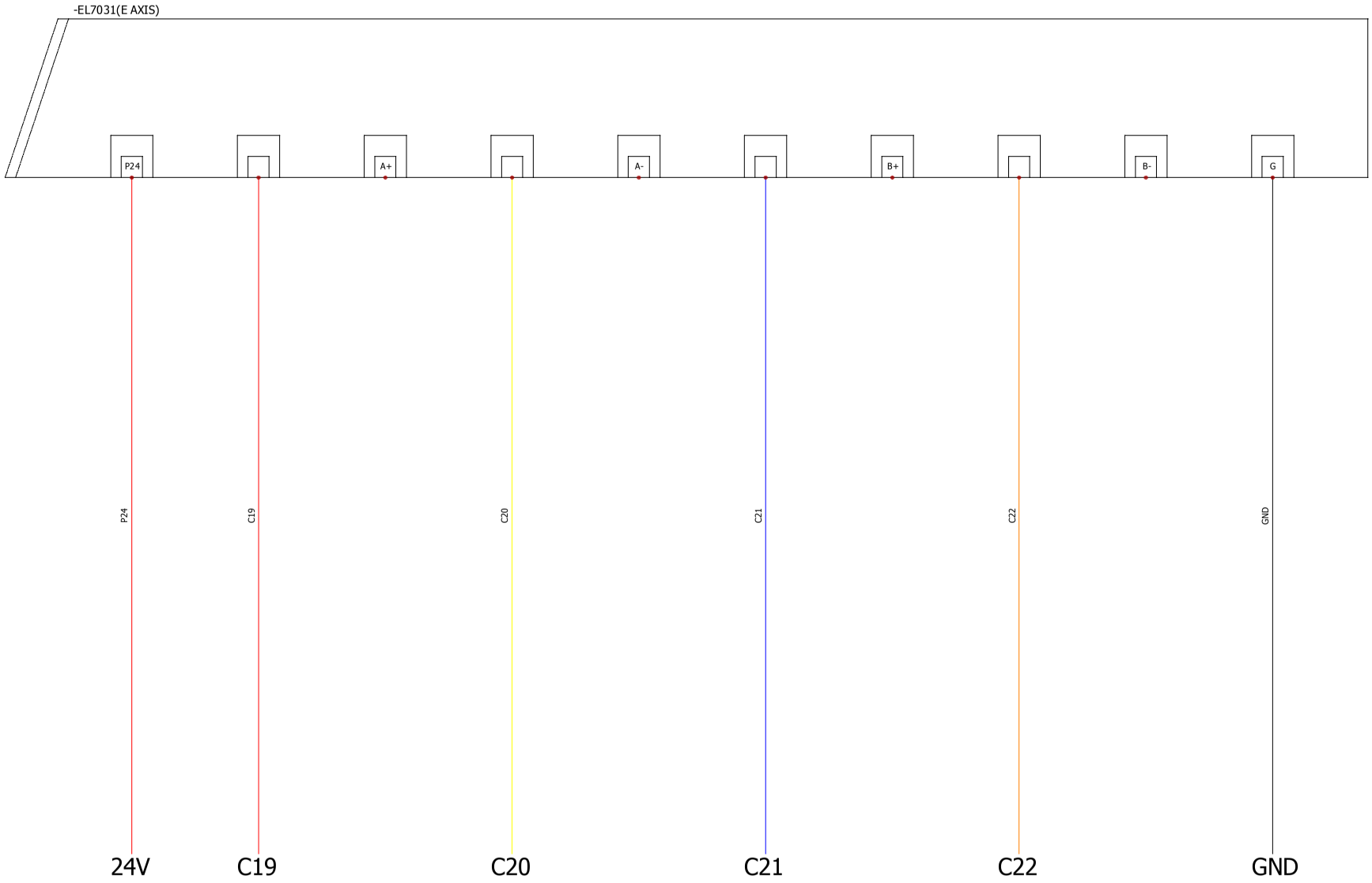

1	2	3	4	5	6	7	8	9	10

PROJECT: PC-BASED 3D PRINTER	TITLE: EL7031(E AXIS)			PREVIOUS 12	REVISION 0
		0	28/1/2018 Vincent	NEXT 14	SCHEME 13
CONTRACT:	UTAR	REV. DATE NAME CHANGES			
		DRAWN BY: Vincent Hoong	APPROVED BY:		

SOLIDWORKS Electrical

1	2	3	4	5	6	7	8	9	10

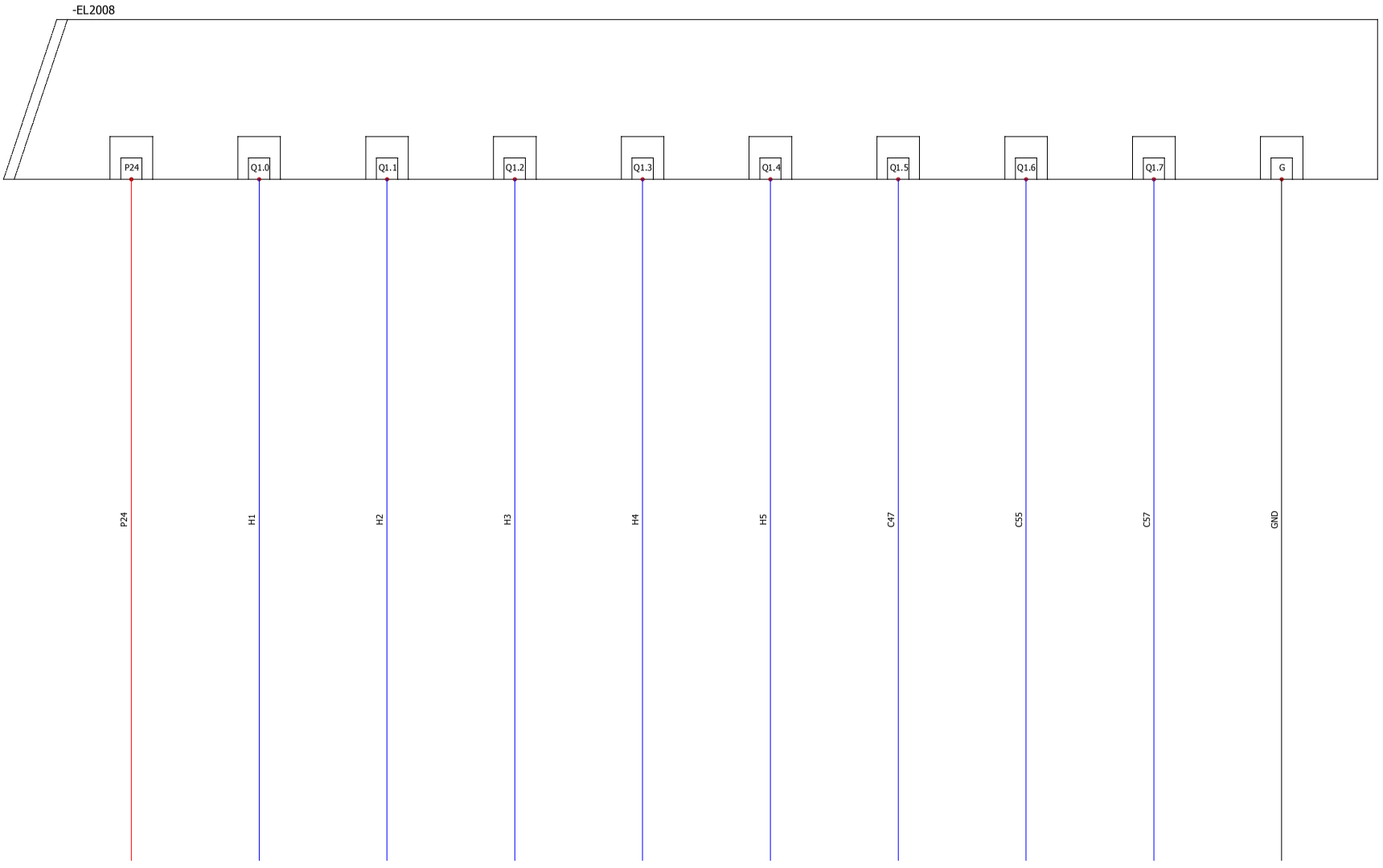

PROJECT: PC-BASED 3D PRINTER	TITLE: EL2008 OUTPUT (1)			PREVIOUS 13	REVISION 0
		0	27/1/2018 Vincent	NEXT 15	SCHEME 14
CONTRACT:	UTAR	REV. DATE NAME CHANGES			
		DRAWN BY: Vincent Hoong	APPROVED BY:		

SOLIDWORKS Electrical

Document realized with version :2015.0.3.24

1	2	3	4	5	6	7	8	9	10

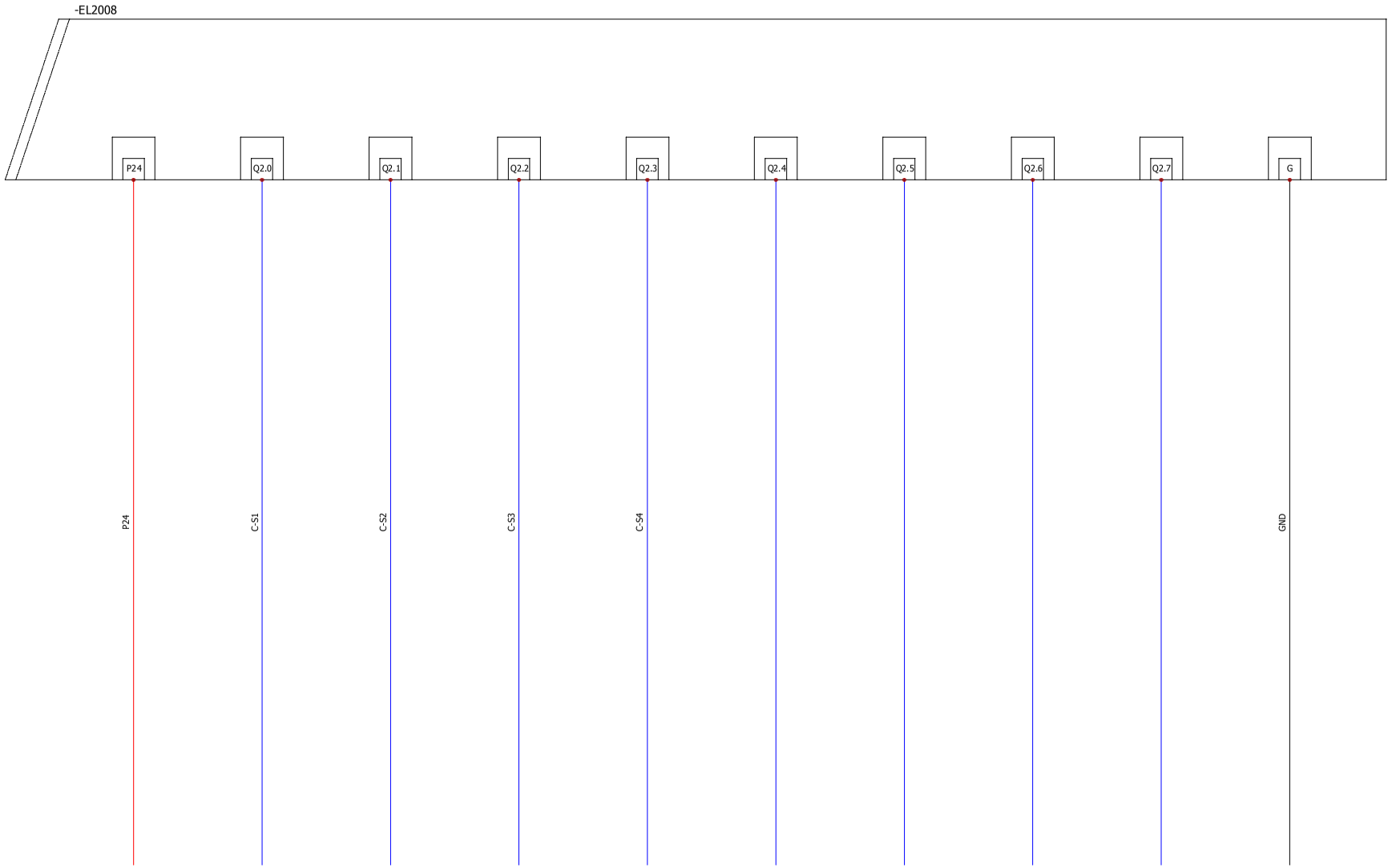

PROJECT: PC-BASED 3D PRINTER	TITLE: EL2008 OUTPUT (2)			PREVIOUS 14	REVISION 0
		0	28/1/2018 Vincent	NEXT 16	SCHEME 15
		REV.	DATE NAME CHANGES		
CONTRACT:	UTAR	DRAWN BY: Vincent Hoong	APPROVED BY:		

SOLIDWORKS Electrical

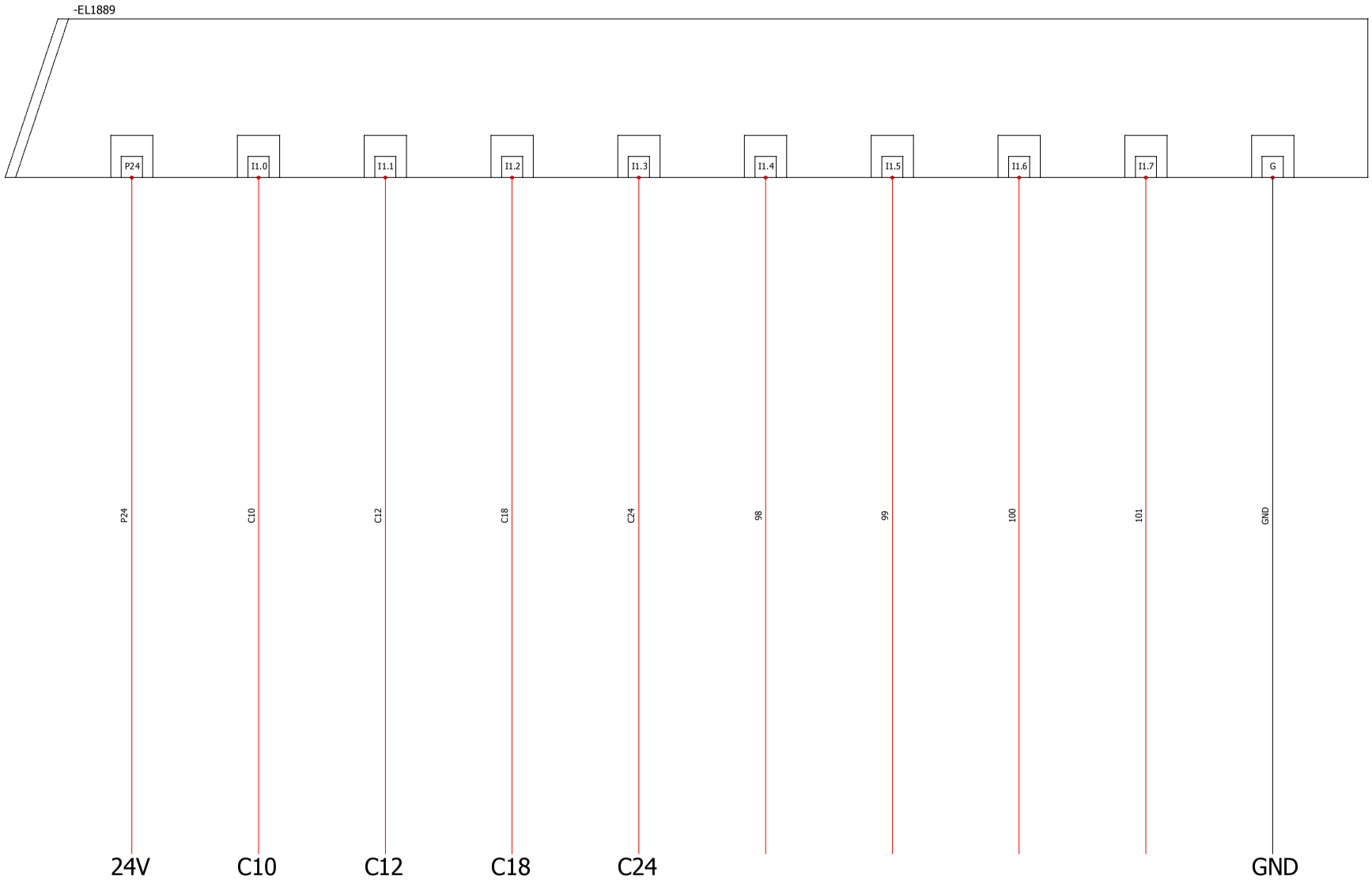

1	2	3	4	5	6	7	8	9	10

PROJECT: PC-BASED 3D PRINTER	TITLE: EL1889 INPUT				PREVIOUS 15	REVISION 0
		0	28/1/2018	Vincent	NEXT 17	SCHEME 16
CONTRACT:	UTAR	REV.	DATE	NAME	CHANGES	
		DRAWN BY: Vincent Hoong			APPROVED BY:	

SOLIDWORKS Electrical

72 Way Socket Details

Port	Item Description	Label	Colour
1	X axis Stepper Motor (A+)	Stepper X	Red
2	X axis Stepper Motor (A–)	Stepper X	Yellow
3	X axis Stepper Motor (B+)	Stepper X	Blue
4	X axis Stepper Motor (B–)	Stepper X	Orange
5	Y axis Stepper Motor (A+)	Stepper Y	Red
6	Y axis Stepper Motor (A–)	Stepper Y	Yellow
7	Y axis Stepper Motor (B+)	Stepper Y	Blue
8	Y axis Stepper Motor (B–)	Stepper Y	Orange
9	X axis End Stop Switch	Endstop X-axis	Red
10	X axis End Stop Switch	Endstop X-axis	Black
11	Y axis End Stop Switch	Endstop Y-axis	Red
12	Y axis End Stop Switch	Endstop Y-axis	Black
13	Z axis Stepper Motor (A+)	Stepper Z	Red
14	Z axis Stepper Motor (A–)	Stepper Z	Yellow
15	Z axis Stepper Motor (B+)	Stepper Z	Blue
16	Z axis Stepper Motor (B–)	Stepper Z	Orange
17	Z axis End Stop Switch	Endstop Z-axis	Red
18	Z axis End Stop Switch	Endstop Z-axis	Black
19	Extruder Stepper Motor (A+)	Extruder	Red
20	Extruder Stepper Motor (A–)	Extruder	Yellow
21	Extruder Stepper Motor (B+)	Extruder	Blue
22	Extruder Stepper Motor (B–)	Extruder	Black
23	Emergency Stop Switch	Emergency Stop	Red
24	Emergency Stop Switch	Emergency Stop	Black
25	Material Extruder 1 Stepper Motor (A+)	Ext 1	White
26	Material Extruder 1 Stepper Motor (A–)	Ext 1	Brown
27	Material Extruder 1 Stepper Motor (B+)	Ext 1	Blue
28	Material Extruder 1 Stepper Motor (B–)	Ext 1	Black
29	Material Extruder 2 Stepper Motor (A+)	Ext 2	White
30	Material Extruder 2 Stepper Motor (A–)	Ext 2	Brown
31	Material Extruder 2 Stepper Motor (B+)	Ext 2	Blue
32	Material Extruder 2 Stepper Motor (B–)	Ext 2	Black
33	Mixer Stepper Motor (A+)	Mixer	Black
34	Mixer Stepper Motor (A–)	Mixer	Blue
35	Mixer Stepper Motor (B+)	Mixer	Orange
36	Mixer Stepper Motor (B–)	Mixer	Yellow

Port	Item Description	Label	Colour
37	Thermocouple 1 (Chomel)	T1	Red
38	Thermocouple 1 (Alumel)	T1	Blue
39	Thermocouple 2 (Chomel)	T2	Red
40	Thermocouple 2 (Alumel)	T2	Blue
41	Thermocouple 3 (Chomel)	T3	Red
42	Thermocouple 3 (Alumel)	T3	Blue
43	Thermocouple 4 (Chomel)	T4	Red
44	Thermocouple 4 (Alumel)	T4	Blue
45	Thermocouple 5 (Chomel)	T5	Red
46	Thermocouple 5 (Alumel)	T5	Blue
47	Extra Wires	47/59/60/71/72	Green
48	Extra Wires	-	Purple
49	Heat Cartridge 1	H1	Red
50	Heat Cartridge 2	H2	Red
51	Heat Cartridge 3	H3	Red
52	Heat Cartridge 4	H4	Red
53	Heat Cartridge 5	H5	Red
54	Heat Cartridge Neutral		
55	Cooling Fan 1 (+)	fan 1	Red
56	Cooling Fan 1 (–)	fan 1	Black
57	Cooling Fan 2 (+)	fan 2	Red
58	Cooling Fan 2 (–)	fan 2	Black
59	Extra Wires	47/59/60/71/72	White
60	Extra Wires	47/59/60/71/72	Black
61	Laser Displacement	laser	White
62	Laser Displacement	laser	Brown
63	Laser Displacement	laser	Blue
64	Laser Displacement	laser	Green
65	Laser Displacement	laser	Black
66	Extra Wires	5 extra	White
67	Extra Wires	5 extra	Brown
68	Extra Wires	5 extra	Blue
69	Extra Wires	5 extra	Green
70	Extra Wires	5 extra	Black
71	Extra Wires	47/59/60/71/72	Brown
72	Extra Wires	47/59/60/71/72	Blue

SOLIDWORKS Electrical

PROJECT: PC-BASED 3D PRINTER

TITLE: 72 WAY SOCKET DETAILS

CONTRACT:

UTAR

REV.	DATE	NAME	CHANGES
0	28/1/2018	Vincent	

DRAWN BY: Vincent Hoong

APPROVED BY:

PREVIOUS 16 | REVISION 0

NEXT 18 | SCHEME 17

PROJECT: PC-BASED 3D PRINTER	TITLE: END-STOP AND EMERGENCY SWITCH					PREVIOUS 17	REVISION 0
		0	28/1/2018	Vincent		NEXT 19	SCHEME 18
		REV.	DATE	NAME	CHANGES		
CONTRACT:	UTAR	DRAWN BY: Vincent Hoong			APPROVED BY:		

SOLIDWORKS Electrical

Document realized with version :2015.0.3.24

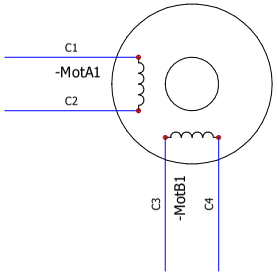

X AXIS

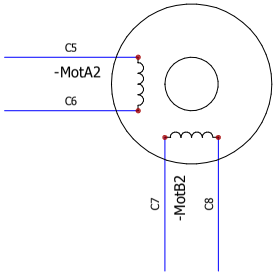

Y AXIS

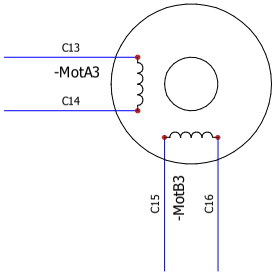

Z AXIS

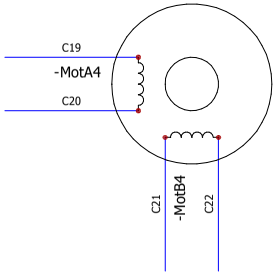

E AXIS

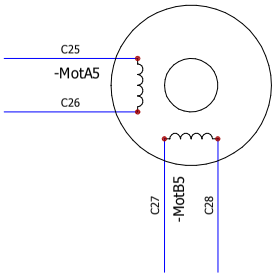

MAT FEED 1

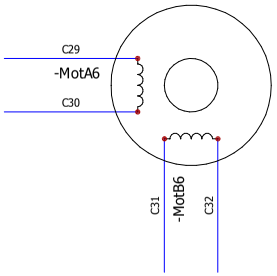

MAT FEED 2

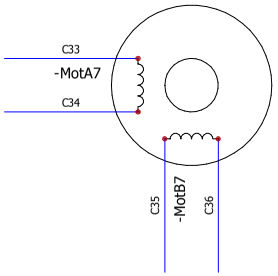

MIXER

PROJECT: PC-BASED 3D PRINTER	TITLE: STEPPER MOTOR			PREVIOUS 18	REVISION 0
		0	28/1/2018 Vincent	NEXT 20	SCHEME 19
CONTRACT:	UTAR	REV.	DATE NAME CHANGES		
		DRAWN BY: Vincent Hoong	APPROVED BY:		

SOLIDWORKS Electrical

Document realized with version :2015.0.3.24

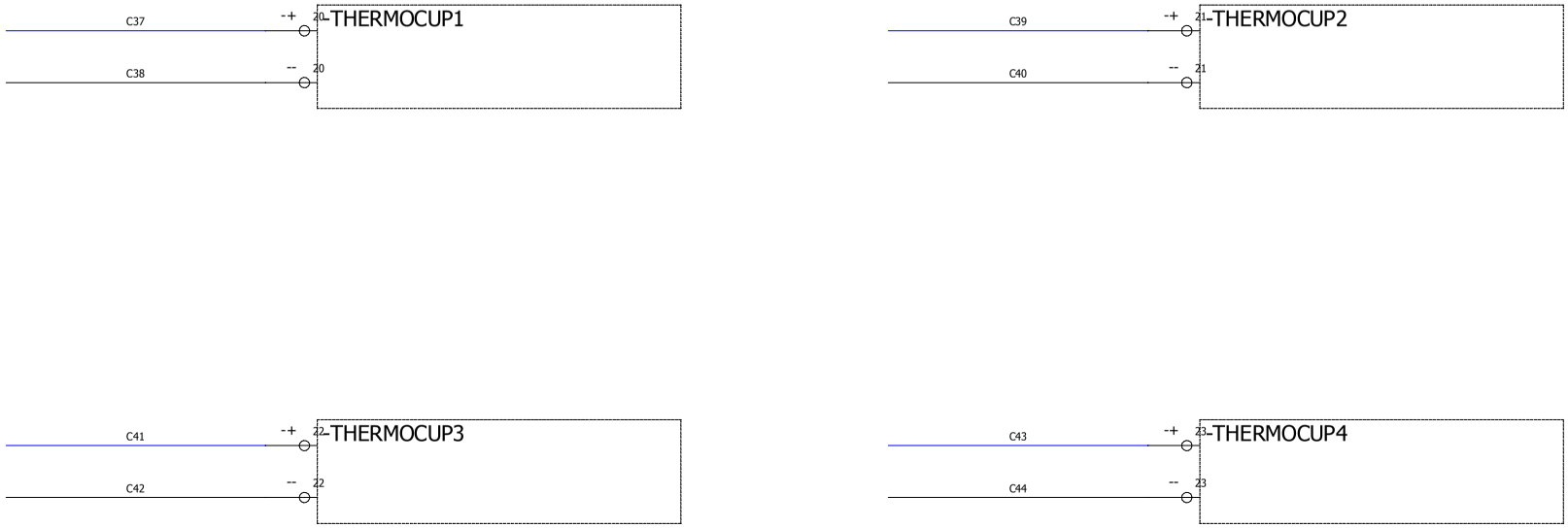

PROJECT: PC-BASED 3D PRINTER		TITLE: THERMOCOUPLE					PREVIOUS 19	REVISION 0
							NEXT 21	SCHEME 20
CONTRACT:		UTAR		0	28/1/2018	Vincent		
				REV.	DATE	NAME	CHANGES	
				DRAWN BY: Vincent Hoong			APPROVED BY:	

SOLIDWORKS Electrical

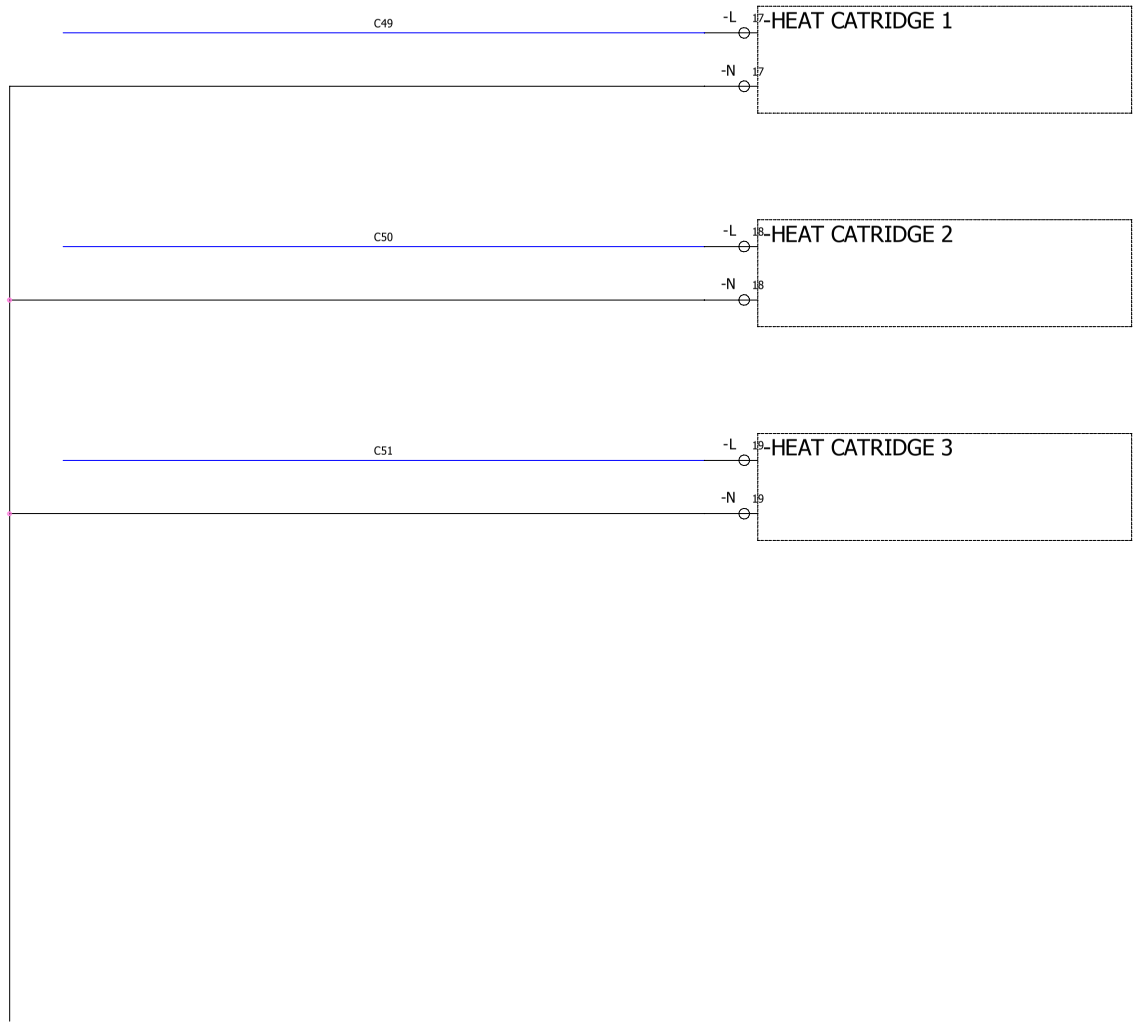

PROJECT: PC-BASED 3D PRINTER	TITLE: HEAT CATRIDGE						PREVIOUS 20	REVISION 0
							NEXT	SCHEME 21
CONTRACT:	UTAR	0	28/1/2018	Vincent				
		REV.	DATE	NAME	CHANGES			
		DRAWN BY: Vincent Hoong			APPROVED BY:			

SOLIDWORKS Electrical

CX5010, CX5020

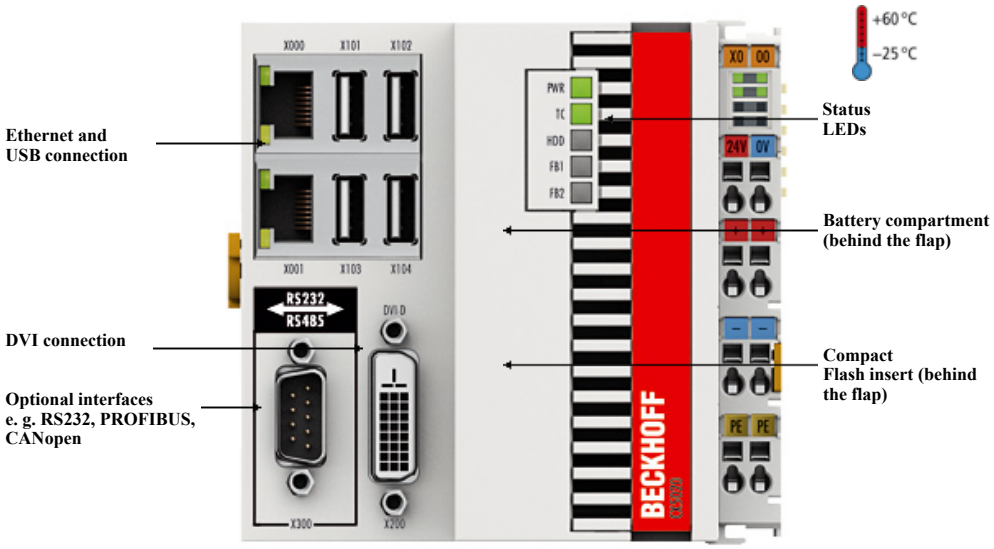

CX5010, CX5020 | Embedded PC series with Intel® Atom™ processor

The CX5010 and CX5020 are Embedded PCs from the CX5000 series based on Intel® Atom™ processors and differ only by the CPU version. The CX5010 has a 1.1 GHz Intel® Atom™ Z510 processor, while the CX5020 has a 1.6 GHz Intel® Atom™ Z530 processor. Apart from the clock speed, the two processors also differ by the fact that the Z530 features hyperthreading technology, i.e. it has two virtual CPU cores for more effective execution of software.

Depending on the installed TwinCAT runtime environment, the CX5010/CX5020 can be used for the implementation of PLC or PLC/Motion Control projects (with or without visualisation).

The extended operating temperature range between -25 and +60 °C enables application in climatically demanding situations.

The order identifier of the CX5000 devices is derived as follows:

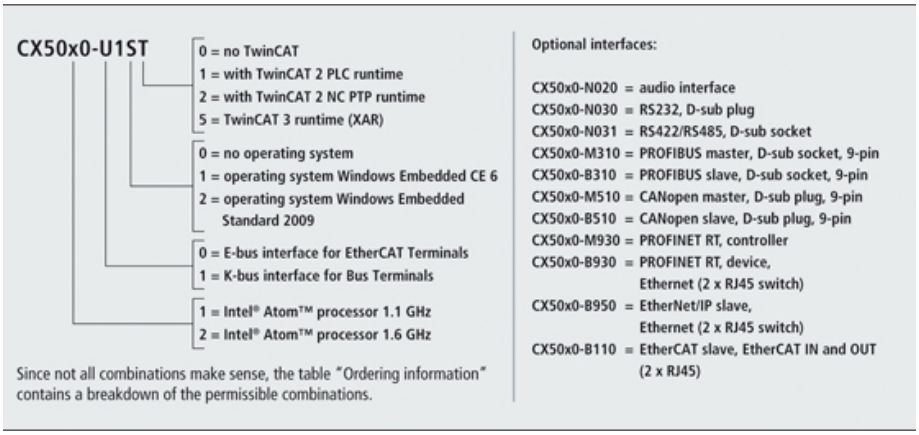

Technical data	CX5010-x1xx	CX5020-x1xx
Processor	processor Intel® Atom™ Z510, 1.1 GHz clock frequency (TC3: 40)	processor Intel® Atom™ Z530, 1.6 GHz clock frequency (TC3: 40)
Flash memory	128 MB Compact Flash card (optionally extendable)	
Internal main memory	512 MB RAM (internal, not expandable)	512 MB RAM (optionally 1 GB installed ex factory)
Persistent memory	integrated 1-second UPS (1 MB on Compact Flash card)	
Interfaces	2 x RJ45, 10/100/1000 Mbit/s, DVI-D, 4 x USB 2.0, 1 x optional interface	
Diagnostics LED	1 x power, 1 x TC status, 1 x flash access, 2 x bus status	
Clock	internal battery-backed clock for time and date (battery exchangeable)	
Operating system	Microsoft Windows Embedded CE 6 or Microsoft Windows Embedded Standard 2009	

Control software	TwinCAT 2 PLC runtime or TwinCAT 2 NC PTP runtime	
I/O connection	E-bus or K-bus, automatic recognition	
Power supply	24 V DC (-15 %/+20 %)	
Current supply E-bus/K-bus	2 A	
Max. power loss	12 W (including the system interfaces)	12.5 W (including the system interfaces)
Dimensions (W x H x D)	100 mm x 106 mm x 92 mm	
Weight	approx. 575 g	
Operating/storage temperature	-25…+60 °C/-40…+85 °C	
Relative humidity	95 %, no condensation	
Vibration/shock resistance	conforms to EN 60068-2-6/EN 60068-2-27	
EMC immunity/emission	conforms to EN 61000-6-2/EN 61000-6-4	
Protection class	IP 20	
TC3 performance class	performance (40); please see here for an overview of all the TwinCAT 3 performance classes	

Ordering information	E-bus	K-bus	no operating system	Windows Embedded CE 6	Windows Embedded Standard 2009	optional TwinCAT 3	TwinCAT 2 PLC runtime	TwinCAT 2 NC PTP runtime
CX5010-0100	x	–	x	–	–	–	–	–
CX5010-0110	x	–	–	x	–	x	–	–
CX5010-0111	x	–	–	x	–	–	x	–
CX5010-0112	x	–	–	x	–	–	x	x
CX5010-0120	x	–	–	–	x*	x	–	–
CX5010-0121	x	–	–	–	x*	–	x	–
CX5010-0122	x	–	–	–	x*	–	x	x
CX5010-1100	–	x	x	–	–	–	–	–
CX5010-1110	–	x	–	x	–	x	–	–
CX5010-1111	–	x	–	x	–	–	x	–
CX5010-1112	–	x	–	x	–	–	x	x
CX5010-1120	–	x	–	–	x*	x	–	–
CX5010-1121	–	x	–	–	x*	–	x	–
CX5010-1122	–	x	–	–	x*	–	x	x
CX5020-0100	x	–	x	–	–	–	–	–
CX5020-0110	x	–	–	x	–	x	–	–
CX5020-0111	x	–	–	x	–	–	x	–
CX5020-0112	x	–	–	x	–	–	x	x
CX5020-0120	x	–	–	–	x*	x	–	–
CX5020-0121	x	–	–	–	x*	–	x	–
CX5020-0122	x	–	–	–	x*	–	x	x
CX5020-1100	–	x	x	–	–	–	–	–
CX5020-1110	–	x	–	x	–	x	–	–
CX5020-1111	–	x	–	x	–	–	x	–
CX5020-1112	–	x	–	x	–	–	x	x
CX5020-1120	–	x	–	–	x*	x	–	–
CX5020-1121	–	x	–	–	x*	–	x	–
CX5020-1122	–	x	–	–	x*	–	x	x

Accessories	
CX1900-0204	1 GB DDR2 RAM for CX5020, instead of 512 MB DDR2 RAM; pre-assembled ex factory
CX1800-0400	Windows Embedded Standard 7 E instead of Windows Embedded Standard 2009; requires at least 1 GB RAM and 8 GB Compact Flash; supported devices: CX5020
CX1800-0401	Windows Embedded Standard 7 P 32 bit instead of Windows Embedded Standard 2009; requires

	at least 1 GB RAM and 8 GB Compact Flash; supported devices: CX5020
CX1900-00xx	Optionally expandable memory ex factory. Instead of 128 MB Compact Flash card: 1, 2, 4 and 8 GB Compact Flash card
CX1900-00xx	Aditionally expandable memory: 1, 2, 4 and 8 GB Compact Flash card
CX1900-001x	Formatting a Compact Flash card (bootable)

Optional interfaces	
CX5010-N020	audio interface, 3 x 3.5 mm jack sockets, Line In, Mic In, Line Out or 5.1 Surround
CX5010-N030	RS232 interface, D-sub plug, 9-pin
CX5010-N031	RS485 interface, D-sub socket, 9-pin, configuration as an end point, without echo, termination on
CX5010-N031-0001	RS485 interface, D-sub socket, 9-pin, configuration as an end point, with echo, termination on
CX5010-N031-0002	RS485 interface, D-sub socket, 9-pin, configuration as drop point, without echo, termination off
CX5010-N031-0003	RS485 interface, D-sub socket, 9-pin, configuration as drop point, with echo, termination off
CX5010-N031-0004	RS422 interface, D-sub socket, 9-pin, configuration as full duplex end point, termination on
CX5010-B110	EtherCAT slave interface, EtherCAT IN and OUT (2 x RJ45)
CX5010-M310	PROFIBUS master interface, D-sub socket, 9-pin
CX5010-B310	PROFIBUS slave interface, D-sub socket, 9-pin
CX5010-M510	CANopen master interface, D-sub plug, 9-pin
CX5010-B510	CANopen slave interface, D-sub plug, 9-pin
CX5010-M930	PROFINET RT, controller interface, Ethernet (2 x RJ45)
CX5010-B930	PROFINET RT, device interface, Ethernet (2 x RJ45 switched)
CX5010-B950	EtherNet/IP slave interface, Ethernet (2 x RJ45 switched)
CX5020-N020	audio interface, 3 x 3.5 mm jack sockets, Line In, Mic In, Line Out or 5.1 Surround
CX5020-N030	RS232 interface, D-sub plug, 9-pin
CX5020-N031	RS485 interface, D-sub socket, 9-pin, configuration as an end point, without echo, termination on
CX5020-N031-0001	RS485 interface, D-sub socket, 9-pin, configuration as an end point, with echo, termination on
CX5020-N031-0002	RS485 interface, D-sub socket, 9-pin, configuration as drop point, without echo, termination off
CX5020-N031-0003	RS485 interface, D-sub socket, 9-pin, configuration as drop point, with echo, termination off
CX5020-N031-0004	RS422 interface, D-sub socket, 9-pin, configuration as full duplex end point, termination on

CX5020-B110	EtherCAT slave interface, EtherCAT IN and OUT (2 x RJ45)
CX5020-M310	PROFIBUS master interface, D-sub socket, 9-pin
CX5020-B310	PROFIBUS slave interface, D-sub socket, 9-pin
CX5020-M510	CANopen master interface, D-sub plug, 9-pin
CX5020-B510	CANopen slave interface, D-sub plug, 9-pin
CX5020-M930	PROFINET RT, controller interface, Ethernet (2 x RJ45)
CX5020-B930	PROFINET RT, device interface, Ethernet (2 x RJ45 switched)
CX5020-B950	EtherNet/IP slave interface, Ethernet (2 x RJ45 switched)
Product announcement	CX50x0-B950: estimated market release 1st quarter 2016

*CX50x0 systems with Microsoft Embedded Standard 2009 require Compact Flash with a capacity of at least 2 GB (must be ordered separately).

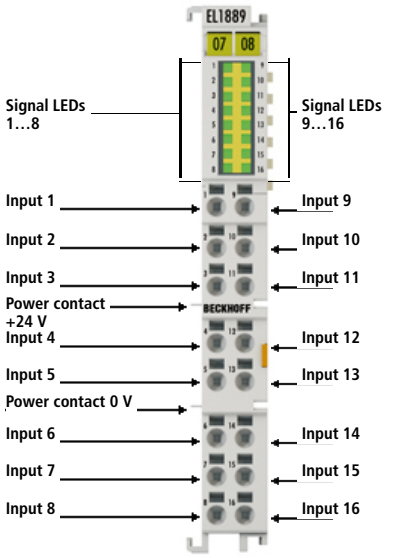

Top view

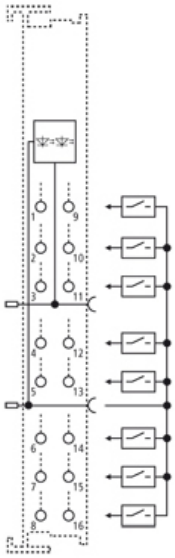
Contact assembly

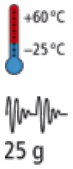

EL1889 | HD EtherCAT Terminal, 16-channel digital input 24 V DC, 0 V (ground) switching

The EL1889 digital input terminal acquires the binary control signals from the process level and transmits them, in an electrically isolated form, to the higher-level automation device. The EtherCAT Terminal contains 16 channels, whose signal states are displayed by LEDs. The terminal is particularly suitable for space-saving use in control cabinets. By using the single-conductor connection technique, a multi-channel sensor can be connected in the smallest space with a minimum amount of wiring. The power contacts are looped through.

The EL1889 EtherCAT Terminal takes the 24 V power contact as its reference for all inputs. The conductors can be connected without tools in the case of solid wires using a direct plug-in technique.

The HD EtherCAT Terminals (High Density) with increased packing density feature 16 connection points in the housing of a 12 mm terminal block.

Technical data	EL1889
Connection technology	1-wire
Number of inputs	16
Nominal voltage	24 V DC (-15 %/+20 %)
"0" signal voltage	18…30 V
"1" signal voltage	0…7 V
Input current	typ. 3 mA
Input filter	typ. 3.0 ms
Distributed clocks	–
Current consumption power contacts	typ. 35 mA
Current consumption E-bus	typ. 110 mA
Electrical isolation	500 V (E-bus/field potential)
Bit width in the process image	16 inputs
Configuration	no address or configuration setting
Conductor types	solid wire, stranded wire and ferrule
Conductor connection	solid wire conductors: direct plug-in technique; stranded wire conductors and ferrules: spring actuation by screwdriver
Rated cross-section	solid wire: 0.08…1.5 mm²; stranded wire: 0.25…1.5 mm²; ferrule: 0.14…0.75 mm²
Weight	approx. 55 g
Operating/storage temperature	-25…+60 °C/-40…+85 °C
Relative humidity	95 %, no condensation
Vibration/shock resistance	conforms to EN 60068-2-6/EN 60068-2-27
EMC immunity/emission	conforms to EN 61000-6-2/EN 61000-6-4
Protect. class/installation pos.	IP 20/variable (see documentation)
Approvals	CE, UL, Ex

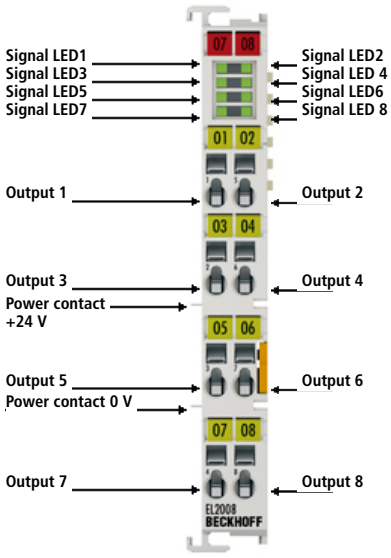

Top view

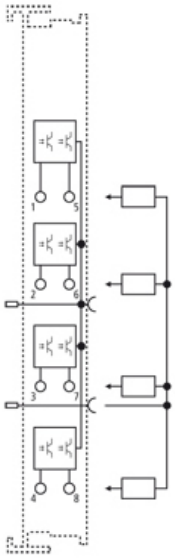

Contact assembly

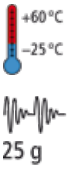

EL2008 | 8-channel digital output terminal 24 V DC, 0.5 A

The EL2008 digital output terminal connects the binary control signals from the automation unit on to the actuators at the process level with electrical isolation. The EtherCAT Terminal indicates its signal state via an LED.

Technical data	EL2008 | ES2008
Connection technology	1-wire
Number of outputs	8
Rated load voltage	24 V DC (-15 %/+20 %)
Load type	ohmic, inductive, lamp load
Distributed clocks	–
Max. output current	0.5 A (short-circuit-proof) per channel
Short circuit current	typ. < 2 A
Reverse voltage protection	yes
Breaking energy	< 150 mJ/channel
Switching times	typ. T_{ON}: 60 µs, typ. T_{OFF}: 300 µs
Current consumption E-bus	typ. 110 mA
Electrical isolation	500 V (E-bus/field potential)
Current consumption power contacts	typ. 15 mA + load
Bit width in the process image	8 outputs
Configuration	no address or configuration setting
Weight	approx. 55 g
Operating/storage temperature	-25…+60 °C/-40…+85 °C
Relative humidity	95 %, no condensation
Vibration/shock resistance	conforms to EN 60068-2-6/EN 60068-2-27
EMC immunity/emission	conforms to EN 61000-6-2/EN 61000-6-4
Protect. class/installation pos.	IP 20/see documentation
Pluggable wiring	for all ESxxxx terminals
Approvals	CE, UL, Ex

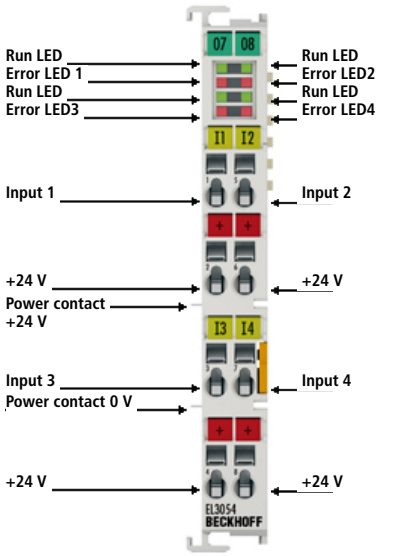

Top view

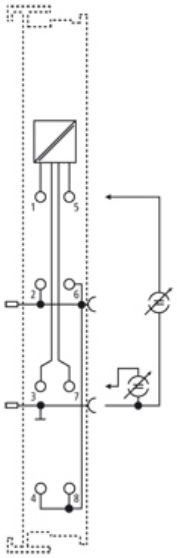

Contact assembly

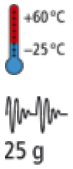

EL3054 | 4-channel analog input terminal 4…20 mA, single-ended, 12 bit

The EL3054 analog input terminal processes signals in the range between 4 and 20 mA. The current is digitised to a resolution of 12 bits and is transmitted (electrically isolated) to the higher-level automation device. The input electronics are independent of the supply voltage of the power contacts. In the EL3054 with four inputs, the 24 V power contact is connected to the terminal in order to enable connection of 2-wire sensors without external supply. The power contacts are connected through. The signal state of the EtherCAT Terminal is indicated by light emitting diodes. The error LEDs indicate an overload condition and a broken wire.

Technical data	EL3054 | ES3054
Number of inputs	4 (single-ended)
Technology	single-ended
Signal current	4…20 mA
Distributed clocks	–
Internal resistance	85 Ω typ.
Input filter limit frequency	1 kHz
Dielectric strength	max. 30 V
Conversion time	0.625 ms default setting, configurable
Resolution	12 bit (16 bit presentation, incl. sign)
Measuring error	< ±0.3 % (relative to full scale value)
Electrical isolation	500 V (E-bus/signal voltage)
Current consumption power contacts	–
Current consumption E-bus	typ. 130 mA
Bit width in the process image	inputs: 16 byte
Configuration	no address or configuration setting required
Special features	standard and compact process image, activatable FIR/IIR filters, limit value monitoring
Weight	approx. 60 g
Operating/storage temperature	-25…+60 °C/-40…+85 °C
Relative humidity	95 %, no condensation
Vibration/shock resistance	conforms to EN 60068-2-6/EN 60068-2-27
EMC immunity/emission	conforms to EN 61000-6-2/EN 61000-6-4
Protect. class/installation pos.	IP 20/variable
Pluggable wiring	for all ESxxxx terminals
Approvals	CE, UL, Ex

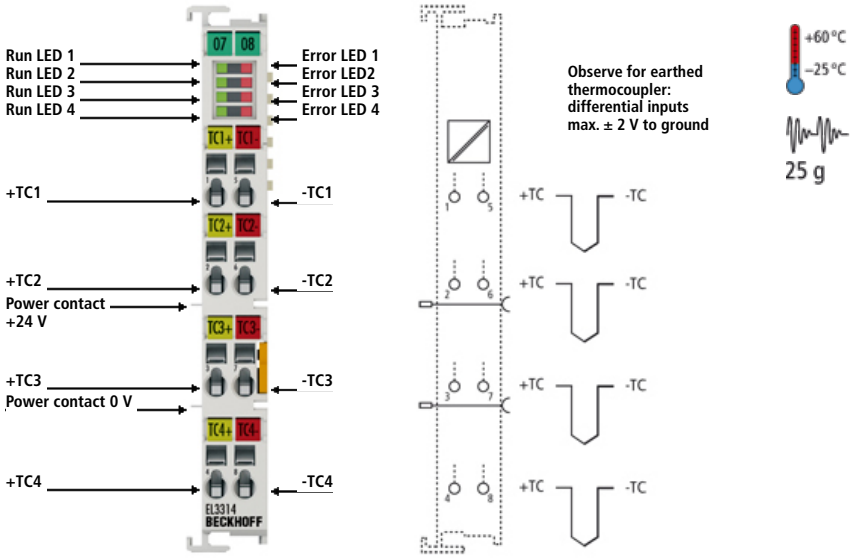

EL3314 | 4-channel thermocouple input terminal with open-circuit recognition

The EL3314 analog input terminal allows four thermocouples to be connected directly. The EtherCAT Terminal circuit can operate thermocouple sensors using the 2-wire technique. A microprocessor handles linearisation across the whole temperature range, which is freely selectable. The error LEDs indicate a broken wire. Compensation for the cold junction is made through an internal temperature measurement at the terminal. The EL3314 can also be used for mV measurement.

Technical data	EL3314
Number of inputs	4
Power supply	via the E-bus
Thermocouple sensor types	types K, J, L, E, T, N, U, B, R, S, C (default setting type K), mV measurement
Distributed clocks	–
Input filter limit frequency	typ. 1 kHz; dependent on sensor length, conversion time, sensor type
Connection method	2-wire
Wiring fail indication	yes
Conversion time	approx. 2.5 s up to 20 ms, depending on configuration and filter setting, default: approx. 250 ms
Temperature range	in the range defined in each case for the sensor (default setting: type K; -200…+1370 °C); voltage measurement: ±30 mV…±75 mV
Resolution	0.1 °C per digit
Measuring error	< ±0.3 % (relative to full scale value)
Electrical isolation	500 V (E-bus/signal voltage)
Current consumption power contacts	–
Current consumption E-bus	typ. 200 mA
Bit width in the process image	4 x 32 bit TC input, 4 x 16 bit TC output
Configuration	no address setting, configuration via the controller
Special features	open-circuit recognition
Weight	approx. 60 g
Operating/storage temperature	-25…+60 °C/-40…+85 °C
Relative humidity	95 %, no condensation
Vibration/shock resistance	conforms to EN 60068-2-6/EN 60068-2-27
EMC immunity/emission	conforms to EN 61000-6-2/EN 61000-6-4
Protect. class/installation pos.	IP 20/variable
Approvals	CE, UL, Ex

Related products	
EL3314-0010	4-channel thermocouple input terminal, high-precision, with open-circuit recognition
EL3314-0020	4-channel thermocouple input terminal, high-precision, with open-circuit recognition, with calibration certificate
EL3314-0090	4-channel thermocouple input, 16 bit, TwinSAFE SC

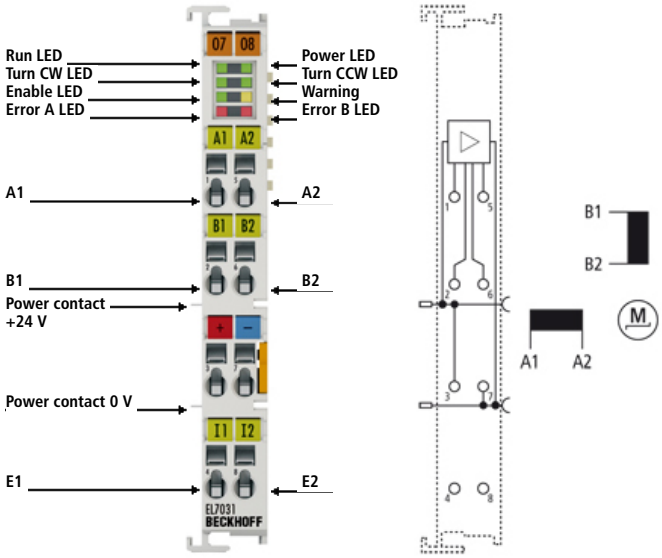

Top view | Contact assembly

EL7031 | Stepper motor terminal 24 V DC, 1.5 A

The EL7031 EtherCAT Terminal is intended for the direct connection of different small Stepper Motors. The slimline PWM output stages for two motor coils are located in the EtherCAT Terminal together with two inputs for limit switches. The EL7031 can be adjusted to the motor and the application by changing just a few parameters. 64-fold micro-stepping ensures particularly quiet and precise motor operation.

Technical data	EL7031 | ES7031
Technology	direct motor connection
Number of outputs	1 stepper motor, 2 phases
Number of inputs	2
Number of channels	1 stepper motor, 2 digital inputs
Load type	uni- or bipolar stepper motors
Nominal voltage	24 V DC (-15 %/+20 %)
Power supply	24 V DC via the power contacts, via the E-bus
Max. output current	1.5 A (overload- and short-circuit-proof)
Max. step frequency	1000, 2000, 4000 or 8000 full steps/s (configurable)
Step pattern	64-fold micro stepping
Current controller frequency	approx. 25 kHz
Diagnostics LED	error phase A and B, loss of step/stagnation, power, enable
Resolution	approx. 5000 positions in typ. applications (per revolution)
Electrical isolation	500 V (E-bus/signal voltage)
Current consumption power contacts	typ. 30 mA + motor current
Current consumption E-bus	typ. 120 mA
Distributed clocks	yes
Control resolution	approx. 5000 positions in typ. applications (per revolution)
Special features	travel distance control
Weight	approx. 50 g
Operating/storage temperature	0…+55 °C/-25…+85 °C
Relative humidity	95 %, no condensation
Vibration/shock resistance	conforms to EN 60068-2-6/EN 60068-2-27
EMC immunity/emission	conforms to EN 61000-6-2/EN 61000-6-4
Protect. class/installation pos.	IP 20/see documentation
Pluggable wiring	for all ESxxxx terminals
Approvals	CE, UL

Accessories	
EL9576	brake chopper terminal, 72 V, 155 µF
AS20xx | AS10xx	Product overview stepper motors
Leitungen und Getriebe	Prefabricated connecting cables in IP 20 and IP 67 protection for AS10xx stepper motors

Related products	
EL7037	stepper motor EtherCAT Terminal, I_{MAX} = 1.5 A, 24 V, IP 20, vector control
EL7041	stepper motor EtherCAT Terminal, I_{MAX} = 5 A, 50 V, IP 20
EL7047	stepper motor EtherCAT Terminal, I_{MAX} = 5 A, 50 V, IP 20, vector control
EP7041-0002	stepper motor EtherCAT Box (industrial housing), I_{MAX} = 5 A, 50 V, IP 67
KL2531	stepper motor Bus Terminal, I_{MAX} = 1.5 A, 24 V, IP 20
KL2541	stepper motor Bus Terminal, I_{MAX} = 5 A, 50 V, IP 20